NOVEL DESIGN OF ENERGY CONTROL ALGORITHM USED IN SOLAR POWERED BATTERYLESS ENERGY HARVESTING SYSTEM TO POWER WIRELESS SENSOR NODE

by

Hoi Wah Lo

Thesis Submitted in Partial Fulfillment
of the Requirements for the Degree of
Master of Applied Science

in the
School of Mechatronic Systems Engineering
Faculty of Applied Sciences

SIMON FRASER UNIVERSITY
Fall 2019

APPROVAL

Name: Hoi Wah Lo

Degree: Master of Applied Science

Title of Thesis: Novel Design of Energy Control Algorithm used in Solar Powered Batteryless Energy Harvesting System to power Wireless Sensor Node

Examining Committee: Patrick Palmer, Chair
Professor, School of Mechatronic Systems Engineering

Zoë Druick, Senior Supervisor
Professor, School of Communication

Ivan V. Bajić, Supervisor
Professor, School of Engineering Science

Eldon Emberly, External Examiner
Professor, Department of Physics

Date Approved: November 28, 2019

Abstract

'Internet of Things' (IoT) technology is becoming one of the most important driving forces in human productivity in recent years. New generation of 'super sensors', in the form of wireless sensor nodes (WSN) are the most important components in IoT. Powering these devices using traditional batteries creates a tough battery longevity problem, where the rigorous demands on the batteries require them to be replaced once every few years. This is further worsened by the huge number of devices in a typical IoT application, with their demand in power becoming a serious issue. It is commonly considered that one of the best ways to power these wireless sensor nodes is to use energy harvesters with solar energy harvesting.

Due to the unpredictable nature of solar irradiation, a problem to be solved is how a wireless sensor node powered by a solar energy harvester can have continual operation while simultaneously deliver the highest possible service duty. This thesis presents a new energy control algorithm that addresses this bottleneck problem.

Firstly, the analysis of past research using PID Control, Fuzzy Logic, and Adaptive Dynamic algorithm is provided, which reveals significant shortfalls. The use of a solar irradiation prediction model by one group of researchers results in significant system shutdown ("dead time") when actual solar irradiation deviates from the prediction model. Another group of researchers maintain the terminal voltage of the supercapacitor at a certain set point but this approach is not able to avoid system shut down, and it demands an unacceptable operating condition in which certain amount of light must be present for the system to operate. After analysis of these past projects, the design deficits and imprecise design objectives in these researches are elaborated.

Secondly, a proposal of a new energy control algorithm with the use of a precise two branch equivalent model is presented, with the employment of Model Predictive Control (MPC) theories to compute important control parameters. An augmented MPC control algorithm is designed based on three new principles, in order to handle the two mingled system input variables of system operating current and system sleep mode current of the WSN.

Thirdly, the resulting new energy control algorithm is implemented in a self designed wireless sensor node embedded system. The purpose of this self designed system is to conduct comprehensive field tests to validate the performance and the robustness of the energy control algorithm.

Finally, detail results with analysis of the four field tests is presented. The four field tests include the first test with normal operating condition, the second test as a stress test with an obstructed solar panel, the third as an additional stress test with a defective supercapacitor, and the fourth field test under abnormally adverse operating conditions. Except for the third field test which exhibits some time duration (2.8% of the total testing duration) with non-maximized WSN operation, all other field tests demonstrate full fulfillment of the new energy control algorithm's design objectives.

The last part of this thesis summarizes the conclusion of the research. And the research contribution in the field of IoT as well as in other numerous application areas are interpreted.

Thesis Senior Supervisor: Dr. Zoë Druick

Title: Novel Design of Energy Control Algorithm used in Solar Powered Batteryless Energy Harvesting System to power Wireless Sensor Node

Dedication

To my heavenly father and mighty God, who revived my life with his everlasting love and blessings,

To my beloved wife, for her support, encouragement, patience and endless love, and

To my dear son, for his encouragement, sharing, love and inspirations

Acknowledgments

I would like to express my sincere thankfulness and gratitude to my senior supervisor, Professor Zoë Druick, to my supervisor Professor Ivan V. Bajic, to my external examiner Professor Eldon Emberly, and to my thesis defense examination chair Professor Patrick Palmer. Their participation and invaluable guidance as members of my supervisory committee and of my examination committee will be remembered for many years to come.

My special thanks to Dr. Jeff Derksen and Miss Sheilagh Macdonald of SFU Graduate and Postdoctoral Studies for their help and care to form my thesis defense examination committee and to arrange for my thesis defense examination.

Table of Contents

APPROVAL ii
Abstract iii
Dedication v
Acknowledgments vi
Table of Contents vii
List of Figures ix
List of Tables xi
CHAPTER 1 INTRODUCTION 1
1.1 Motivation 1
1.2 Objective and Scope 4
1.3 Research Process and Thesis Organization 5
CHAPTER 2 ANALYSIS OF RELATED RESEARCH 7
2.1 Anatomy of an Energy Harvesting System 8
2.2 Research of SPBL Harvesters 9
2.3 Research of MPPT 11
2.4 Research of DC-DC Converters 12
2.5 Research of Supercapacitors Modelling 14
2.6 Research of Energy Control Algorithm 15
2.6.1 Earlier research of Energy Control Algorithm 17
2.6.2 Latest research of Energy Control Algorithm 20
2.7 Conclusion 24
CHAPTER 3 RESEARCH PROBLEM AND OBJECTIVE IDENTIFICATION 25
3.1 Importance of Problems Identification and Intuition of Solution 25
3.2 Addressing Problems and Objectives Identification 26
3.3 Research Problem Identification 28
3.4 Research Objectives Definition 29
3.5 Conclusion 29
CHAPTER 4 POSSIBLE SOLUTION 30
4.1 Irrelevance of Energy Neutral Operation (ENO) 30
4.2 Importance of Predictive Control 31
4.3 Two Branch Model for a Supercapacitor 33
4.4 Mitigating WSN Sleep Mode and Supercapacitor Leakage Current 35

4.5 Conclusion 36
CHAPTER 5 MODEL PREDICTIVE CONTROL THEORIES AND PLANT MODELLING 37
5.1 Model Predictive Control (MPC) Theories 38
5.2 SPBL Energy Harvester State Space Model 40
5.3 State Space Model Parameters Identification 43
5.3.1 Instruments used in model parameter identification 45
5.3.2 Two branch model parameters identification experiments 46
5.4 Conclusion 54
CHAPTER 6: PROPOSED NOVEL DESIGN OF ENERGY CONTROL ALGORITHM 55
6.1 MPC Energy Control Algorithm Formulation 55
6.1.1 Consideration on the best tool to generate MPC algorithm 55
6.1.2 MPC Algorithm design prerequisite to define State Space Model of Plant 57
6.1.3 MPC Algorithm Design with 'Matlab' MPC toolbox 62
6.1.4 Explicit MPC Algorithm Design used in this research 70
6.1.5 Rationale on the choice to use Explicit MPC Algorithm 72
6.2 Augmented MPC Energy Control Algorithm Formulation 74
6.2.1 Augmented MPC Energy Control Algorithm Design Approach 74
6.2.2 Augmented MPC Energy Control Algorithm Design for 22 hours Continuous Maximized Operation 78
6.3 Conclusion 80
CHAPTER 7: SYSTEM IMPLEMENTATION AND FIELD TESTS 81
7.1 Algorithm Implementation in WSN Embedded System 81
7.2 Data Error Analysis 83
7.3 Field Validation and Testing of Augmented MPC Energy Control Algorithm 84
7.4 Interpretation of field test results 90
7.5 Conclusion 95
CHAPTER 8: CONCLUSION AND suggestion for future works 96
BIBLIOGRAPHY 97
Annex A 'Matlab' MPC Design Process with screen shots 102
Annex B FOUR Sets of Testing Data 110
Annex C Three Sets of Matlab Design Files 111

List of Figures

Figure 1-1 Technology Roadmap – The Internet of things 1
Figure 1-2 Internet of Things - 6 Key Elements 2
Figure 1-3 Wireless Sensor Network 3
Figure 1-4 Basic Components of an Energy Harvesting System 4
Figure 2-1 Anatomy of an Energy Harvesting System 8
Figure 2-2 Conceptual Diagram of the Harvester Platform 9
Figure 2-3 Power-Voltage Plot of a Solar PV Module 11
Figure 2-4 Normalized Output Voltage vs Normalized Output Current Curve in a Buck-Boost Converter 13
Figure 2-5 Block Diagram of an EH-powered Wireless Sensor 16
Figure 4-1 Charging and discharging performance comparison among 2 Branch Model, 1 Branch Model and a real Supercapacitor 34
Figure 5-1 Basic idea of Model Predictive Control 38
Figure 5-2 Simplified circuit model of a Solar Energy Harvester with Energy Storage in a Supercapacitor 41
Figure 5-3 Constant source equipment used - 'Fluke' Model 341A Voltage Calibrator 45
Figure 5-4 Current sink equipment used - LM358 Op-Amp Controlled IRL530N MOSFET Circuit 45
Figure 5-5 Supercapacitor Two Branch Model with Variable Leakage Resistance [20] 47
Figure 5-6 Two Points (P1 and P2) Charging Method to determine Two Branch Model parameters 48
Figure 6-1 'Matlab' model simulation of an MPC Controller on a SPBL Energy Harvester with Two Branch Circuit Equivalent Model 57
Figure 6-2 SPBL energy harvester with supercapacitor two branch equivalent model circuit diagram 58
Figure 6-3 'Matlab' MPC Design Process 64
Figure 7-1 Self designed wireless sensor node embedded system 82
Figure 7-2 WSN embedded system placed in a plastic case on top of a sundeck for field tests 86
Figure 7-3 Graph (1) Field Test under simulated greenhouse operating environment 87
Figure 7-4 Graph (2) Field Test under Stress Test I 88
Figure 7-5 Graph (3) Field Test under Stress Test II 89
Figure 7-6 Graph (4) Field Test under extreme abnormal operating condition 90

Figure A-1 'Matlab' MPC Design Process 1 - Define Plant's State Space Model 102
Figure A-2 'Matlab' MPC Design Process 2 - Create 'Simulink' Plant's Model connected to a MPC Controller.....103
Figure A-3 'Matlab' MPC Design Process 3 - Open 'Simulink' MPC Designer Design Function for Plant's Linearization 104
Figure A-4 'Matlab' MPC Design Process 4 - Specify Operating Point of Linearization.....105
Figure A-5 'Matlab' MPC Design Process 5 - Observe Defaulted MPC Algorithm Design.....106
Figure A-6 'Matlab' MPC Design Process 6 - Specify Required MPC Algorithm Design Condition 1 107
Figure A-7 'Matlab' MPC Design Process 7 - Specify Required MPC Algorithm Design Condition 2 108
Figure A-8 'Matlab' MPC Design Process 8 - Final MPC Algorithm Design Computation of Required Supercapacitor Discharge Time.....109

List of Tables

Table 6-1 'Matlab' MPC Algorithm simulation result on SPBL energy harvester 67

Table 6-2 Experimental Validation of 'Matlab' MPC Design Computation 69

Table 6-3 AMPC Algorithm parameters for Augmented MPC Energy Control Algorithm for 22 hours continuous operation.....78

CHAPTER 1 INTRODUCTION

1.1 Motivation

The motivation of the research as presented in this thesis originates from the realization of the importance of 'Internet of Things' (IoT). With the vast power provided by our global internet infrastructure, 3.7 billions people out of our world's total population of 7.5 billions (49.2%) are now connected by the internet [1]. Huge productivity gains achieved by the internet have made internet indispensable to our modern global economy. Undoubtedly, IoT will become the next step in our quest to improve human productivity.

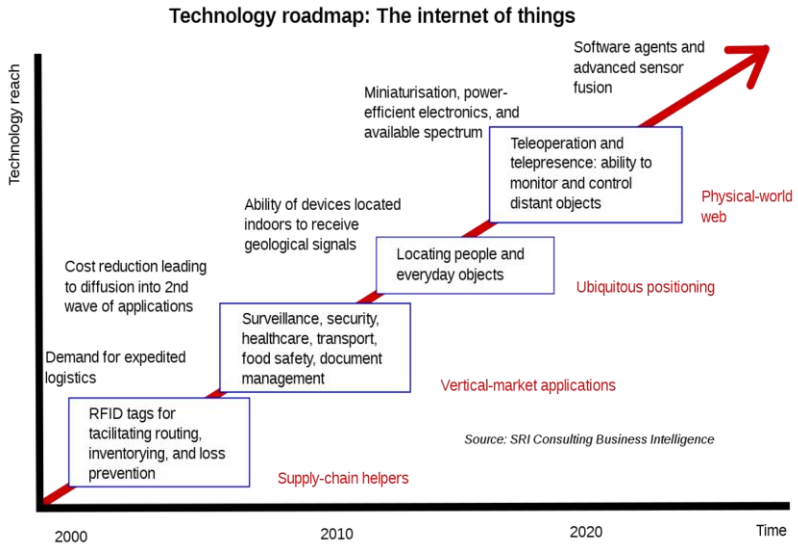

Figure 1-1 Technology Roadmap – The Internet of things [40]

IoT allows objects to be sensed or controlled remotely across existing network infrastructure, creating opportunities for more direct integration of the physical world into computer-based systems. This results in improved efficiency, accuracy and economic benefits, in addition to reduced human intervention [2]. Among the four core elements (sensing, communication, cloud based capture and consolidation and delivery of information) of IoT, the most important elements are sensing and

communication. They are the critical first and second steps of IoT workflow [3], as can be seen in following diagram FIGURE 1-2:

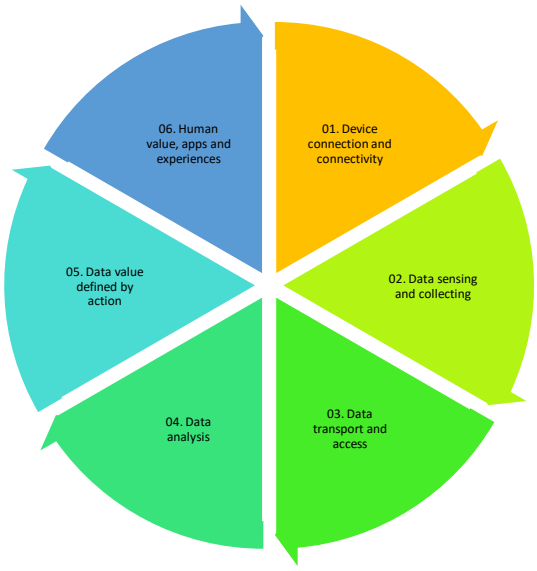

Figure 1-2 Internet of Things - 6 Key Elements

As such, the idea of developing a new generation of 'super sensors' with functions and capabilities needed in our anticipating world of IoT [4] has emerged in recent years. Despite the rapid pace of technologies advancement, there is still no officially or internationally acknowledged definition of what a 'super sensor' should be.

While the definition and standard of 'super sensors' keep on evolving, there is a common viewpoint that the wireless sensor nodes used widely in the application of IoT is a typical type of 'super sensors' that we strive to develop.

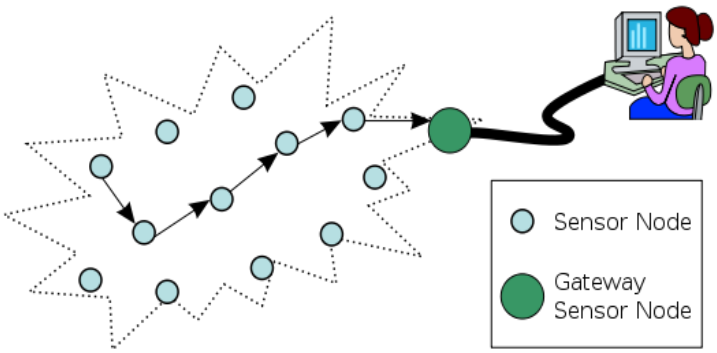

Figure 1-3 Wireless Sensor Network [41]

"Super sensors" require several key elements, such as wireless capability, high sensitivity sensing, robustness, and self powered capability [5]. By far, the ability to be self powered, without the use of traditional batteries, is the most important requirement for the development of the new generation of "super sensors". The relatively short life of traditional rechargeable batteries (2-5 years), their adverse environmental impacts, and the high replacement costs have made it impossible to use batteries in a typical IoT application, where potentially hundreds of sensors are employed. How to power the new generation of 'super sensors' is a technological 'bottleneck. The current research trend is to employ self powered energy harvesting technologies to harvest ambient energy resources like solar energy [7] . The growing popularity and importance of energy harvesters is provided by the evidence that many big integrated circuits manufacturers supply numerous models of energy harvesters integrated circuits in the past ten years ('Texas Instrument', 'Linear Technology', 'Analog' etc.). Energy is stored in a supercapacitor rather than in a battery, because a supercapacitor has a much longer life span of up to 40 years. While this may provide a promising solution, there are still conceptual and technical barriers, noticeably in the frequent shutdown of energy harvesters during unfavorable and unpredictable energy harvesting circumstances, awaiting to be solved [6]. Once these barriers are overcome, the new generation of 'super sensors' can potentially operate autonomously for the whole life time of the sensors, which may be up to 40 years.

It is obvious that the new generation of 'super sensors' can properly support IoT applications only after the technological challenges in the self powered energy harvesting unit are solved. Therefore, this research, as presented in this thesis, focuses on the development of a novel energy control algorithm and aims to tackle the most pressing self powered energy harvesting challenges.

1.2 Objective and Scope

The core objective of this research is to develop a novel energy control algorithm for a solar powered batteryless (SPBL) energy harvester subsystem. The SPBL energy harvester subsystem can be used to power a wireless light spectrum sensor node connected to a wireless sensor network, as an example of a possible application. This research focuses on the power management control portion as shown in the following diagram FIGURE 1-4 :-

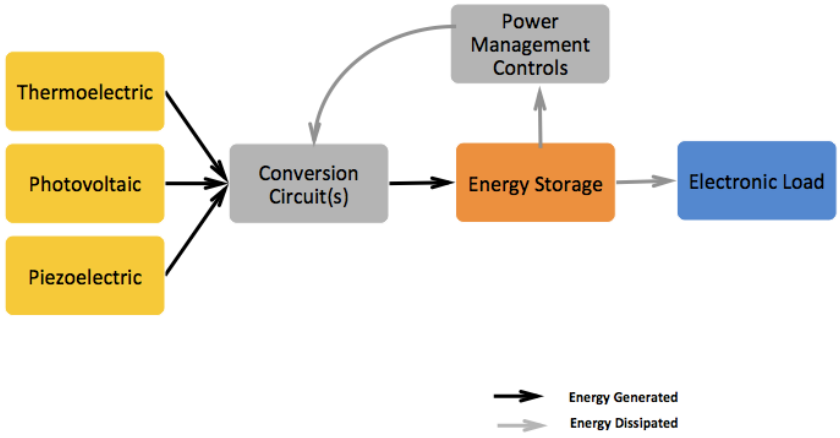

Figure 1-4 Basic Components of an Energy Harvesting System

After thorough analysis, it is clear that existing research of solar powered energy harvesting subsystem (which will be elaborated in Chapter 2) such as DC-DC converter, maximization of solar energy harvesting with Maximum Power Point Tracking (MPPT) and energy storage devices charging and discharging modelling/utilization are mature, with very good efficiency. The remaining critical portion to be improved on is the energy control algorithm, for which existing research is still nascent for practical commercial usage.

While a hardware platform of an embedded wireless light spectrum sensor node system (for greenhouse automation purpose, amount of artificial lighting in different light spectrum is compensated to facilitate the growing of vegetables and fruits, depending on the light spectrum composition of natural light in different weather condition) is designed and built during this research, that is not the core research focus. Instead, it is used as a testing platform to validate the performance of the new energy control

algorithm developed in this thesis. The design of the self powered energy harvester unit with a novel energy control algorithm can either be used in the embedded wireless light spectrum sensor node system as in this case, or in any other wireless sensor node for any other wireless sensor network.

The aspiration and the focus of this research are on the novel design of the energy control algorithm used in the SPBL energy harvester. Once it is proven able to solve existing technological barriers, it can be used in any other similar wireless sensor network and that will create valuable contributions.

Specifically, the new design of the energy control algorithm strives to achieve two clearly defined objectives, which are still present as outstanding research problems:

(a) the enabling of the SPBL energy harvester to supply continuous power to the wireless sensor node (WSN) even in situation of highly fluctuating weather conditions; and

(b) its ability to provide power to maximize the service duty cycle of the WSN.

The scope of the research includes both software simulation and actual hardware implementation of the algorithm in C codes in a self designed WSN embedded system. Extensive field tests are performed to validate the algorithm's performance and its robustness under different operating conditions.

1.3 Research Process and Thesis Organization

The research process begins with the study of past ten years' related research in energy control algorithm in solar powered batteryless energy harvester powering wireless sensor nodes. The weaknesses of existing research and the lessons learned from the past decade's research are summarized. Specific design objectives and design directions are then laid out. With support from the most appropriate plant equivalent model and control theories, these design objectives include the design of a new energy control algorithm, together with the C codes implementation of the algorithm in a self designed hardware platform. The detailed design of the new energy control algorithm is the core focus of this research.

The first four chapters provide general introduction, past research reviews, specific research problem and objectives identified, and the possible directions for solution.

Chapter 5 firstly explains the need and justification of a precise two branch equivalent model for the controlled plant (the solar powered batteryless energy harvester) and identifies the model parameters using specific charging and discharging tests. Then the reasons for the choice of Model Predictive Control (MPC) theories to compute important control parameters are elaborated and their distinctive

advantages in this application highlighted. At the end of the chapter, it explains why MPC theories alone, despite the importance of the theories, are not sufficient to derive a usable energy control algorithm for this case. New design concepts and principles to sort out the mingled plant operating current and plant sleep mode current are necessary to provide a full solution to achieve the design objectives.

In Chapter 6, new design principles to handle the two mingled control variables are analyzed and proposed in detail. These unique design principles are then applied and combined with the use of the MPC theories computed control parameters to develop a complete new energy control algorithm.

Chapter 7 documents the embedded system implementation and field tests. It focuses on the actual implementation of the new energy control algorithm (in C codes) in a wireless sensor node embedded system as well as the validation of the energy control algorithm's performance with four carefully selected field tests. The actual C code software implementation of the new energy control algorithm in a microcontroller based wireless sensor node embedded system demonstrates that the research in this thesis is ready to be put into practical use. The four field tests conducted show satisfactory results which fulfill the design objectives and demonstrate strong robustness of the energy control algorithm in adverse operating condition.

A summary of this research work, its key contributions and its future works is provided in the final chapter of this thesis.

The structure of this thesis report is as follows:

Chapter 1: Introduction

Chapter 2: Analysis of related research

Chapter 3: Research problem and objective identification

Chapter 4: Possible solution

Chapter 5: Model Predictive Control Theories and plant modelling

Chapter 6: Proposed novel design of energy control algorithm

Chapter 7: System implementation and field tests

Chapter 8: Conclusion and interpretation of research contribution

CHAPTER 2 ANALYSIS OF RELATED RESEARCH

SPBL harvester has been recognised as an ideal powering device for WSN. However, in real life applications, most WSNs are still powered with button cell batteries. There are obviously technological or financial barriers prohibiting the use of SPBL harvester. On the cost side, using SPBL harvester as a power device will surely increase the cost of an embedded WSN system. Yet the added technical advantages and the potential for economies of scale will more than compensate the added cost. Hence, the financial consideration should not be considered as the barriers. The objective of this research is, therefore, to find out the possible technological barrier(s) and to provide a suitable solution.

This chapter starts with the anatomy of the structure and the system components of an SPBL energy harvester. It follows with the analysis of research related to different system components of the energy harvester. The conclusion of the analysis shows that the energy control algorithm represents the most critical research still encountering outstanding technological barriers.

Following the above conclusion, subsequent analysis effort focuses on the research related to energy control algorithm for SPBL harvesters. In Spring 2017, at the beginning of this research, related research papers in the past ten years were exhaustively searched and reviewed. Among them, five most relevant and outstanding research papers were identified. Towards the end of this research in January 2018, another search of related research was conducted. Two more most relevant research papers [27][28] were identified for a final analysis and comparison. It is concluded that both the Fuzzy Logic Energy Management Algorithm research [28] and the research as presented in this thesis provide the best practical solution, in spite of the two totally different design approaches. A detailed analysis of these past seven research papers with a focus on the best paper [28] is provided.

At the end of the chapter, the contribution of analysis of these related research is summarized.

2.1 Anatomy of an Energy Harvesting System

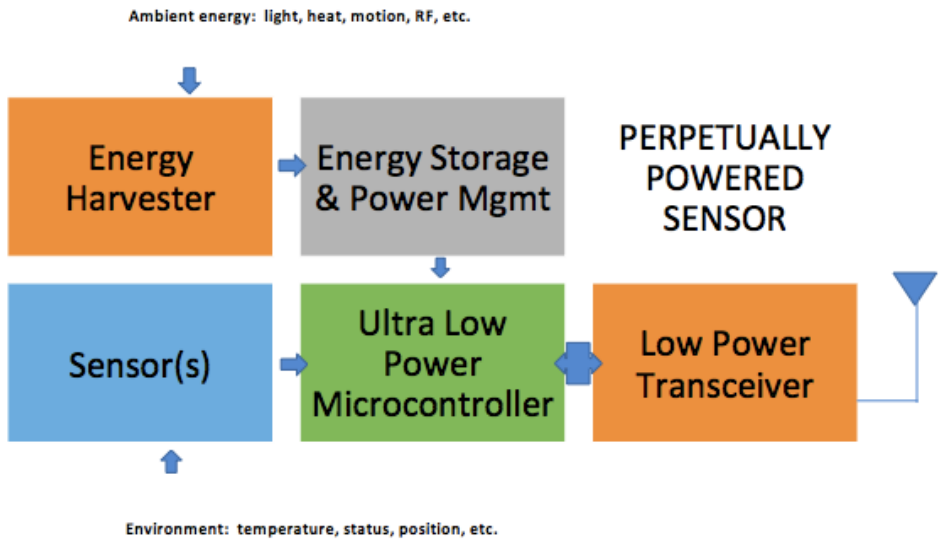

Figure 2-1 Anatomy of an Energy Harvesting System

There are many available ambient energy sources for energy harvesting. And many tools have become commercially available to help harvest these energy sources. Among them, the miniature solar panel has a distinctive advantage of providing the highest energy density (100s of mw/cm^2 in direct sunlight, vs 10s of mw/cm^2 of thermal energy, 100s of µw/cm^2 of piezoelectric devices, and 100s of pw/cm^2 by RF devices), the lowest maintenance requirements and the longest operating life (20-50 years) [7].

On the other hand, starting from year 2007 and with ever increasing certainty in the last four years, batteryless operation for wireless sensor nodes has become an indispensable requirement. This is due to the environmental harms of batteries and the practical difficulty to replace hundreds of batteries every few years in a typical IoT application [8]. Solar cells are not as friendly to the environment as other ambient energy harvesters (such as wind, thermal, vibration etc.), but they are mostly chosen due to their energy efficiency, cost, size, along with other reasons. The new energy control algorithm derived in this research applies equally well to other energy harvesters using other energy harvesting sources.

With consideration of the above two important reasons, this research focuses on designing a new energy control algorithm for a self powered energy harvester unit, using a miniature solar panel for energy harvesting and a supercapacitor as energy storage element instead of a rechargeable battery. A solar powered and batteryless (SPBL) energy harvester provides the most promising solution in powering

wireless sensor nodes for the IoT applications.

2.2 Research of SPBL Harvesters

There are many research studies done on SPBL harvesters in the last ten years, but their research focus and content do not deviate significantly from the paper done by D. Brunelli and L. Benini [9] . The iconic research of D. Brunelli and L. Benini and their other team members in the University of Bologna was published in 2009 [9]. Their research, as well as other similar research, is analyzed below.

A typical SPBL harvester schematic diagram is usually found in the beginning of the research papers.

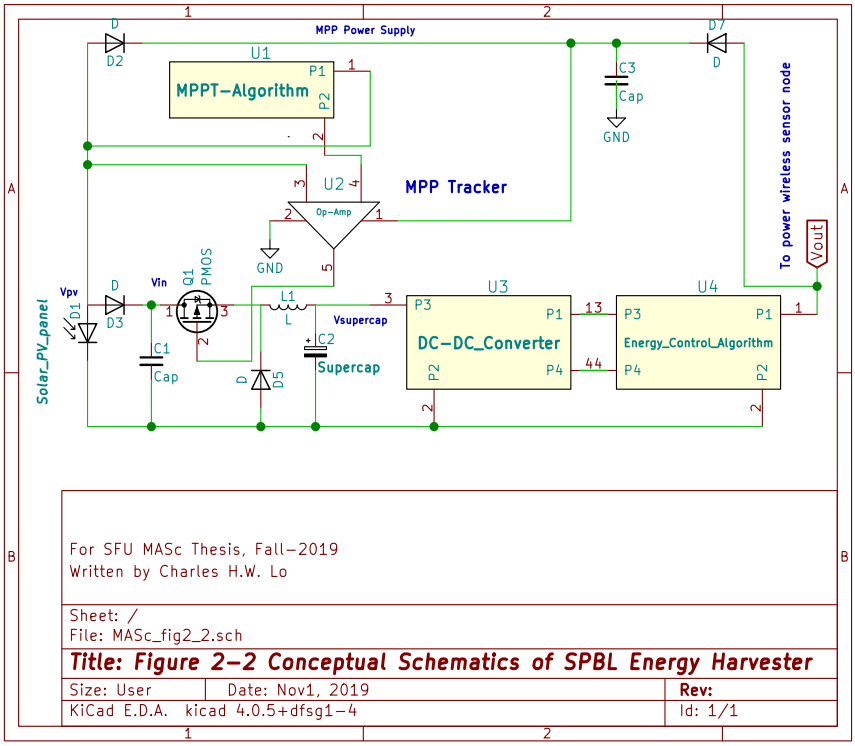

Figure 2-2 Conceptual Diagram of the Harvester Platform

Schematics in Figure 2-2 shows that solar energy harvested is maximized by locating at the optimal energy harvesting current operating point (known as maximum power point tracking). Solar energy harvested is used to charge up the supercapacitor as an energy storage device with an efficient charging circuit. Energy stored in the supercapacitor is then converted to a suitable output voltage level (typically 3.3 V, or sometimes 2V for new generation of microcontrollers) by a DC-DC converter so as to power a wireless sensor node embedded system.

Based on this conceptual diagram of the SPBL harvester, researchers focus on handling or solving four core technical issues in a SPBL harvester:

(1) MPPT (Maximum Power Point Tracking) of the miniature solar modules.

(2) DC-DC inverters' efficiency and effectiveness.

(3) Special charging and discharging characteristics of the supercapacitors (also known as ultracapacitors or double layered capacitors), which are used to replace traditional rechargeable batteries.

(4) Energy management and control methodologies and algorithm.

Overwhelming majority of research efforts before year 2012 were spent on areas (1), (2) and (3). Research focusing on area (4) constitutes most of research efforts in the past five years from year 2012 to year 2017. These past research studies are summarised in the four major research areas in the following sections.

2.3 Research of MPPT

Due to the special energy capturing properties of solar module as shown in the following graph, its maximum power being captured is located at a different point of voltage and current under different solar irradiation and temperature operating conditions. Maximum Power Point Tracking (MPPT) method is used to enable the solar module to operate as close to the Maximum Power Point (MPP) as possible. Among the numerous proposed methods, the fractional open-circuit technique is used predominantly, due to its best effectiveness in terms of cost and power consumption in microscale PV systems [9].

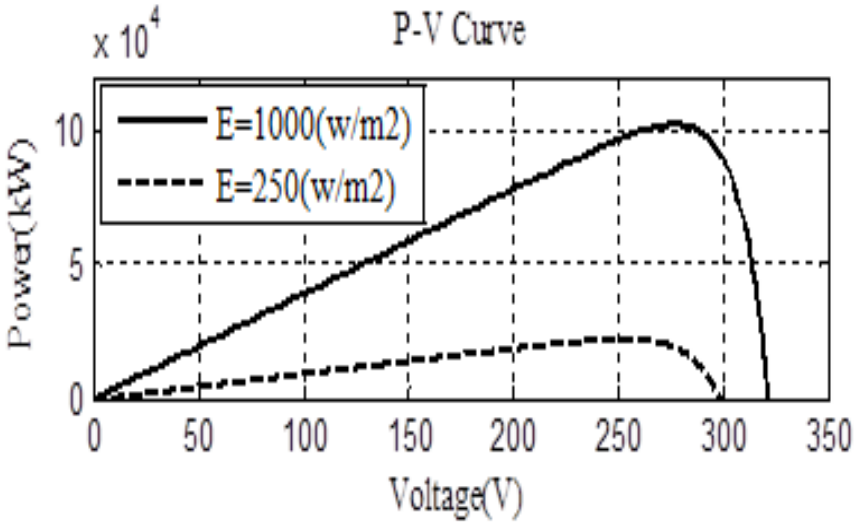

Figure 2-3 Power-Voltage Plot of a Solar PV Module [45]

As seen in the above figure 2-3, the maximum power point lies at around output voltage of 275V of the solar module. A maximum power point tracking circuit aims to provide a loading circuit in order to move the solar module output voltage to this maximum power operating point.

In the MPPT research paper presented by Oscar Lopez-Lapena and his team in 2010, a modified and improved type of the Perturb and Observe (P&O) method is proposed. It offers a more accurate, but costlier, solution than the fractional open-circuit technique [10]. Individual MPPT tracking efficiency is not reported in [9] while it is reported as 92% in [10]. A Linear Technologies Corporation (LTC) DC-DC boost converter with efficiency of 97% is used in [9] to provide a stable 3.3 V supply. An off-the-shelf Pulse Frequency Modulation (PFM) dc/dc boost converter is used in [10] for the same purpose to convert energy from the supercapacitor to the required 3.3 V used to power a wireless sensor node. Overall SPBL

energy harvester efficiency is reported as 80% in [9] while it is reported as 92% in [10].

Another research paper proposes an innovative MPPT method, in which a closed loop predictive method is used to predict the voltage and current operating point of the solar module using the charging time calculation of the supercapacitor [11]. Using this closed loop method, a more accurate tracking of the MPPT is achieved compared to the fractional open-circuit technique, but at the same time, it avoids using the more complex voltage and current sensing circuit needed in the P&O method. To test the proposed MPPT technique, similar to what is used in [9] & [10], a commercially available MAX1795 boost converter is used to construct a SPBL harvester. Overall efficiency of the harvester is reported to be over 90%.

Due to the obvious cost effectiveness consideration, the simpler and cheaper fractional open-circuit technique is predominantly adopted in commercial SPBL harvester integrated circuits. As can be seen in the analysis in this section, research on MPPT is mature without much room for further improvement.

2.4 Research of DC-DC Converters

The research papers of [9], [10] & [11] show that commercially available DC-DC boost converter integrated circuits (ICs) are used to construct their proposed SBPL harvesters. These boost converter ICs, such as the LTC 3401 and the MAX 1795 boost converter, are typically supplied by global leading silicon chip manufacturers. Most of them provide comprehensive functionality with very high power conversion efficiency. In many older generation DC-DC boost converter ICs, traditional Pulse Width Modulation (PWM) technique is used for the DC to DC power conversion. Traditional PWM technique generally works satisfactorily, but at low loads its efficiency decreases rapidly. The graph below, as illustrated in [43], shows a typical efficiency curve of a DC-DC converter.

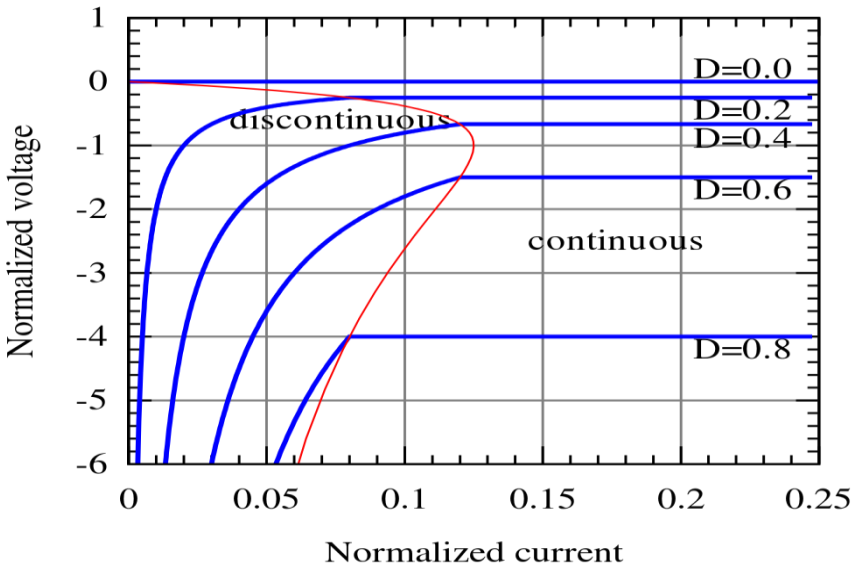

Figure 2-4 Normalized Output Voltage vs Normalized Output Current Curve in a Buck-Boost Converter [43]

There are two types of power losses in the light load region. The first type occurs from current ripple-induced conduction losses. The second type is called "V-I overlap" switching losses due to rapid switching cycle. In light load region, these two types of power losses become much more significant as compared with the small load current. As a result, the efficiency in the light load region is seriously hampered.

To mitigate the inefficiency in the low load region in a PWM DC/DC converter, three popular complementary switching techniques are commonly used, namely 'Soft Switching', 'Forced Discontinuous Mode' and 'Pulse Skipping' [13].

Using the 'Forced Discontinuous Mode', the LTC3401 boost converter used in [9] exhibits a very high average power conversion efficiency of up to 97%. Using the 'Pulse Skipping' technique, the MAX1795 used in [10] also exhibits a very high average power conversion efficiency of up to 95%. There are also numerous other commercial boost converters in integrated circuits forms employing the three low-load complementary switching techniques mentioned, all with power conversion efficiency above 95%.

It is shown that employing Pulse Frequency Modulation (PFM) in the low load region of a boost converter becomes an increasingly popular trend [14]. It is apparent that, based on the analysis in this

section, research on the design of DC-DC boost converter has become mature, without much room for further improvements.

2.5 Research of Supercapacitors Modelling

Double layered capacitors (also known as ultracapacitors or supercapacitors) have much higher capacitance and energy density compared to traditional aluminium electrolytic capacitors. They were first developed in 1989 by 'Panasonic', followed with mass commercial production in the early 90's. Unlike electrolytic capacitors, supercapacitors do not have dry-up problems over time. Compare with rechargeable batteries, which have a limited life span of several years due to chemical reaction degradation, supercapacitors' charging and discharging processes do not use chemical reaction and, therefore, they enjoy an average life time of 20 to 40 years. These features have made supercapacitors excellent energy storage devices for powering low power embedded systems. However, researchers discover that supercapacitors' charging and discharging characteristics are different from traditional electrolytic capacitors. They also discover that the normal energy storage formulae (E (Energy) = 1/2 CV^2) do not conform totally to these types of capacitors. This creates difficulty in predicting the energy stored in the supercapacitors and to derive power management scheme of their powered embedded systems [15] & [16].

In [17] published in 2000 and in [18] published in 2007, it is argued that there are two distinctive characteristics of supercapacitors which are crucial for energy modelling and power prediction calculation:

1. Supercapacitors suffer from energy loss due to internal charge distribution, even without taking into consideration of charge leakage. The charging and discharging cycle efficiency rate is 93% in the initial cycle and stabilizes to about 97% after 3 cycles.

2. Supercapacitors suffer from much worse leakage problems than rechargeable batteries. Depending on the capacitor's size, model and manufacturer, early generations of supercapacitors suffer from stored energy losses by 5 – 25% in the first 24 hours [17]. However, as of 2017, most supercapacitor manufacturers can reduce the leakage current to a very small value of single-digit figure or double-digit figure of Microampere [37]. In a self discharge experiment in this research, testing data shows that a 5-Volt, 20-Farad supercapacitor bank discharges only about 0.1 V in 22 hours. While this self discharged energy is greatly reduced compared to ten years ago, it still needs to be put into consideration in the energy budget calculation for the design of energy control algorithm.

These problems, which cause difficulties in calculating energy available from the supercapacitors, are mitigated in [9] by arbitrarily oversizing the supercapacitors during the design stage and by relying on the daily replenishing of solar energy to the supercapacitors. However, it is obvious that a detailed mathematical model of the supercapacitors needs to be developed to take into consideration of the above two distinctive characteristics of supercapacitors, so that precise energy control of the SPBL energy harvester can be achieved.

First proposed by [19], then adapted by [20], and further improved by [21], a practical and accurate two branch equivalent model is commonly acknowledged as the best model for use for modelling supercapacitors. It is also used for the modelling of the supercapacitor in the SPBL energy harvester in this research, which will be elaborated in detail in later chapters.

In summary, research on the design of supercapacitor and its manufacturing technologies has matured without much room for further improvement. The research on supercapacitors' modelling has also matured where a practical and accurate two branch equivalent model can be used with great precision.

2.6 Research of Energy Control Algorithm

Past research shows significant improvements and maturity in the first three technological areas of SPBL energy harvester, namely MPPT, DC-DC converters and supercapacitors charging and discharging characteristics modelling. The only remaining key research area for improvement is the research in energy control algorithm. Once a practical and high-performance energy control algorithm is derived, SPBL energy harvester will allow the new generation of 'super sensor' to deliver its full capability. As seen in the diagram below, the power controller design methodologies and control algorithm has become the focus of research effort in recent years.

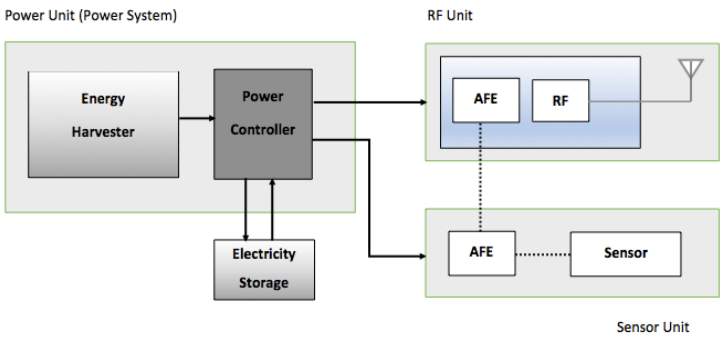

Figure 2-5 Block Diagram of an EH-powered Wireless Sensor

As mentioned in sections 1.1 and 1.2, the objective and scope of this research are to solve an outstanding energy control problem in the SPBL energy harvester. The prevailing problem is that under situations where environmental factors are volatile, the SPBL energy harvester fails to effectively supply sufficient power to the WSN on a continuous basis while maximizing the WSN service duty. To solve this problem, it requires the implementation of a new energy control algorithm, which can satisfy the two seemingly contradictory objectives.

Since there are very few WSNs powered by SPBL energy harvesters in the commercial market, one may assume that a practical and applicable energy control algorithm is still not available for full commercialization. At the early stage of this research (Spring 2017), an extensive search was performed with the intention to identify all past related research of energy control algorithms for SPBL harvesters that have similar scope and objectives to this research. The result of the search confirms the assumption that there were in fact no fully successful energy control algorithm as of early 2017. Among all related research papers found, five papers are considered to provide the better solutions [22], [23], [24], [25], [26]. Although these five papers provide better solutions than the others, there are significant weaknesses which prohibit their effective use as commercial WSN products.

At the completion stage of designing the new energy control algorithm in this research, in Spring 2018, another extensive search was conducted with the aim to identify the newest related research studies by other researchers. Two additional research papers were identified to provide effective solution to the same problems as addressed in this research [27], [28]. Between them, [28] is considered to provide a satisfactory and practical solution to the research problem while [27] shows certain design weaknesses. Using a completely different design approach compared with the design in this research, [28] provides a

similar satisfactory solution. However, [28] uses Nickel Cadmium rechargeable battery as the energy storage device in the SPBL energy harvester. As mentioned in section 1.1 Motivation, batteries require regular replacement in every few years and such maintenance are not possible in many large scale IOT application using hundreds of wireless sensor nodes. In contrast, the design of the new energy control algorithm as presented in this thesis provides a more appropriate and practical solution for SPBL energy harvester using supercapacitor for energy storage.

In the following section 2.6.1, an analysis of the five research papers reviewed in year 2017 is presented. Section 2.6.2 elaborates an analysis of the two most recent research papers reviewed in January 2018. As mentioned, [28] appears to provide an alternative satisfactory solution for SPBL energy harvester compared with the design in this research, should its design be modified to using supercapacitor instead of Nickel Cadmium rechargeable battery as energy storage device.

2.6.1 Earlier research of Energy Control Algorithm

In early 2017, five most related research studies of energy control algorithm for SPBL energy harvester powering WSN were identified. Among these five research papers, the first group (Group 1) employs different types of closed-loop feedback controllers (such as state space LQR controller, PID controller and Model Predictive Controller), but all with a hard-to-realize and unreliable solar energy harvesting prediction model [22], [24], [25]. The second group of research (Group 2) aims to correct the weaknesses of the first group by avoiding the use of a solar energy harvesting prediction model, and by seeking to achieve an 'Energy Neutral Operation' (ENO) for the storage element (either a rechargeable battery or a supercapacitor) to maintain at a stable charging level [23], [26]. While Group 2 research succeeds in improving on Group 1's research significantly, their inherent weaknesses still prohibit their successful practical usage.

Group 1 researchers focus on achieving a longer time span of an energy neutral operation. Their designs rely heavily on solar energy harvesting prediction using solar irradiation prediction models. Based on historical record of solar irradiation in a specific location, solar irradiation prediction model predicts future solar irradiation which would be difficult due to daily unpredictability such as cloud cover. With an assumption that there will be a regular replenishment of solar energy as harvested everyday in the daytime to provide for the energy consumption in the night time, the storage element (either a rechargeable battery or a supercapacitor) is sized optimally for the reasons of cost and system size. The longer period balance of energy is achieved by coping with the energy harvested (estimated by the solar irradiation prediction models) with the optimal energy consumed.

The energy control algorithms presented in all three Group 1 research papers can utilize the storage element to mitigate the energy fluctuations on a daily basis. However, they fail to achieve an energy neutral operation should the solar irradiation prediction models deviate significantly from reality. For example, several days of heavy rain with very low solar irradiation, deviating from the prediction average, will easily deplete all energy stored in the storage element. Then it results in the shutting down of the energy harvester and its powered WSN. This frequent 'dead-time' (shutting down of the WSN due to energy depletion of the storage device of the energy harvester) is validated in [26] in its field testing of the model used in [24]. Although energy will eventually be replenished and energy neutral operation will eventually be able to resume, the frequent 'dead-time' is totally unacceptable in a highly risk averse commercial environment.

Group 2 research papers seek other design methods to avoid 'dead-time' due to short term solar irradiation prediction inaccuracies. In [23] and [26], solar irradiation prediction models are eliminated due to its short-term unreliable nature. Instead, [23] and [26] focus on tracking the output voltage of the storage element at a healthy operating voltage level by adjusting the power duty cycle supplied to the WSN. An ENO can be achieved because of such adjustment to the power duty cycle to cope with the solar energy harvested. In both papers, the storage element is used as a 'last resort' buffer to steal some time for last minute operation when an ENO is not attainable. This happens when energy harvested is not equal to energy consumed during certain period. Hence, it diminishes the huge value of the storage element in enabling continuous power operation of the energy harvester in period of zero energy harvesting.

This undesirable result may be due to the nature and the strength of the PID controller and adaptive dynamic controller, which is able to track the terminal voltage of the supercapacitor at a particular setpoint by its fast close-loop feedback control. While it helps preventing the supercapacitor from discharging further, the very important advantage of the energy storage capacity of the supercapacitor is not utilized. The important charging and discharging characteristics of the supercapacitor is not employed to use the stored energy optimally.

It is obvious that Group 2 researchers neglect the crucial storage capability advantages of the storage element. Both [23] and [26] do not use any modelling of the supercapacitor to employ fully the charging and discharging characteristics of the storage device. As both [23] and [26] try to achieve ENO (while at the same time maximizing the power duty cycle percentage), their algorithm tracks and controls the supercapacitor's operating voltage to stay at a pre-set nominal value, so as to prevent the energy harvester from entering into discharge stage in the case where no new solar energy is harvested.

However, their focus to achieve ENO proves to provide negative consequence, which is shown in different manners and with different results in [23] and [26].

In [23], to achieve ENO, a minimum level of light must be present to balance the minimum power duty cycle percentage defined in its PID control algorithm. This operational pre-requisite implies that if there is no light present, there will be no incoming solar energy harvested to support the minimum power duty cycle, hence not achieving ENO. However, this operation requirement is unreasonable, as the energy harvester still needs to provide power to send out wireless data at night. This is not necessarily an unavoidable result. When the supercapacitor starts to discharge from its nominal voltage (which the PID controller aims to track), there remains the valuable discharging power and discharging period that one can use to continue operating the wireless sensor node before the minimum operating voltage is reached. A very important fact that works to our benefit is that, during the discharge period from the nominal supercapacitor voltage to the minimum operating voltage (of the wireless sensor node), no light is needed to power the operation of the WSN and the energy harvester is operating at a non-ENO status.

[23] does not utilize much of the value of the storage and discharge characteristics of the supercapacitor although it refers in its paper the work of [26] which does mitigate this odd result of the requirement of the control algorithm to operate only in the presence of light. In [23], it says, “In [4] (i.e. [26]), a new concept of energy neutrality, known as ENO-Max, is proposed. An adaptive controller is constructed for the node to minimize the cost function and satisfy the ENO-Max condition. The power manager only considers the battery level to adapt the duty cycle. Therefore, this approach does not need to characterize harvesting sources and consumed energy. However, the energy storage model based on battery level is only considered in the linear region of the rechargeable battery.”. The statement clearly does not reflect accurately the value of paper [26] which already solved the problem of operating with no light in a 'hidden' and 'subtle' manner. This will be elaborated further in the next paragraph.

[26] succeeds in avoiding the problem of using a solar energy prediction model used by Group 1 researchers. At the same time, it does not have the problems in [23] where a certain low light level is needed for operation. In fact, [26] reports a zero-percentage operation downtime as written in its experiments. This compares well to the work of [23] where a double-digit percentage downtime is reported. A more detail analysis of [26] shows that it includes a minimum duty cycle percentage in its design, to prevent the supercapacitor from discharging prematurely before the next solar energy harvesting cycle restarts. The reason for setting a minimum duty cycle percentage as a soft constraint to the LQR (Linear Quadratic Regulator) algorithm is not mentioned explicitly but it is apparently set to ensure a zero-percentage operation downtime. The mechanism and mathematics of how to determine the

parameter of the minimum duty cycle percentage is not mentioned in the paper, but it is likely determined by an intrinsic estimation of when the next solar energy harvesting cycle will happen. As the minimum duty cycle percentage in its experiments and simulation is set at a very low level, it is building a very big safety buffer for the supercapacitor to be able to discharge for a significant period before reaching the minimum operating voltage.

However, the design of setting a minimum duty cycle percentage results in two weaknesses. Firstly, optimization to achieve the highest possible duty cycle percentage is sacrificed. Secondly, should the next solar energy harvesting period arrive only after an unexpected but extended rainy period of many days, the energy harvester will still run into a total energy depletion of its supercapacitor which will make it inoperable.

From our analysis as presented in this section, [26] is the best research but its weaknesses still prohibit it from successful and practical usage as a SPBL energy harvester.

2.6.2 Latest research of Energy Control Algorithm

Upon finishing the design of the new energy control algorithm in January 2018, a search was conducted again to find any new developments in relevant research. As a result, [27] and [28] were identified. [27] appears to provide a similar performance as compared with [26]. [28] demonstrates to be the best relevant research paper that is analyzed in this thesis.

Although both [27] and [28] provide strong relevance and value for comparison, they have several major differences as compared with the research in this thesis. Firstly, both research use Nickel Cadmium rechargeable batteries as storage devices while research design in this thesis uses supercapacitor as energy storage for the SPBL energy harvester. Secondly, both research only validate their energy control algorithm in software simulator and have not yet implement their design on any real hardware platform. On the contrary, this research validates its design both with 'Matlab' software simulator and at the same time completes its actual implementation in a self designed WSN hardware platform. Thirdly, both research designs require measurement of multiple system parameters such as harvested current, consumed current, terminal voltage of battery, and records of past harvested current, etc., while this research requires the sensing of the terminal voltage of the supercapacitor as the single measured parameter. Lastly, the final design and software simulation of the best related research paper [28] is based on an indoor operating environment while the design in this thesis focuses on an outdoor operating environment.

As the future IoT application cannot use WSNs that require batteries replacement in every few

years, it is puzzling why Nickel Cadmium battery is still selected in both [27] and [28]. It is possible that the design of the energy control algorithm of [27] and [28] is modified to use supercapacitor as energy storage device instead, so that their designs will be suitable to operate on a SPBL energy harvester. However, such modification will involve very different design consideration due to the significant difference of the charging and discharging characteristics of Nickel Cadmium battery and supercapacitor.

Due to these major differences, it is very difficult (if not impossible) to compare directly this research design's performance with those of [27] and [28], whether with software simulation or actual hardware implementation. It is because any meaningful comparison will involve extensive modification of either their design or the design of this research, and then with an additional effort to implement their design into the self designed WSN hardware platform in this research. In view of the practical difficulties and of the time and work scope limitation in this research, it is decided not to conduct the actual experimental comparison. Detailed analysis in the following paragraphs will provide in-depth information for the comparison.

[27] introduces the concept of 'Harvested Energy Utilization (HEU) efficiency' to represent the fraction of the harvested energy that can be effectively utilized by the system in the presence of battery energy storage inefficiencies. As SPBL energy harvester uses supercapacitor as energy storage which has over 95% energy storage efficiency [9], this design concept is irrelevant to the research in this thesis. Moreover, even in the context of using Nickel Cadmium rechargeable battery as energy storage device, its introduction and use of HEU efficiency does not help much in its energy algorithm design. The introduction of this special concept aims to present the idea that it is desirable to use the harvested energy as much as possible to deliver the maximized service duty cycle of the WSN, instead of storing the harvested energy into the battery. To validate this obvious idea, this paper uses mathematical formulae, lemmas and proofs to convert this simple concept into complicated mathematical representations which seems to be unnecessary. This paper refers to a research paper in year 1999 and concludes that supercapacitor suffers from high self discharge rate of more than 50% in a few days. This is obviously an obsolete assumption as modern supercapacitor only has very small leakage current in the order of single or double digits of Microampere [37].

As with [28], [27] requires the measurement of energy harvested and energy consumed in order to determine its control action in the next time slot. Further, on page 8 of this published research, it uses an Exponential Weighted Moving Average (EWMA) filter to calculate the value of $N_{sun}(h+1)$ (Number of sunlots in the next operating cycle). While the intention of its research is to provide a prediction free energy control algorithm, the use of EWMA is one form of prediction of future solar energy harvesting

based on past statistics. And it can still incur errors in its control action when its prediction deviates from reality.

The Section 5.2 Energy Budget Generation of [27] forms the most important section of the whole research paper. Section 5.2 of [27] proposes that when energy level of the battery falls below a certain level which is considered to be risky, a minimum service duty cycle should be used; and when the energy level of the battery is at a healthy level, the control algorithm should use all of the harvested energy to provide the maximized service duty. The risky battery level is determined by the energy gap E_r which depends on a subtle prediction of future solar irradiation in the form of the formulae to compute the value of $N_{sun}(h+1)$ (Number of sun lots in the next operating cycle). The final paragraph of section 5.2 completes its design proposal by including a Fail-Safe Energy reserved to account for some extreme weather conditions. It does not mention how large the Fail-Safe Energy should be but one can interpret that the bigger it is, the less chance that the energy harvester will shut down due to energy depletion of the battery.

It appears that section 3 and section 4 in this research paper convert common sense ideas into sophisticated mathematical formulae which do not provide the needed value to achieve the design objectives. On the other hand, the necessary mathematical handling and computation by Fuzzy Logic theories in [28] and by Model Predictive Control theories in this research provide important core values to the formation of the energy control algorithm.

It is also noted that [27] conducts a performance analysis and comparison with [24], with the use of software simulation. Despite [27] (in its section 6) admitting that [26] is the best research when they conduct their research, they do not compare their design with that of [26] stating that [26] does not consider battery energy storage inefficiencies. Instead, [27] selects to compare their design with that of [24]. This is in fact not a candidate for comparison due to its deficits in frequent dead time out from its use of a solar irradiation prediction model. The result of comparison as presented by [27] is that its design shows a better performance than [24] but this is to be expected. If its comparison target was [26], it would likely show a similar performance between [26] and [27]. It is also important to note that the performance analysis and evaluation by [27] uses a very strong solar irradiation simulation environment (10 hours of strong sunlight every day). This environment does not impose any challenge in testing the system's performance under bad weather condition. There is also no dead time analysis of its energy control algorithm which is the most critical problem that all related research strives to address.

Moreover, one can imagine that if the energy control algorithm of both [27] or [26] are subjected to a bad weather operating environment, a high level of system down time will bound to happen as either

its Fail Safe Energy reserve mechanism or its minimum service duty mechanism is not flexible enough to address large fluctuation of daily solar irradiation in bad weather condition.

The analysis of the most recent related research of [28], on the other hand, reflects that it corrects most of the pitfalls of the work of [27] and provides a practical solution to each addressed research problem. As mentioned previously, the research of [28] could only be identified in January 2018 after the design of the new energy control algorithm of this thesis was finished. Nonetheless, it is found that using totally different design approaches, both the design in [28] and the design in this thesis can provide a satisfactory solution to the addressed research problem.

The core strength of [28] is that it uses a tuning mechanism to address the inflexibilities of the design of [26] and [27] in coping with extremely bad and fluctuating weather condition. As with [26] which uses an established LQ maximization control theory to address the research problem, [28] uses an alternative but equally established Fuzzy Logic control theory which results in its much better execution of the common sense solution as compared with the work of [27]. The inclusion of the tuning parameter K and its tuning appears to be a fuzzy process which depends on actual field tests and experiments to create the best control result. While there are no strong theories to explain the precise tuning process, the proposed parameter K with its tuning mechanism nonetheless provides a practical and usable solution. The function of this tuning parameter K can be easily understood. The value of K serves to exponentially increase or decrease the service duty cycle of the WSN according to weather condition. Its function serves as a similar function of the prediction horizon in this research which is chosen based on the estimated worst-case scenario of how long that no solar energy will be harvested. The selection of a particular value of prediction horizon depends on designer's knowledge of the worst weather condition in a particular location which can be quite accurate. On the other hand, the tuning of the parameter K in [28] depends on numerous field tests and can be quite time consuming.

Nonetheless, both [28] and the research in this thesis are able to reduce system shut down to a bare minimum under fluctuating bad weather condition. As to the performance to achieve another major design objective to maximize the service duty cycle of the WSN, the design proposed in this thesis uses MPC theories to compute the maximized service duty cycle under a certain prediction horizon. As such, maximization of the service duty cycle is guaranteed. It is unknown whether [28] can achieve the same level of maximization as it is not elaborated in its paper. Only the implementation of the two different control algorithms in the same hardware platform, and with extensive field tests, can allow one to conduct a fair comparison. As explained in the beginning of this chapter, it is decided not to conduct this test due to the limitation of time and scope in this MASc research.

As a final remark to the detail analysis of the seven related research papers on energy control algorithm, it is found that the term ENO (Energy Neutral Operation) is used extensively as a foundation of the design concept. Such foundation may not necessarily be helpful to provide the best design solution. In many related research papers, it appears that the design objectives are distorted to achieve an ENO operation rather than to fulfill the original design objectives. While ENO is a fact of truth over a long period of time, the control objectives are to solve a continuous power supply problem in a much shorter time frame and amid unpredictable weather in days and in weeks. To solve this problem, the charging and discharging characteristics of the supercapacitor should be the core focus, rather than the ENO.

2.7 Conclusion

In this chapter, the related research papers in the past ten years on SPBL energy harvester for the powering of WSN are analyzed extensively. The analysis of the research on the major components in a SPBL energy harvester shows that research on MPPT, on DC-DC converter and on supercapacitor's modelling has matured with very good efficiency. Research on energy control algorithm remains to be the most relevant prospect in finding a way to achieve a continuous power supply operation while maximizing the service duty of its powered WSN. The review and analysis of seven most relevant research papers on energy control algorithm provides detail insights on the strength and weaknesses of their design. It is concluded that there is one research paper [28] that can provide a possible practical solution to the addressed research problem subjected to significant design modification to use supercapacitor instead of using Nickel Cadmium battery as energy storage device. The analysis of past related research work in this chapter serves as a useful reference for the research presented in this thesis.

CHAPTER 3 RESEARCH PROBLEM AND OBJECTIVE IDENTIFICATION

3.1 Importance of Problems Identification and Intuition of Solution

During the process of analyzing related research, it is realized that many related research works and papers may not have the research problems clearly identified and defined. Without clear identification of research problems, it risks leading to doubtful and unworkable solutions. In section 3.1, the importance of problem identification and subsequent intuition of solution is elaborated. In the following section 3.2, an example of past related research paper is selected as a lesson learned about the problem of unclear research problems and research objectives identification. After making these observations, the precise research problems and research objectives of this research are defined clearly in section 3.3 and section 3.4.

Many great scientific discoveries start with a sharp observation of a certain scenario, followed with a clear identification of the problem, then with a distinctive intuition of the possible solution. An iconic example is Albert Einstein's discovery of the General Theory of Relativity. He wrote of this process [29], which he called 'The happiest thought of my life':

> "Sitting in a chair in the patent office in Berne (in 1907), a sudden thought occurred to me. If a person falls freely he will not feel his own weight. ..... If the one who is falling drops other bodies, then these remain relative to him in his state of rest ..... ".

Einstein's thought that 'a person falling freely does not feel his own weight' seems rather obvious. Yet from this starting point, he exhausted every possible drop of insight, and removed all the inconsistencies of Newton's theory. By thinking intuitively about a man jumping off a roof in Berlin, Einstein was able to replace gravity by acceleration and discovered his principle of equivalence. That was what happened with the great discovery of the Theory of Relativity in the past century.

There is rarely anyone matching the talent and creativity of Albert Einstein, but we can all benefit from his lessons of observing a scenario out of pure curiosity, and sharply identifying and defining a problem with thoughts of possible intuitive solutions. It is worthy to note that, although Einstein must be totally thorough in understanding the Newtonian Theory of Gravity which was a main stream dominating theory at that time, he did not try to look for a solution from the Newtonian Theory. Instead, he adopted an 'Outside the box' way of thinking.

This brings in an important point and insight. Although it is necessary to review and analyze in depth many of the related research of a specific research topic during the research process, it is of vital importance that one can always think out of the box and has the courage and willingness to always raise questions of 'Why and Why Not?". A common scenario in research works is tapping similar spring mechanism for the 'improvement of unworkable mouse traps', while not being aware that the damages caused to some houses are not done by the mice. This common scenario reflects two problems. Firstly, if the 'unworkable mouse traps' spring mechanisms to kill the mice do not work, what is the use of continuing to suggest alternative ways to improve the spring mechanism? Secondly, if the damage in some houses are not caused by the mice, house damage problem will not be solved even when every fault in the unworkable mouse-trap is corrected.

It is of critical importance for any research work to start with the correct identification and the precise definition of a problem, followed with an intuitive thinking of possible solutions. Although this important starting point is emphasised in many literatures, it is often neglected as evidenced in many related research papers read during our research period. On the other hand, this important point is easily said than done. In one of the MPC (Model Predictive Control) video lectures by Dr. J.A. Rossiter (Reader, University of Sheffield, U.K.) [31], he says this right in the beginning, "If you do not understand the topics thorough enough, do not start to do any design as you will for sure arrive at a totally incorrect result". Therefore, the ability to correctly identify and define a problem has to come from a thorough understanding of the relevant principles and theories behind, together with a broad common knowledge in many related subjects.

3.2 Addressing Problems and Objectives Identification

In section 2.6, five related research papers with core research focus similar to this research are analyzed. It is mentioned that most of the five research papers (though [26] is close to providing a practical solution) are not able to deliver a practical solution to the relevant problem.

With more detailed analysis, it is found that the possible reason behind the failure may be stemmed from identifying wrongly or vaguely the research problems or the research objectives. An example of this problem is provided in the following paragraphs.

In paper [22], the major weakness is its use of a solar energy irradiation prediction model which will fail when weather fluctuates with many days of rainfall. The lack of solar harvesting makes the energy stored in the SPBL harvester totally depleted and the SPBL harvester become inoperable. The root of this failure may be vaguely identified research problems, leading to vaguely defined research objectives.

What is the major problem that the research [22] aims to solve? The closest problem statement can be seen in its section 1.1 Motivation, where it says, “The presence of a limited environmental power source changes the focus of the monitoring device from minimizing energy consumption and maximizing device longevity, to optimizing performance and allocating resources.”.

As the problem statement is vaguely defined, defining the major objectives or intended solution would be difficult, as seen in its section 2.1, “The objective of this thesis is to investigate and address some of the challenges present in remote environmental monitoring systems. The two main difficulties considered are energy scarcity and limited access. The intent is to show that energy management and appropriate system design can guarantee a high level of performance between the extended maintenance periods of the device. This facilitates the ultimate goal of environmental monitoring: the collection of high quality data.”. As both research problems and research objectives are vaguely defined in this case, it appears that a vague solution will be resulted, as reflected in its conclusion section 8.1 which says, “A good energy management strategy will ensure the monitor’s resources are invested in a way that collects high quality data.”.

A further review into its simulation chapter shows that an improvement of percent data points lost from 31.4% to 19.3% when the Fuzzy Logic Controller is used. However, on the other hand, average duty cycle is reduced from 68.6% to 57.8% which is an undesirable side effect, probably due to the extra energy consumed by the controller. As these two results go against each other, one will have difficulty to convince the true improvement made by the controller. Besides the negative effect of the reduction of average power duty cycle, a 19.3% data points lost after a controller (in this case, the Fuzzy Logic Controller) is used can hardly be interpreted as a successful energy control solution.

There is a strong possibility that a better solution could be derived should the research problems and research objectives of the research in [22] be more precisely defined.

3.3 Research Problem Identification

The lessons learnt have been summarised in the previous section. This section presents the precise research problem identification of the research in this thesis.

The research problem in this MASc research is to address the energy control problem in SPBL energy harvester powering wireless sensor node which suffers from two major operation difficulties in the following priorities:

1. Unsustainable operation of the energy harvester due to stored energy depletion during periods of unpredictable and low level of solar energy harvesting. Once stored energy is depleted, the energy harvester fails to supply power to the wireless sensor node and that will make it inoperable. This problem is defined with a parameter called the Time Dead % (T_d *%*), which is the percentage of time when the wireless sensor node ceases to operate as compared to the total time elapsed.
2. Solar power harvested from the energy harvester is not used optimally to provide the best quality of service as supposed to the wireless sensor nodes. Providing the best quality of service by the wireless sensor node means providing the maximum operation (sensing and data transmission by wireless communication) duty cycle. Maximum operation here means the maximum service duty permitted, subjected to a constraint to allow this selected rate of operation to sustain for a certain selected period of zero solar energy harvesting. We define this problem as a non-optimization of a parameter called Duty Cycle of Service % *(Ds%*). *Ds%* is defined as the percentage of time when the wireless sensor nodes' sensor and wireless antenna are turned on as compared to the total time elapsed.

It is elaborated in Chapter 1 that because of the above two major problems, SPBL harvesters are not used in powering WSNs, despite the common consensus that they are much better power supply than batteries. Instead, majority of commercial wireless sensor nodes manufacturers are still using long life button cell types or other types of non-rechargeable batteries (need to be replaced in every 2-5 years) as the source of power.

It is also elaborated in Chapter 2 that technology research of the other elements in the SPBL energy harvesters are very mature with problems satisfactorily solved. The two difficulties, energy control problem 1 and problem 2, as identified above now remain the outstanding and the most pressing technologies problems prohibiting the practical use of SPBL energy harvesters.

They are now defined as the research problems in a clear and precise manner.

3.4 Research Objectives Definition

With research problems precisely defined, it is ready to define the precise research objectives for the new design of the energy control algorithm, with the following priorities:

1. To reduce to minimal, and if possible, to totally eliminate the *Time Dead %* as defined in the last section.
2. To maximize the Duty Cycle of Service % (*Ds%*) of the wireless sensor nodes as defined in the last section.

Once these research objectives are precisely defined, it is very important not to divert or to shift away from them. In fact, the degree that this research will accomplish the two research objectives as defined above is an determining factor to evaluate the research result and contribution.

3.5 Conclusion

In this chapter, the importance of research problems identification and precise definition of research objectives is discussed. An example in a related research paper is borrowed as learning experience that failures to define research problems and research objectives precisely will adversely affect the research results and contributions.

Intuition in seeking a solution for a research problem is essential. While it is important to learn and to obtain references from related research, researcher's creativity and the abilities to 'think out of a box' are extremely crucial in solving research problems. Built upon these elaborated realizations, the research problems and objectives are now clearly defined. Hopefully, the elaborations on how this research is positioned and conducted may be useful as a reference to other research.

CHAPTER 4 POSSIBLE SOLUTION

As discussed in section 3.1, intuition in seeking a solution for the research problems is one of the guideposts in this research, in addition to extensive research and intensive computation. To solve the research problems as defined in the previous chapter, it is prepared that intuition may play an important role in seeking a possible solution. Adapting a thinking 'out of the box' approach by Albert Einstein as mentioned in previous section 3.1, a question is raised on why a concept of Energy Neutral Operation (ENO) is emphasized so heavily by previous research papers.

4.1 Irrelevance of Energy Neutral Operation (ENO)

The first research objective priority is to enable a sustained operation of the energy harvester with the use of its stored energy in the supercapacitor. The natural tendency is to focus on the discharge characteristics of the supercapacitor. That is, the focus is on the duration of discharge from the maximum operating voltage of the wireless sensor node to its minimum operating voltage. Such duration serves as the sustained operating time for the wireless sensor node when there is no incoming solar energy harvested.

In fact, the problem of unsustainable operation of the energy harvester does not exist when solar energy is being harvested. Naturally, the solar energy harvested will be used optimally (or maximally) to provide the maximum *Ds %* to the wireless sensor node. The problem of unsustainable operation starts to exist when there is no solar energy harvested, resulting in the beginning of the energy discharge from the supercapacitor.

In the period when ENO (Energy Neutral Operation, i.e. when solar energy harvested equals to energy being consumed) succeeds, it is entirely not a concern to us. But in the period when ENO fails (when solar energy harvested is less than energy being consumed, resulting in discharge of supercapacitor), it is something that one needs to accept and to mitigate. However, as presented in many other related research papers, researchers try to aim at achieving ENO at all time. There may have an unexpected and undesirable effect of diverting their attention to solve something unsolvable. In fact, the effort spent on solving the unsolvable problem does not benefit in solving the real research problem. On

the contrary, it creates an undue and unnecessary constraint which becomes a big barrier in addressing the defined research objectives. It is because no matter how hard one tries, the energy harvester has to operate under a non-ENO situation at a significant portion of time. In fact, energy neutral will exist, as energy consumed can never be more than energy harvested over a long spectrum. However, when the addressed problem is to sustain the energy harvester in a much shorter time frame of days or even weeks, when no solar energy is harvested, achieving ENO is not possible in such a time domain.

Hence, ENO has not been a relevant perspective in the process of seeking a solution in this research. Only during the analysis of other relevant research papers, it is realised that ENO was put into such a prominent position.

4.2 Importance of Predictive Control

From the beginning of this research, the intuition has always been focused on how to sustain the operation of the energy harvester while aiming to maximize the service duty cycle % (*Ds%*) during the supercapacitor's discharge period from the maximum to the minimum wireless sensor node operating voltage.

Once this thinking direction is determined, the next question to answer is that how long would one expects this workable discharge period to last. Naturally, with the stored energy in the supercapacitor being fixed, the longer one expects the discharge period to last, the smaller amount of the power one is to draw from the supercapacitor (i.e. to decrease *Ds%*).

This thinking process further leads to the realization that the problem actually relates to what one has to do at a present state in order to arrive at a predicted future. More precisely, if the DC operating voltage of the DC-DC converter in the solar energy harvester is from 4.1 V to 2.5V, what is the average *Ds %* that one should used for the discharge period to last for a certain time period (say, *T*)?

At this point, it is realized that the maximized *Ds %* that one can use for a sustained discharge period of *T* relates precisely to the discharge characteristics of the supercapacitor. And it is also realized that the discharge characteristics of the supercapacitor is totally well defined by many past successful research on the workable mathematical models for supercapacitors (noticeably, the two branch equivalent circuit model for supercapacitor).

After some more in-depth thinking, an intuition solution is arrived for the research problem as below:

1. From 4.1 V to discharge to 2.5V, the discharge period is divided into individual time zone, each time zone differs from the other by the discharge time of 0.1 V. That is, discharge process starts from 4.1V to 4.0V, then from 4.1V to 3.9V, etc.

2. At any point during the operable discharge period (i.e. at 4.1V, 4.0V, ... up to minimum voltage point at 2.5V), the period of discharge from this point to the lowest operable voltage (i.e. 2.5V) is expected to last for a period of T (say for example, 22 hours) if the supercapacitor is discharged using a particular service duty cycle % (say $D_{sx)}$.

3. The closer the discharge point goes towards the minimum voltage 2.5V, the smaller the D_{sx} will be. One would expect that D_{sx} at 2.6 V to be much smaller than that at 4.1V.

4. The parameters of D_s (i.e. D_{s1}, D_{s2}, D_{s3}, ... D_{s15}) can be found out from the open-loop discharge curve of the supercapacitor using a discharge period of T (say, 22 hours), with a graphical trial and error method or by using software simulation tool.

5. The use of D_{sx} in the energy control algorithm at a particular discharge point will allow the energy harvester to continue operating for a period of T (say, 22 hours) even at the lowest point of operable voltage discharge (i.e. at 2.6V).

6. The determination of the exact value of the period T (22 hours? 70 hours? 100 hours?) will depend on an estimation of the worst-case scenario of how long the period of zero energy harvesting will last.

7. One may wonder, as solar energy will be harvested at anytime during the supercapacitor's discharge period, whether one has to monitor at real time the input harvested energy as an input disturbance. Apparently, that is what many related research do especially when they use a solar irradiation prediction model. This is determined to be unnecessary in this research. As without monitoring the energy harvested in real time, the design of the energy control algorithm will be more effective and simpler. It is decided that monitoring the terminal voltage of the supercapacitor in real time is sufficient as the terminal voltage level of the supercapacitor already intrinsically reflects accurately the accumulative solar energy harvesting level in the past. The more solar energy is harvested in a certain day, the longer the terminal voltage point of the supercapacitor will stay at a highly or fully charged voltage level (i.e. close to 4.1 V in our SPBL energy harvester's design). The longer the voltage point stays closer to 4.1V, the higher the value of D_s % will be allowed to be used.

At this point, it is determined that the above design direction would be able to deliver an effective and satisfactory solution, although working out D_{sx} with the use of software simulation tool will still be

very time consuming.

Further study and research of related information indicate that this design direction is actually related to a well-defined topic of control theory called Model Predictive Control (MPC). The theory has gained increasing popularity and importance in the last 15 years. The intuition of the 'Moving On Period' of *T* when voltage is discharged from 4.1 V to 2.5V, with each voltage point separated by 0.1V is actually the concept of 'Receding Horizon' which is a major distinctive characteristics of MPC Theory. This concept of 'Receding Horizon' is vital for solving this research problem, as it is difficult if not impossible for other types of control algorithm such as PID, Fuzzy Logic, and Linear Quadratic Regulator to accomplish.

Details of the MPC Theory will be elaborated in the next chapter.

4.3 Two Branch Model for a Supercapacitor

There has always been a question why a two-branch electrical equivalent model is used for supercapacitors (which are double layers capacitors) modelling while the simpler single branch (that is, single time constant) equivalent model is used for ordinary capacitors (single layer capacitors).

After thorough research on supercapacitor modelling comparison, parameters identification, and experimental testing, a detailed comparison between the single branch equivalent model and the two-branch equivalent model for a targeted sample supercapacitor was performed. This detail separate research with testing results found which took 3 months to accomplish, were outside the scope of this thesis. However, this parallel research was done to reinforce the appropriateness of using two branch equivalent model for supercapacitors. A brief elaboration of findings is provided in the following paragraphs.

Once all the parameters of the two models (single branch and two branch) are identified, two 'Matlab' /'Simulink' models are separately built for the two models for their simulation comparison. At the same time, experimental testing using a sample 'ELNA' 5.5V, 1 Farad supercapacitor is performed. Actual experimental results of the charging and discharging performance of the sample supercapacitor are compared in detail with the simulation results using the two different equivalent models.

The research result shows that the precise two branch model demonstrates an almost identical charging and discharging performance as the real supercapacitor. It also shows that the single branch model has serious deviation, that is, big inaccuracies, from the real supercapacitor charging and

discharging performance. This validates the prior conclusion that a precise two branch equivalent model is needed for the supercapacitor modelling instead of the simpler single branch equivalent model. The latter, if used, will result in inaccurate and unacceptable energy control performance of the supercapacitor.

The graph below summarises the comparison of charging and discharging test results. During the whole process of charging up the sample supercapacitor with a constant source of 7.5 mA, the constant current source is removed, with the supercapacitor's terminal voltage settled at a stable voltage, then a constant current load of -5 mA is connected, until its terminal voltage is discharged to 3 volts.

The graph shows clearly that the Two Branch model demonstrates an almost undetectable or negligible deviation from the real test data performance of the supercapacitor. On the other hand, a huge deviation of discharging performance of One Branch Model from real testing data is found.

Real test discharging time of the Two Branch Model = 26.8' – 24' = 2.8' = 168 seconds

Discharging time of 1-Branch Model = 28.3' – 24' = 4.3' = 258 seconds

Discharging time deviation error % of the 1-Branch Model = [(258 – 168) /168] * 100% = 54%

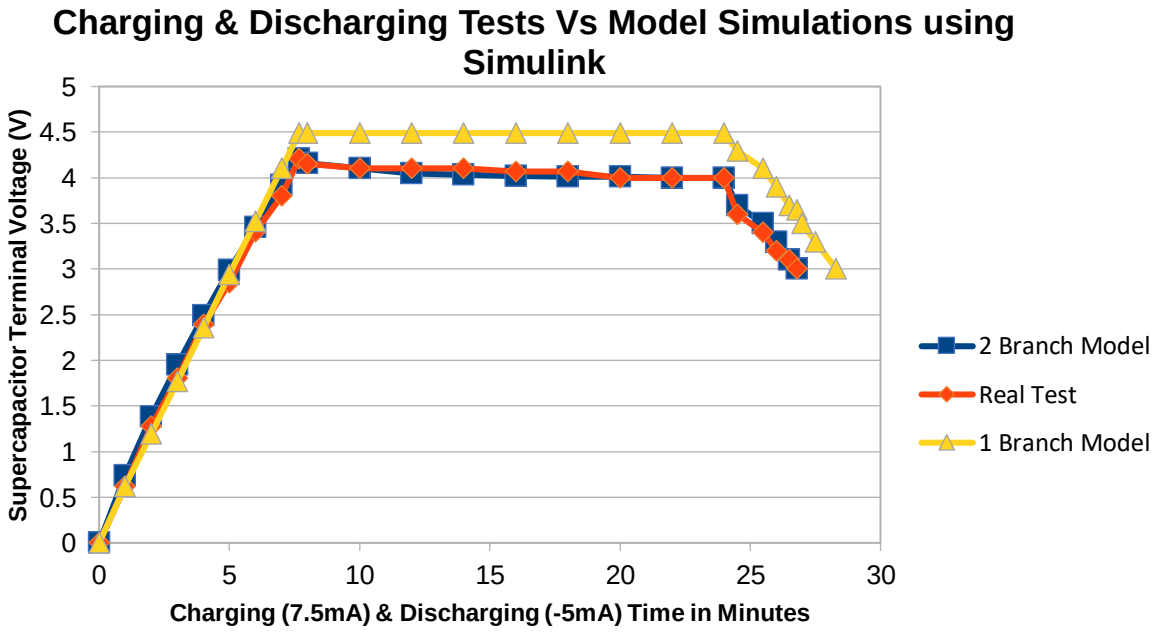

Figure 4-1 Charging and discharging performance comparison among 2 Branch Model, 1 Branch Model and a real Supercapacitor

In the past few years, there has been significant advancement in supercapacitor's technologies and manufacturing development. Nowadays, the leakage current of a supercapacitor has been reduced from the magnitude of a few mini Ampere to a few micro Ampere which is an improvement of 1,000 times. At the same time, the series resistance of the supercapacitor which directly determines how fast an supercapacitor can be charged up has been reduced from a few hundred ohms to the tested data of the sample supercapacitor of only 4 ohm (series resistance R_1 as seen in FIGURE 5-2, with supercapacitor two branch model differential equations 5.9 and 5.10 shown in section 5.2). These advancements in supercapacitor have no doubt further established it as an ideal storage device to power the new generation of wireless sensor nodes in the upcoming new age of Internet of Things.

Although the core of this research work is not intended to drill into intensive supercapacitor modelling, the research work in this part of supercapacitor modelling research helps to reinforce the confidence and knowledge in deploying an accurate Two Branch model for the supercapacitor. The Two Branch model has its distinctive characteristics and is an integral element in the design of the new generation of wireless sensor nodes.

4.4 Mitigating WSN Sleep Mode and Supercapacitor Leakage Current

The impact of the sleep mode current of the wireless sensor node and the impact of the leakage current of the supercapacitor are both uncontrollable, yet either of them can be eliminated. As the system is operating, they will be present. However, these uncontrollable currents determine the voltage range of operation of the supercapacitor.

The design of the energy control algorithm incorporates the realization of the issue. The minimum operable terminal voltage of the supercapacitor, the total voltage discharge due to sleep mode current, as well as the total voltage discharge due to leakage current are specifically identified and mitigated in the design. The need to reserve certain energy to sustain the sleep mode operation of the embedded system under the continuous effect of leakage current for the desirable operation time is addressed.

Therefore, if the energy control algorithm works properly, the voltage discharge would never be discharged down below the minimum operable terminal voltage.

4.5 Conclusion

By intuitive thinking, vigorous research and validation, as well as intensive modelling and computation, it is preliminary concluded that in order to develop possible solutions, there are four core concepts to be followed as guideposts.

Firstly, Energy Neutral Operation should not be treated as a constraint in finding a workable solution to the research problem. Secondly, Model Predictive Control is instrumental to the sustained successful operation of the energy harvester while maximizing the service duty cycle. Thirdly, only the two branch model is suitable for the deployment of a supercapacitor to reflect its distinctive characteristics. Fourthly, the impact of sleep mode current of the wireless sensor node and the impact of leakage current of the supercapacitor need to be separately addressed and mitigated.

Based on these core concepts, it is confident that a workable solution will be successfully developed.

CHAPTER 5 MODEL PREDICTIVE CONTROL THEORIES AND PLANT MODELLING

In the previous chapter, a preliminary solution for the research problem is identified. The core of the solution depends on how the magnitude of certain inputs can be computed to achieve certain desirable outputs after a determined period. It is possible to obtain these certain inputs by tedious trial and errors experiments. A better way to obtain these inputs is by utilizing modern software simulation tools. After careful search and evaluation, it shows that Model Predictive Control (MPC) theories allow one to compute precisely the values of the desirable inputs.

Most importantly, MPC theories use linear quadratic optimization method to compute the desirable inputs, and result in an optimized (maximized or minimized depending on the particular application) solution with singularity. It means that for a particular optimization task in a defined time frame (as is called 'Prediction Horizon' in MPC theories), MPC theories and their computation provide the only optimized solution. This implication of singularity in its solution contrasts with the solution in many related research papers analyzed. These research papers tend to imply that there can be numerous different solutions to this single research problem. Due to the observation of the solution singularity in this research problem and the fact that MPC theories have very mature tools available, it is highly likely that anyone who want to solve the same research problem optimally will have to employ MPC tools in some form to derive their solution.

However, as elaborated in the next chapter, using MPC theories alone is not sufficient to provide the solution to our research problem. There are certain supplementary design principles that one needs to apply for each individual design problem. In this chapter, MPC theories as well as the plant modelling are introduced to partially solve the research problem. The solution of the remainder of the research problem will be provided by three unique design principles as presented in Chapter 6.

5.1 Model Predictive Control (MPC) Theories

References are made to [30], [32], [33] & [34] for MPC control theories. In particular, [32] provides the background theories for our MPC algorithm.

[32] mentions that the only advanced control methodology with a major impact on industrial control engineering is Model Predictive Control. There are three major distinctive characteristics with this methodology: (1) handling multivariable control variables problems naturally; (2) allowing operation closer to constraints and actuator limitations; and (3) 'receding horizon' idea with relatively low control update rates.

FIGURE 5-1 below shows the basic idea of Model Predictive Control [42] :-

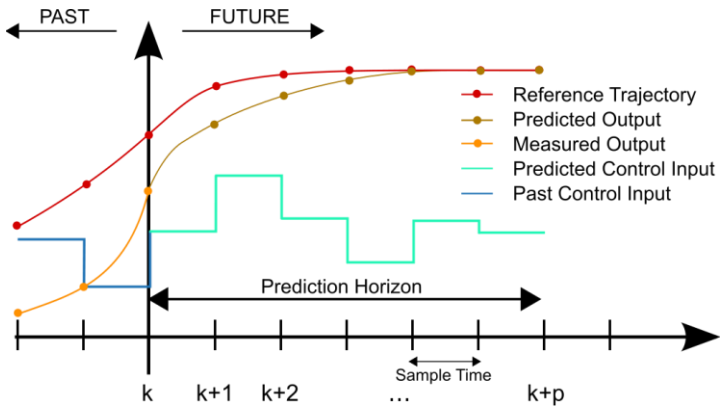

Figure 5-1 Basic idea of Model Predictive Control [42]

To enable predicted output(s) to follow a reference endpoint result or a reference trajectory at the end of a desired period (called prediction horizon), predicted control input(s) is computed using MPC control algorithm with allowance for different system's constraints. Once a future input trajectory has been chosen, only the first element of that trajectory is applied as the input signal to the plant. The whole cycle of output measurement and input trajectory determination is repeated, one sampling interval later, with a new output measurement being obtained. Since the prediction interval remains of the same length as before, but slides along by one sampling interval at each step, this way of controlling a plant is often called a receding horizon strategy.

In generalized form, suppose that the 'plant' being controlled has an input vector u and a state

vector x, and has nonlinear behaviour governed by the vector differential equation $dx/dt = f(x, u)$, and suppose that the control objective is to minimize a 'cost function' which has the form

$$V(\boldsymbol{x}, \boldsymbol{u}, t) = \int_0^T l(\boldsymbol{x(t)}, \boldsymbol{u(t)}, t)\, dt + F(x(T)) \tag{5.1}$$

where $l(x(t), u(t), t)$ is some function which is never negative, and that the control input is constrained to be in some set $u(t) \in U$.

The difficulty of the general optimal control problem arises because it is a function optimization problem. Instead of ordinary calculus, it needs the Calculus of Variations to find the optimal input function among all possible ones. The main idea of Model Predictive Control is to avoid this difficulty by restricting the set of possible inputs to such as extent that the optimization is performed only over a finite set of parameters or 'decision variables', rather than over a set of functions. Most commonly this is done by cutting up some time into discrete intervals, optimizing over a finite horizon, and hence over a finite number of intervals, and assuming that the input signal is held constant during each interval, or even over several intervals. The future values of the input signal are then the decision variables

Using a linearized, discrete-time, state space model of the plant, in the form

$$\boldsymbol{x}(k+1) = A\boldsymbol{x}(k) + B\boldsymbol{u}(k) \tag{5.2}$$

$$\boldsymbol{y}(k) = C_y \boldsymbol{x}(k) \tag{5.3}$$

$$\boldsymbol{z}(k) = C_z \boldsymbol{x}(k) + D_z \boldsymbol{u}(k) \tag{5.4}$$

where x is an n-dimensional state vector, u is an l-dimensional input vector, y is an m_y dimensional vector of measured outputs, and z is an m_z dimensional vector of outputs which are to be controlled, either to particular set-points, or to satisfy some constraints, or both.

Then with the mathematical manipulation to solve $x(k+1)$ at a certain linearized point using numerical iteration computation techniques, the following states prediction is derived with notation used in [32] :

$$\boldsymbol{x}_{\rightarrow k+1} = [A\ A^2 \ldots\ldots A^n]^T \boldsymbol{x}_k + H_x [\boldsymbol{u}_{k|k}\ \boldsymbol{u}_{k+1|k} \ldots\ldots\ \boldsymbol{u}_{k+n-1}]^T \tag{5.5}$$

where *Hx* is an n x n matrix with matrix elements of *A* & *B* multiples

$$\boldsymbol{x}_{\rightarrow k+1} = P_x \boldsymbol{x}_k + H_x \boldsymbol{u}_{\rightarrow k} \tag{5.6}$$

where the first component $P_x x_k$ depends on the past, and the second component $H_x u_{\rightarrow k}$ depends upon decision input variables,

And output prediction as:

$$\boldsymbol{y}_{\rightarrow k+1} = [CA \;\; CA^2 ..... \; CA^n]^T \boldsymbol{x}_k + H[\boldsymbol{u}_{k|k} \; \boldsymbol{u}_{k+1|k} ..... \; \boldsymbol{u}_{k+n-1}]^T \tag{5.7}$$

$$\boldsymbol{y}_{\rightarrow k+1} = P \boldsymbol{x}_k + H \boldsymbol{u}_{\rightarrow k} \tag{5.8}$$

where *H* is a n x n matrix with matrix elements of *C, A and B* multiples

The above formulae computation and algorithm coding implementation is a well defined but tedious task. Fortunately, popular mathematical computation and simulation software tools such as 'Matlab' are available to simplify the process. Although 'Matlab' does not provide a detailed elaboration of the principles and theories behind its 'MPC' tool box, [35] provides a detailed theoretical analysis on the software that may be used in this context. 'Matlab' also has a 'Coder' tool box which converts its 'MPC' algorithm to C codes, to be transported for programming into selected embedded hardware systems.

5.2 SPBL Energy Harvester State Space Model

All Model Predictive Control Theories documents including [30], [32], [33] & [34] highlight the importance of a precise mathematical model of the plant so that a desired accurate feedback control can be achieved. There are other fast rate feedback control algorithms, such as PID controller, which can tolerate an imprecise plant model by fast rate close loop feedback corrections. In contrast, Model Predictive Control mostly applies to low rate feedback applications with heavy numerical computation which depends on a precise plant model. An inaccurate plant model will lead to an inaccurate future state projection. Its low rate feedback nature cannot correct accumulative sample computation errors.

In this research thesis, the plant to be controlled is a solar energy harvester with a supercapacitor as the storage element. The focus is to fully utilize the energy stored in the supercapacitor to achieve a

sustained operation of a wireless sensor node. The plant is the supercapacitor with a single input (solar electricity harvested as measured in current) and a single output (electricity for the wireless sensor node embedded system, also measured in current).

Research and analysis of the most suitable supercapacitor mathematical model is found in documents [17], [18], [19], [20] & [21] and in particularly [19] and [21]. The simplified two branch model first proposed by [19] in 2007 is the most practical and accurate model. In order to validate and justify the necessity of using the two branch model instead of using a simpler single branch model (one that is used for ordinary single layer capacitor), separate research on supercapacitors' modelling with detailed experiments was conducted in Fall, 2017. As briefly explained in section 4.3, the Fall 2017 research data shows a 50% overestimation of supercapacitor's discharge time if a single branch model is wrongly used. The separate supercapacitor's modelling research is outside the scope of this MASc research and therefore will not be discussed in detail in this research thesis.

FIGURE 5-2 below is a simplified circuit model of a solar energy harvester with energy storage in a supercapacitor.

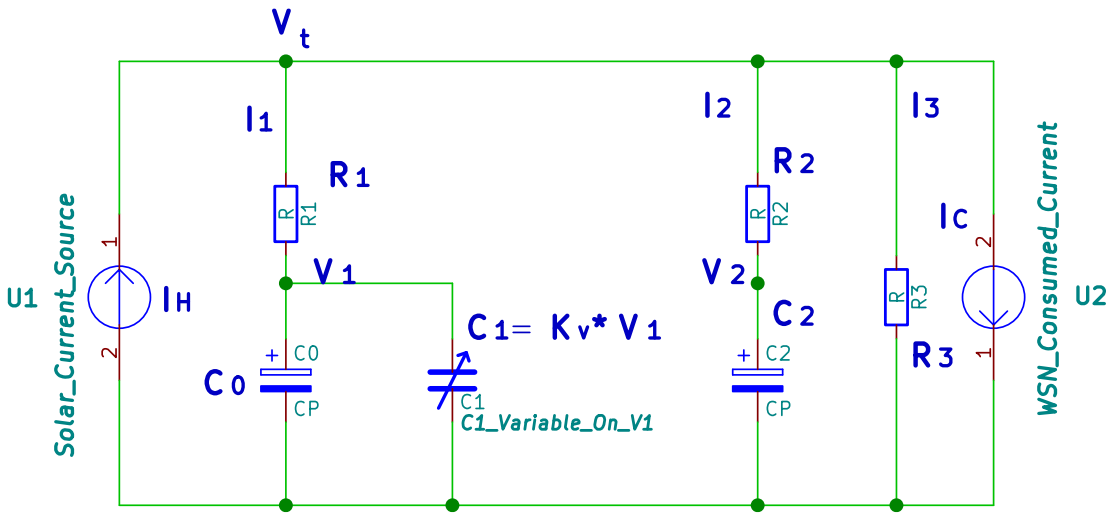

Figure 5-2 Simplified circuit model of a Solar Energy Harvester with Energy Storage in a Supercapacitor

I_H : electricity current harvested by a miniature solar panel

I_C : current used to supply the wireless sensor node

R_1: first branch series resistance

C_o: main storage capacitance in the first branch circuit

K_V: variable factor to determine a variable capacitance in the first branch circuit

R_2: second branch series resistance

C_2: second branch capacitance

R_3: parallel resistance of the supercapacitor

Apart from I_H, which represents the electricity current harvested by a miniature solar panel, and I_C which represents the current used to supply the wireless sensor node embedded system, the above circuit diagram represents an equivalent electrical two branch model of a supercapacitor as proposed by [19]. Due to the double layer structure of the supercapacitor, its characteristics are significantly different from that of an ordinary single layer capacitor. The capacitance of the first branch, which is responsible for the main energy storage, is composed of a constant term (C_0) and a variable term proportional to the voltage of the C_0 terminal (K_V*V_1). The second branch of R_2 & C_2 represents the voltage redistribution phenomena inside the device according to medium and long-term effect.

Circuit mathematical handling of the two branches model derives two differential equations for the state space representation formulation of the SPBL energy harvester:

$$\frac{dV_1}{dt} = \frac{V_t - V_1}{R_1 C_0 + R_1 K_v V_1} \tag{5.9}$$

$$\frac{dV_2}{dt} = \frac{V_t - V_2}{C_2 R_2} \tag{5.10}$$

In this research, after a supercapacitor bank with capacitance of 20 Farad is selected for our self designed wireless sensor node embedded system (as will be explained in the next section), a series of charging and discharging tests are conducted to determine all the supercapacitor's equivalent two branch model parameters (C_0, C_1, C_2, R_1, R_2 & R_3) so that the four matrices *A*, *B*, *C* and *D* of the supercapacitor's state space model can be computed (detail of their computations is provided in section 6.1.2).

The supercapacitor bank's equivalent two branch model parameters identification is presented in section 5.3 of this chapter. The computation of the four matrices in the supercapacitor bank's state space model is presented in subsection 6.1.2 in the next chapter.

5.3 State Space Model Parameters Identification

Following mainly the recommendation of [19] as well as the '6-steps process' for supercapacitor's two branch model parameters identification as suggested by [36], model parameters for the 5V, 20F supercapacitor bank are identified as: R_1 = 0.115 ohm, R_3 = 0.118 Mohm, C_0 = 18.883 F, K_V = 1.905 F/V, C_2 = 0.335 F, R_2 = 716.439 ohm. For the understanding of the accuracy of the values of identified parameters, a section of data error analysis is provided in section 7.2.

To mitigate a potential problem of the shift in values of these parameters over the lifetime of the supercapacitor, specification of the datasheet of the supercapacitor used in this research ('AXA' model 1647 – 5V, 5F) is studied for the impact [37]. It is specified in the datasheet that the lifetime of the supercapacitor will only be impacted negatively when either the operating temperature is over 40 degree Celsius or the input voltage is over 70% of its rated value (5V * 0.7 = 3.5 V). As the WSN is targeted to be used in a greenhouse automation application, it is unlikely that operating temperature will be over 40 degree Celsius and the average charging voltage of the supercapacitor in a daily cycle (day and night) will also be under 3.5 V (charging voltage at night will be reduced to almost zero at night). The datasheet

also states that the *MTTF* (Mean Time To Failure, commonly refer to as the lifetime) is 80 years. At the end of its lifetime, capacitance value of the supercapacitor will be degraded by 30%, and its series resistance value will be increased by 2 times. There is no information presented in the datasheet as to the change of these parameters at the mid point of its lifetime, i.e., at about 40 years. Although it appears that the change of values of these parameters at its half lifetime point (after 40 years of operation) will be minimum, further study and research needs to be done to find out its precise impact.

It is vital to identify the supercapacitor bank's model parameters and the subsequent computation of its state space model matrices are vital, as MPC algorithm can only work with a precisely defined plant model. If the model parameters are identified inaccurately, the MPC algorithm will compute an inaccurate output which leads to inaccurate control action. Inaccurate control action in this case will cause the supercapacitor's discharge time deviating from the original expectation. In this research, the model parameters identification is very time consuming and it even involves design of a testing instrument to accomplish the unique task. Fortunately, for potential commercial product development, model parameters identification needs to be done just one time for every supercapacitor model used.

As the precise two branch equivalent model parameters identification constitutes an important part of our research, the following subsections are devoted to elaborating the whole process.

5.3.1 Instruments used in model parameter identification

Two important pieces of testing Equipment are used in the model parameters identification process. They are a precision constant current source and a precision constant current drain (load), as shown in the two photos as shown below.

Figure 5-3 Constant source equipment used - 'Fluke' Model 341A Voltage Calibrator

Figure 5-4 Current sink equipment used - LM358 Op-Amp Controlled IRL530N MOSFET Circuit

These two pieces of important testing equipment, as shown in the above photos, are used for the charging and discharging tests during the parameter identification process of the two branch equivalent model. The first equipment is an accurate current source which can supply a constant current down to a small magnitude of μA. For the precision constant current source, a Fluke Model 341A Voltage Calibrator, which has a current limiting function down to μA, serves the requirement. The second equipment is an accurate current load (sink) that can draw a constant controlled current down to a small magnitude of μA. For the precision current sink, as there is no suitable equipment available for the testing, there is a need to make a choice between buying a new equipment and building an equipment for this research. A decision is made to build one which employs a simple but practical circuit using a LM358 operating amplifier integrated circuit to control a precise current down to a small magnitude of μA flowing through a IRL530N MOSFET power transistor. Both instruments prove to work flawlessly.

'Maxwell' testing guidelines [36] states the requirement to use a Bitrode Test System or any other test system which can be used to charge and discharge supercapacitors with test cycle programming and data acquisition capabilities. Using a Bitrode Test System may be more convenient and efficient. However, it is an expensive piece of equipment. In turn, the two pieces of equipment that we use prove to do a good job in this context.

5.3.2 Two branch model parameters identification experiments

The testing procedures of this research follow closely the testing methodology proposed by the work of [19]. As mentioned in the previous chapter, the work of [19] is original and novel and serves to provide a great tool for other research including this one.

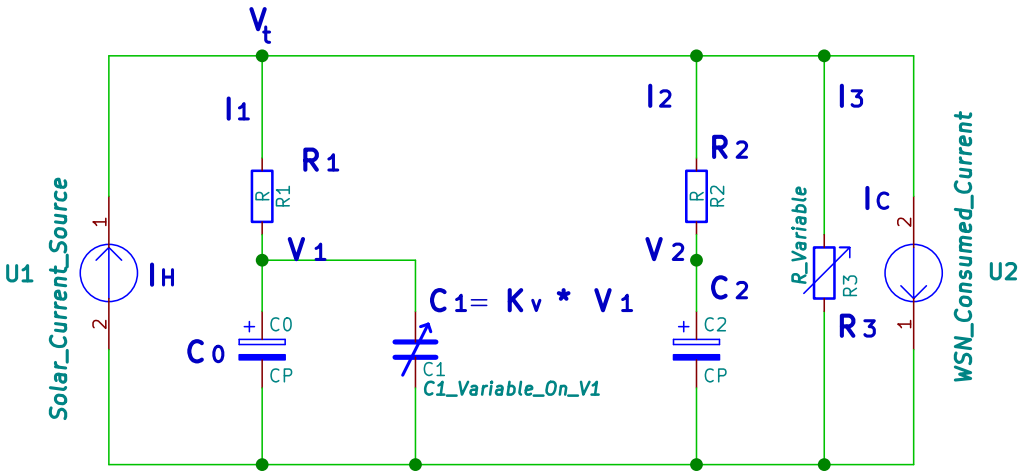

Figure 5-5 Supercapacitor Two Branch Model with Variable Leakage Resistance

The above diagram shows a typical supercapacitor two branch equivalent model with a variable leakage resistance as proposed in the work of [20]. In the original work of [19], the leakage resistance R_3 is taken as a constant value. Whether the leakage resistance can be taken as fixed or variable depends heavily on its magnitude. The larger the magnitude, the smaller its non-linear characteristics will impact the overall self discharge characteristics of the supercapacitor. As will be presented later in this section for the identification of R_3, it is found to be of a very big magnitude of 0.118 Mohm. As such, it is decided to use the two branch model with a fix R_3 as proposed by [19] rather than the two branch model with a variable R_3 as proposed by [20]. This assumption later proves to be reasonable as validated by later experiments because it does not affect the accuracy of the two branch model used.

Two Branch Equivalent Model Parameters Identification Method [19] is presented below:

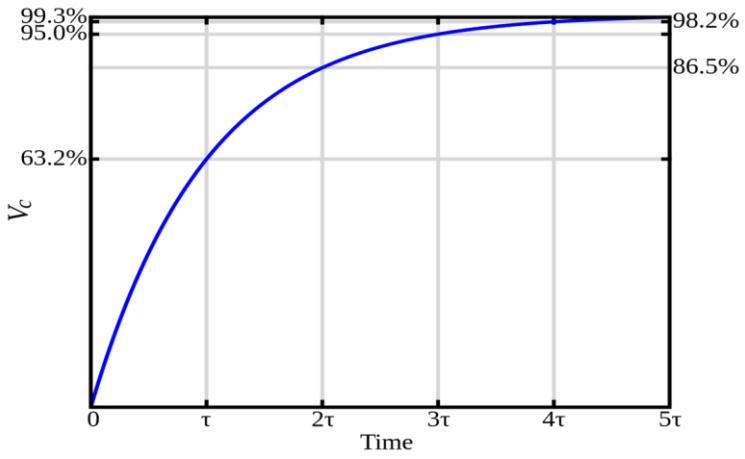

Figure 5-6 Two Points (P1 and P2) Charging Method to determine Two Branch Model parameters [44]

Assume first that the capacitance of the first branch, which is the main storage, is composed of a constant term (C_o) and a variable term proportional to with the voltage at the DLC terminals ($k_v \cdot V$). The merit of this hypothesis has already been verified in many past research. Instead, the second branch represents the voltage redistribution characteristics inside the device according to medium and long term. From the structural point of view, the equivalent circuit should be similar to others that have already been analyzed in other literatures. However, in contrast to these literatures, [19] introduces a new identification procedure.

As in many other cases, this is based on the analysis of the results obtained from charging the supercapacitors from zero volt to the nominal value with a constant current. First of all, the values of the parameters of the immediate branch are determined, in case it absorbs the full current injected into the device during the charge phase (the branch R_2 & C_2 is uninfluential).

The R_1 resistance is calculated by measuring the potential difference ΔV between the two terminals during the first charge moment and subdividing it for the total charge current, assuming all the capacitances still discharged:

$$R_1 = \frac{\Delta V}{I_c} \tag{5.11}$$

The two components of the total capacitance of the short term branch are determined through an unique procedure. In order to explain the method, the tie between voltage and current at the terminals of

a condenser of variable capacitance is considered at first:

$$\mathrm{i} = (\mathrm{C_0} + \mathrm{K_v}\,\mathrm{V_c})(\frac{\mathrm{dV_c}}{\mathrm{dt}}) \tag{5.12}$$

Equation (5.12) can be integrated separating the variable elements. The result of the integration, in case of a constant current charge (I_c) and after having moved to the second member the current, is the following:

$$t = f(V) = \left(\frac{C_0}{I_c}\right)V + \left(\frac{1}{2}\right)\left(\frac{K_v}{I_c}\right)V^2 \tag{5.13}$$

This is the tie time-voltage at the capacitance terminals, that will be exploited in order to identify the parameters.

As it can be seen observing the (5.13) the inverse curve $t = f(V_c)$ during the entire charge phase is a second order polynomial of the following type:

$$\mathrm{t} = \mathrm{C_2V^2} + \mathrm{C_1V} \tag{5.14}$$

Combining (5.13) and (5.14), the values C_o and k_v are gained directly, according to the coefficients and the value of the charge current:

$$C_o = C_1\, I_c \quad \& \quad K_v = 2C_2\, I_c \tag{5.15}$$

Since I_c value is imposed, it is sufficient to know C_1 & C_2 to reach the parameters.

To obtain the values of C_1 & C_2, it is adequate to know only two points of the voltage-time curve of FIGURE 5-6.

Having the points *P 1* (t_1 , V_2) and *P 2* (t_2 , V_2) , obtained from the two measures, the following relations holds true :

$$t_1 = C_2 V_1^2 + C_1 V_1; \quad \text{and}$$

$$t_2 = C_1 V_2^2 + C_1 V_2 \tag{5.16}$$

Solving the above equations (5.16) in the two variables C_1 and C_2 we have:

$$C_1 = \frac{t_1}{V_1} - \frac{V_1 t_2 - t_1 V_2}{V_2^2 - V_1 V_2}; \quad \text{and}$$

$$C_2 = \frac{V_1 t_2 - t_1 V_2}{V_1 V_2^2 - V_1^2 V_2} \tag{5.17}$$

Substituting the (5.17) into the (5.15) we obtain the wanted parameters:

$$C_0 = \left[\frac{t_1}{V_1} - \frac{V_1 t_2 - t_1 V_2}{V_2^2 - V_1 V_2}\right] I_c; \text{ and}$$

$$\mathrm{k_v} = 2\left[\frac{\mathrm{V_1 t_2 - t_1 t_2}}{\mathrm{V_1 V_2^2 - V_1^2 V_2}}\right] \mathrm{I_c} \tag{5.18}$$

In order to obtain satisfactory results, the points *P 1* and *P 2* must be chosen necessarily to cover the entire charge phase as much as possible.

Once the identification of the first branch has been completed it is possible to determine the parameters of the second branch. In this case, the time constant $\tau_2 = R_2 \cdot C_2$ must be fixed.

The behaviour of the device during the medium-long period depends strictly on the choice of this value. In fact, if the time constant is too small, a good accuracy in the medium term would be reached, but errors would be created in the long period. Choosing instead a time constant too high, accuracy in the medium term would be sacrificed. The value must be chosen optimally for the best balance. After some

tests it has been decided the value of τ_2 = 240 s is acceptable.

Once the time constant has been chosen, the voltage must be measured according to a time equal to three times τ_2 and a charge report must be performed to calculate C_2, assuming that also the charge process of the branch 2 is completed and therefore all the capacitances are at the same voltage level:

$$\mathrm{Q_{total}} = \mathrm{I_c T_c} = \mathrm{C_2 V_{2f}} + \left[\mathrm{C_0} + \left(\frac{\mathrm{K_v}}{2}\right)\mathrm{V_{2f}}\right]\mathrm{V_{2f}} \tag{5.19}$$

In (5.19) all the quantities are known, except C_2 , which can be calculated easily.

At this point, only the determination of the value of R_2 remains, that is carried out by simply employing the definition of time constant:

$$\mathrm{R_2} = \frac{\tau_2}{\mathrm{C_2}} \tag{5.20}$$

Summary of the 4 formulae to calculate the four model parameters of the 2 branch model is as follows:

$$C_0 = \left[\frac{t_1}{V_1} - \frac{V_1 t_2 - t_1 V_2}{V_2^2 - V_1 V_2}\right] I_c \tag{5.21}$$

$$k_v = 2\left[\frac{V_1 t_2 - t_1 t_2}{V_1 V_2^2 - V_1^2 V_2}\right] I_c \tag{5.22}$$

$$Q_{total} = I_c T_c = C_2 V_{2f} + \left[C_0 + \left(\frac{K_v}{2}\right) V_{2f}\right] V_{2f} \tag{5.23}$$

$$\mathrm{R_2} = \frac{\tau_2}{\mathrm{C_2}} \tag{5.24}$$

With the method explained above, C_0, K_V, C_2 & R_2 are identified. And with the 6 steps testing procedure recommended by the 'Maxwell' supercapacitor testing guidelines [36], R_1 & R_3 are identified. With all these parameters identified, the two branch model parameters identification experiments are performed:

1. Identification of R_1

With method proposed by [19],

Charge up the supercapacitor to 4.1V, let it settle for 4 minutes for a typical supercapacitor internal charge redistribution as reflected by the two-branch equivalent circuit.

Measure V_t = 3.94V,

At V_t = 3.94V, under a discharge current of 86.9 mA, V_t increases by 0.01 V.

R_1 = 0.01/0.0869 = 0.115 Ω

So R_1 = 0.115 Ω

2. Identification of C

With method proposed by [19],

Charge up the supercapacitor to 4.1V, let it settle for 4 minutes for a typical supercapacitor internal charge redistribution as reflected by the two-branch equivalent circuit.

Measure V_t = 3.98V.

At V_t = 3.98V, under a discharge current of 93.0 mA, V_t is discharged to 2.5 V, in 344 seconds.

C = (93 x 344) / (3.98 – 2.5) = 21612 mF = 21.612 F

So C = 21.612 F

3. Identification of R_3

With method proposed by [20],

From a parallel RC circuit discharge formula with a single time constant,

$$v(t) = v_0\text{^}(-\frac{t_{dis}}{\tau_{le}}) \quad (5.25)$$

where $v(t)$ = Supercapacitor terminal voltage after discharge time of t from initial voltage v_o

v_o = Supercapacitor initial terminal voltage prior to discharge test

Γ_{le} = Time constant of the parallel leakage RC equivalent circuits

t_{dis} = discharge test time duration

and as,

$\Gamma_{le} = R_3 \times C$ (per the definition of the RC time constant)

$\rightarrow \quad R_3 = \frac{\tau_{le}}{C}$

To find R_3,

At 4:03 pm (Jan 17, 18), V_t = 3.61 V, allow supercapacitor to self discharge, until,

At 9:50 am (Jan 18,18), measure V_t = 3.52 V

Time elapsed = 64380s

ln (3.52/3.61) = -0.02525

Γ_{le} = 64380/0.02525 = 2549702.97

$R_3 = \Gamma_{le}/C$ & as C is found out to be 21.612 F in 2,

So R_3 = 2549702.97/21.612 = 0.117933 MΩ

4. Identification of C_o & k_v

Firstly, discharge the supercapacitor bank to zero charge,

Then, charge up the supercapacitor bank with I_c = 23.9 mA,

At 2.0V, t_1 = 28' 57" = 1737s

At 3.7V, t_2 = 57' 46" = 3466s

At 3.7V, charging is stopped and wait for 12 mins (720s), then measure V_{2f} = 3.65V

Calculation of C_o & k_v based on above set of data is :-

V_1 = 2 – (23.9/1000) x 0.115 = 1.99725

V_2 = 3.7 – (23.9/1000) x 0.115 = 3.69725

$C_0 = [t_1/V_1 - (V_1.t_2 - t_1.V_2)/(V_2^{2-} V_1.V_2)] \,.\, I_c$ (From formula (5.21))

C_0 = 18.8832F (by substituting in V_1, V_2, t_1, t_2 & I_c)

$k_V = 2\,[(V_1.t_2 - t_1.t_2) / (V_1.V_2^2 - V_1^2 . V_2)] \,.\, I_c$ (From formula (5.22))

k_V = 1.9052 F/V (by substituting in v_1, v_2, t_1, t_2 & I_c)

5. Identification of C_1 & C_2

$$Q_{total} = I_c \,.\, T_c = C_2.V_{2f} + [\, C_o + (K_V/2).V_{2f}].V_{2f} \qquad (5.22)$$

Plug in V_{2f} = 3.65V, T_c = 3466s, with I_c = 0.0239A as measured in 4,

and with C_0 = 18.8832 & K_V = 1.9052 F/V identified in 4,

C_2 = 0.33499F

Using formula (5.24),

$R2 = \tau_2 / C_2$ = 240/0.33499 = 716.439Ω

5.4 Conclusion

In this chapter, MPC theories and their detailed mathematical computation are elaborated. The computation allows the determination of certain controlled input variables so that predicted outputs can be achieved in a certain prediction horizon. The distinctive characteristics of constraints handling and 'receding horizon' concepts in MPC theories are highlighted. These characteristics make the theories particularly applicable to slow speed and long time domain applications similar to this research.

The second part of this chapter presents the importance of using a precise two branch equivalent model of the supercapacitor for the accurate control action by the MPC algorithm. A unique method to identify the two branch equivalent model parameters is used. Experiments are conducted to find out all the model parameters for a supercapacitor bank used in this research (detail of their computations is provided in section 6.12).

Findings in this chapter may be used as a reference in other MPC algorithm applications with the use of supercapacitors which require precise modelling and model parameters identifications.

CHAPTER 6: PROPOSED NOVEL DESIGN OF ENERGY CONTROL ALGORITHM

In Chapter 3, experience of other researchers is learned to reinforce the importance of precise definition of the research problem and research objectives. With clear research problem and research objectives, an intuition of possible solutions is presented in Chapter 4. It indicates in Chapter 5 that the important control parameters can be computed using Model Predictive Control (MPC) theories.

In the first part of this chapter, section 6.1, the methods to compute important control parameters using MPC algorithm are presented. This will deliver partially the solution to achieve our research objectives. In the second part of this chapter, section 6.2, important augmentations are proposed on top of the MPC algorithm. They will deliver the important remaining part of our novel energy control algorithm. By the augmentation of the MPC energy control algorithm, a complete solution to our research objectives is obtained.

6.1 MPC Energy Control Algorithm Formulation

6.1.1 Consideration on the best tool to generate MPC algorithm

In section 5.1, MPC theories and their mathematical formulae are presented in detail. Based on the computation of these formulae, which involve vigorous computation of matrices, control variables are computed. Before the actual design of MPC algorithm to solve the design problem, a decision must be made on how one can most efficiently and effectively roll out the desired algorithm to compute the required control parameters.

Reference [32], which is a major textbook for graduate study of MPC theories, presents all its MPC algorithm solutions with the use of 'Matlab' Simulink MPC toolbox. This for sure provides a strong indication that 'Matlab' Simulink MPC toolbox is a very relevant tool. However, during the design process in this research, a major difficulty is encountered in using the MPC algorithm generated by 'Matlab'. The major difficulty is that MPC algorithm generated by 'Matlab' is composed of M codes

which is the high-level language created by 'Matlab' to handle matrices computation. While M codes is efficient in handling matrices computation with very strong simulation capabilities, M codes cannot be implemented directly in any WSN hardware platform. Most WSN hardware platforms, including the one that is designed in this research, can only be implemented with C codes, as most microcontrollers manufacturers only provide C compiler for system programming.

To solve this problem, 'Matlab' Simulink provides an utility program called 'Coder', which allows one to convert its control algorithm (such as 'MPC' tool box in this case) from M codes into C codes. The process of using 'Coder' to convert M codes into C codes is tedious and it involves porting of C codes to adapt to individual microcontroller in which significant configuration modification is required. At the same time, as the computation of MPC algorithm by the microcontroller involves time consuming and memory consuming computations, it is desirable to use fast speed microcontroller with relatively large memory. In many cases, the skills of 'Explicit MPC algorithm' implementation is employed to compute important MPC parameters with software simulation, before implementing the algorithm in the microcontroller.

In this application where the cost of hardware is an important consideration factor, a low cost 16-bit microcontroller is used with a relatively small flash memory of 128Kbyte. To avoid the heavy MPC algorithm computational time required in using the small microcontroller, it is decided to use the technique of 'Explicit MPC algorithm' implementation. That is, important MPC parameters are computed in a laptop computer and the resulting control parameters are used in the final control algorithm in the microcontroller.

In the following subsections 6.1.2 and 6.1.3, the complete process of generating the MPC algorithm M codes to compute the important MPC control parameters is presented in detail.

6.1.2 MPC Algorithm design prerequisite to define State Space Model of Plant

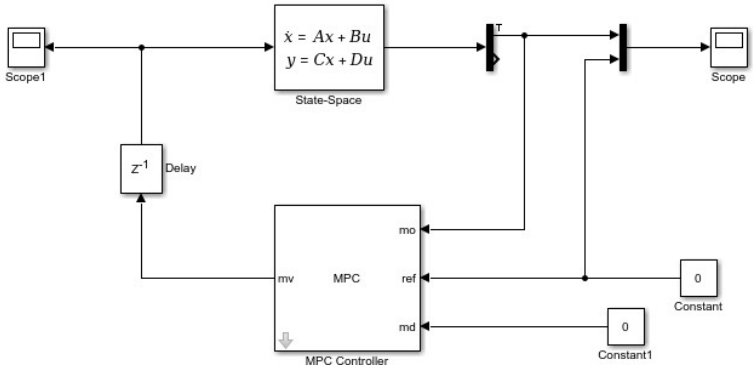

Figure 6-1 'Matlab' model simulation of an MPC Controller on a SPBL Energy Harvester with Two Branch Circuit Equivalent Model

As seen in above FIGURE 6-1, 'Matlab' Simulink MPC tool box allows the design of the MPC algorithm in the form of a controller with comprehensive input of design parameters such as manipulated output, prediction horizon, control horizon etc. However, the use of the MPC tool box comes with a prerequisite requirement that the plant's state space model representation needs to be determined precisely. In this research, the plant to be controlled is the SPBL energy harvester with a two branch equivalent model of the supercapacitor. The process of the plant's precise model determination is presented as follows.

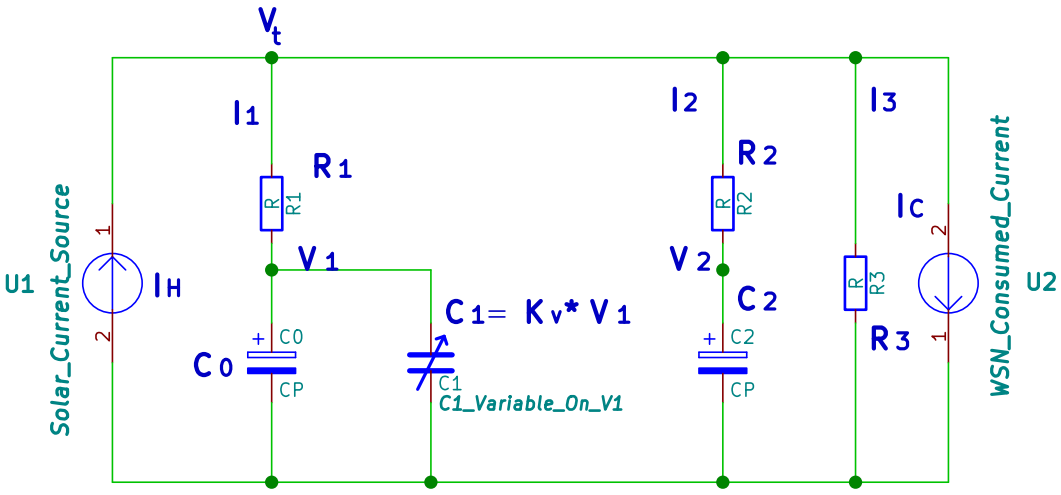

Figure 6-2 SPBL energy harvester with supercapacitor two branch equivalent model circuit diagram

Our aim is to derive a state space model for the supercapacitor, with a state space representation in the following form:

$$\frac{\mathrm{dx}}{\mathrm{dt}} = \mathrm{A}\mathbf{x} + \mathrm{B}\mathbf{y}$$

$$\mathrm{z} = \mathrm{C}\mathbf{x} + \mathrm{D}\mathbf{y}$$

Where x *(state vector)* $= [V_1, V_2]^T$,

y *(input vector)* $= [(I_H - I_C), 0]^T$,

z *(output vector)* $= [V_t, 0]$,

A is a 2x2 state matrix, B is a 2x2 input matrix,

C is a 2x2 output matrix, and D is a 2x2 feedthrough matrix

State space representation is written in the following form:

$$\frac{\mathrm{dx}}{\mathrm{dt}} = \mathrm{A}\mathbf{x} + \mathrm{B}\mathbf{y}$$

$$\mathrm{z} = \mathrm{C}\mathbf{x} + \mathrm{D}\mathbf{y} \qquad (6.0)$$

Applying Kirchoff's Law to the nodes in the above circuit diagram FIGURE 6-2,

$$I_1 = \frac{V_t - V_1}{R_1} \tag{6.1}$$

$$I_2 = \frac{V_t - V_2}{R_2} \tag{6.2}$$

$$(I_H - I_C) = \frac{V_t - V_1}{R_1} + \frac{V_t - V_2}{R_2} + \frac{V_t}{R_3} \tag{6.3}$$

From (6.3),

$$V_t = \left[\frac{R_2 R_3}{\Delta R}\right] V_1 + \left[\frac{R_1 R_3}{\Delta R}\right] V_2 + \left[\frac{R_1 R_2 R_3}{\Delta R}\right](I_H - I_C) \tag{6.4}$$

where $\Delta R = R_2.R_3 + R_1.R_3 + R_1.R_2$

$$C_1 \left(\frac{d}{dt}\right) V_1 = I_1 = V_t - V_1 \tag{6.5}$$

Put (6.4) into (6.5),

$$C_1 \left(\frac{d}{dt}\right) V1 = \left[\frac{R_2 R_3}{\Delta R}\right] V_1 + \left[\frac{R_1 R_3}{\Delta R}\right] V_2 + \left[\frac{R_1 R_2 R_3}{\Delta R}\right](I_H - I_C) - V_1$$

$$= \left[\frac{R_2 R_3}{\Delta R} - 1\right] V_1 + \left[\frac{R_1 R_3}{\Delta R}\right] V_2 + \left[\frac{R_1 R_2 R_3}{\Delta R}\right](I_H - I_C) \tag{6.6}$$

$$C_2 \left(\frac{d}{dt}\right) V_2 = I_2 = V_t - V_2 \tag{6.7}$$

Put (6.4) into (6.7),

$$C_2 \left(\frac{d}{dt}\right) V_2 = \left[\frac{R_2 R_3}{\Delta R}\right] V_1 + \left[\frac{R_1 R_3}{\Delta R}\right] V_2 + \left[\frac{R_1 R_2 R_3}{\Delta R}\right](I_H - I_C) - V_2$$

$$= \left[\frac{R_2R_3}{\Delta R}\right] V_1 + \left[\frac{R_1R_3}{\Delta R} - 1\right] V_2 + \left[\frac{R_1R_2R_3}{\Delta R}\right] (I_H - I_C] \quad (6.8)$$

So, comparing (6.6), (6.8) and (6.4) with state space representation form (6.0), below matrices parameters are derived:

$A_{11} = \left(\frac{1}{C_1}\right)[\frac{R_2R_3}{\Delta R} - 1];$ $A_{12} = \left(\frac{1}{C_1}\right)[\frac{R_2R_3}{\Delta R}];$

$A_{21} = \left(\frac{1}{C_2}\right)[\frac{R_2R_3}{\Delta R}];$ $A_{22} = \left(\frac{1}{C_2}\right)[\frac{R_2R_3}{\Delta R} - 1];$

$B_{11} = \left(\frac{1}{C_1}\right)[\frac{R_1R_2R_3}{\Delta R}];$ $B_{21} = \left(\frac{1}{C_2}\right)[\frac{R_1R_2R_3}{\Delta R}];$

$C_{11} = \frac{R_2R_3}{\Delta R};$ $C_{12} = \frac{R_1R_3}{\Delta R};$

$C_{21} = 0;$ $C_{22} = 0;$

$D_{11} = \frac{R_1R_2R_3}{\Delta R};$ $D_{12} = 0;$

$D_{21} = 0;$ $D_{22} = 0;$

Note that $C_1 = C_0 + Kv.\ V_1$, and $V_1 \approx V_t$ (terminal voltage of the supercapacitor) due to the very small value of R_1 . At any particular terminal voltage point of the supercapacitor, $C_1 = C_0 + Kv.\ V_t$.

Due to the nonlinear nature of the state space model, it needs to be linearized at a particular operating point so as to allow the precise MPC algorithm to be applicable at that particular operating point. Recalling from Chapter 4, the solution intuition involves the determination of the control action starting from the highest terminal voltage of the supercapacitor at 4.1V, with the next control action to be determined after decrement of 0.1V (i.e. 4.0V), until the terminal voltage of the supercapacitor reaches its minimum operable voltage of 2.5V.

As such, the desirable MPC energy control algorithm needs to determine the maximized current consumed (I_c) (which is the single input variable in the state space plant model) allowed at each individual voltage point of V_t = 4.1V, 4.0V, 3.9V,..... until V_t is discharged down to 2.5V. As the supercapacitor's discharge characteristics behaves in a nonlinear manner due to its double layer's structure, linearization of the state space model at each control point is necessary to guarantee an accurate control action taken by the MPC algorithm. In this application, the accurate control action is the

computation of an accurate figure of the maximized consumption current (I_c) that can be used in the next time slot.

With the above process to determine the precise state space model's *A,B,C,D* matrices performed, and with each particular V_3 operating point's C_1 determined by $C_1 = C_0 + Kv.\ V_t$, one is able to provide the precise state space plant model for the MPC energy control algorithm to compute the precise I_c to be used at each particular voltage point of the supercapacitor.

Below shows the 'Matlab' script written to compute model parameters for the plant's state space model at V_t = 2.6V :-

w:pPr><w:r><w:t><![CDATA[% parameters of my VLR_state_space discrete (Jan18,18) - for 4x5F supercap bank

```
R1=0.115;
R2=716.439;
R3=117933;
C0=18.8832;
CV=1.9052*2.6;
%1.9052 is the value of Kv, and V is average charging voltage : 2.6V
C1=C0+CV;
C2=0.33499;
CR1=C1*R1;
CR2=C2*R2;
RR=R2*R3+R1*R3+R1*R2;
A11=(1/CR1)*(R2*R3/RR-1);
A12=(1/CR1)*(R1*R2/RR);
A21=(1/CR2)*(R2*R3/RR);
A22=(1/CR2)*(R1*R3/RR-1);
A=[A11 A12
  A21 A22];
B11=(1/CR1)*(R1*R2*R3/RR);
B21=(1/CR2)*(R1*R2*R3/RR);
B=[B11
  B21];
C11=(R2*R3/RR);
C12=(R1*R3/RR);
C21=0;
```

```
C22=0;
C=[C11 C12
  C21 C22];
D11=(R1*R2*R3/RR);
D21=0;
D=[D11
  D21];
Ts= 1/100;
sys = ss(A,B,C,D);
sys_d = c2d(sys,Ts,'zoh')
% note that a delay block is added to connect model's MV
% and plant's input to avoid direct feedthrough not allowed
% controller (spent several hours to debug this on May13,17
% modified into a discrete model by the last three lines of script (Sep24,17)
]]></w:t></w:r></w:p></w:body></w:document>
```

Note that the continuous state space model is converted into a discrete state space model by the 'Matlab' function *sys_d = c2d(sys, Ts, 'zoh')* in which the sampling time *Ts* is chosen to be equal to 0.01s.

The precise state space model parameters is now determined for each linearized operating point. The MPC controller's design is presented in the following section to compute the desirable I_c at each voltage operating point of the supercapacitor.

6.1.3 MPC Algorithm Design with 'Matlab' MPC toolbox

As a decision is made to use 'Matlab' MPC toolbox to design the control algorithm necessary to compute the input variable (which is I_c, the current consumed), 'Matlab' MPC toolbox user manuals are referenced intensively for the work presented in this subsection [38], [39], [35].

In order to fully understand ‘Matlab’ MPC toolbox design process, the user manuals [38] and [39] need to be thoroughly read through. For a grasp of the design process, a quick summary is provided as below.

The first step of the design process involves choosing a particular operating point, with the use of a function called 'Trim Model'. After linearization of the model at the chosen operating point, a default simulation with some defaulted input/output parameters and some defaulted simulation scenario will be

performed. The resulting manipulated inputs and outputs will be displayed after the simulation. One can select a function to edit the simulation scenario to reflect the particular design criterion. Depending on the plant's state space model, multiple inputs, multiple outputs, input disturbances and output disturbances etc. can be selected. In this research, the plant's model is relatively simple, with only one single manipulated input (I_c), one targeted output (V_3), and with no input or output disturbances. The function of 'Simulation Setting' can then be used to set up the targeted output to allow the MPC algorithm to compute the desirable control action. The MPC algorithm use an optimized manipulated input to arrive at the desired targeted output. Finally, the 'tuning' function is used to input the suitable control parameters, which are the sample time, prediction horizon, control horizon, and the manipulated input constraints.

In this application, the MPC algorithm is required to compute the maximized current consumed (I_c) that is allowed to be used at any particular terminal voltage of the supercapacitor (V_3, say, at 3.7V), so that the duration of discharge can last for 22 hours before V_3 reaches the minimum operable voltage of 2.5V. Once I_c is computed by the MPC algorithm, one can then calculate the duty cycle % that can be used based on the fact that the operating current of the WSN is measured to be equal to 80 mA. Maximized duty cycle % ($D_{s,\,max}$) is simply equal to I_c/80mA * 100%.

However, using above principle in the first trial of algorithm design simulation shows a failure with a special scenario. With a sampling rate of 0.01 second, the simulation lasts for about 30 minutes, and then 'Matlab' simulation stops with an error message, “simulation ceases due to memory overflow”. Obviously, as the prediction horizon is specified to be a rather long duration of 22 hours, the laptop computer's memory is insufficient to perform such a simulation which requires a very large system memory.

After more thoughts, an alternative approach is used to compute the desirable maximized duty cycle % in an indirect manner, which is presented in below paragraphs.

In this design, there exists a specific manipulated input constraint of the manipulated input variable I_c (consumed current). The constraint is the fixed operating current value of 80 mA of the WSN during its data sensing and wireless data transmission period. This constraint is set in the MPC designer as a constant constraint throughout the duration of control horizon, which is set to be the same as the prediction horizon (meaning that influence of this input constraint is maintained throughout the whole period of the prediction horizon). Under such design and simulation criterion, a design simulation is conducted to find out the time elapsed for the decrease of 0.1V of our targeted output (V_3) from its existing linearized operating point (V_3 = 4.1V, 4.0V, 3.9V, etc.). In the MPC designer function, a step input reference signal of -0.1V is used for the reference signal of our desired output.

The important parameters that one wants to find out from the MPC controller's algorithm in this research is the discharge time of every 0.1V, starting from the maximum terminal voltage of the supercapacitor at 4.1V (4.1V is the boost converter charging voltage of our SPBL energy harvester), down to the minimum operable terminal voltage of the supercapacitor at 2.5V (DC-DC converter supplying 3.3V to the WSN will stop operation once input voltage drops below 2.5V). Through the MPC toolbox designer's functions, we are able to find out these important parameters.

The MPC algorithm design uses 'Matlab' MPC toolbox to compute the important discharge time parameter of the selected 20-Farad supercapacitor bank. The entire process of design to compute the discharge time of the supercapacitor's terminal voltage to discharge from 2.6V to 2.5 is demonstrated as in the following 8 processes.

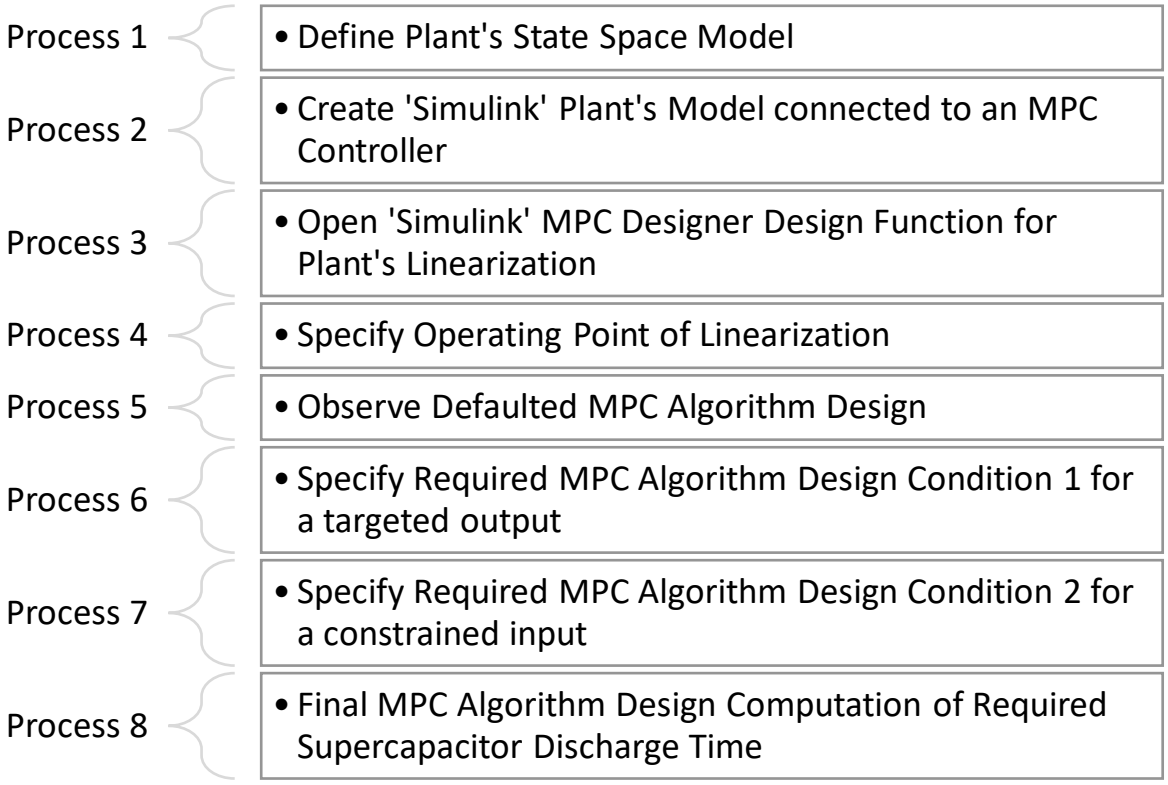

Figure 6-3 'Matlab' MPC Design Process

Detail of the design process, from process 1 to process 8, is included in Annex A. Summary for each step is provided as follows.

6.1.3.1 Define Plant's State Space Model

The first step in using 'Matlab' Simulink MPC designer is to define the controller plant's precise state space model. In this case, the controlled plant is the solar energy harvester state space model as defined precisely previously in section 6.1.2.

6.1.3.2 Create 'Simulink' Plant's Model connected to a MPC Controller

The second step in the 'Matlab' MPC design process is to create a 'Simulink' plant's model connected to a MPC controller. Note that in this case, there is no external disturbance and there is no external reference and these manipulated inputs are set to zero constant. A delay block with defaulted delay time value is connected from the manipulated variable output from the MPC controller to the manipulated input port of our plant as a design requirement of the 'Matlab' controller. The output from the plant is highlighted with a 'Trim' function *T* so that a linearization point of the plant output can be defined in the later design process of plant's linearization at a particular operating point.

6.1.3.3 Open 'Simulink' MPC Designer Design Function for Plant's Linearization

The third step in the 'Matlab' MPC design process is to open 'Simulink' MPC Designer design function for plant's linearization. Select the MPC controller icon to go into the MPC Designer's main menu. In the MPC Designer's main menu, select function of MPC structure so that the option to create a new operating point (function of 'Trim Model') can be seen.

6.1.3.4 Specify Operating Point of Linearization

The fourth step in the 'Matlab' MPC design process is to specify the operating point of linearization of the plant by defining the plant's output voltage. Select the 'Trim Model' function in design process 3 so that a menu to specify the linearization point can be seen. The plant's output voltage is the terminal voltage of the supercapacitor which is this MPC computation is set to 2.6 volts.

6.1.3.5 Observe Defaulted MPC Algorithm Design

The fifth step in the 'Matlab' MPC design process is to observe how the defaulted MPC algorithm generates a defaulted output response with a defaulted manipulated controller's input. After clicking the

'Start trimming' function in design process 4, the MPC controller generates a defaulted MPC control algorithm with defaulted output and defaulted manipulated input at the specified operating point (in this case, at output voltage of 2.6V).

The defaulted MPC algorithm design condition is defined with a prediction horizon of ten seconds; with a control horizon set from the first second to the end of the ten seconds period; and its output reference at the end of the prediction horizon is set at 3.6V FIGURE_A_5 (in Annex A) . With this defaulted design criterion, the manipulated control input can be seen from the Input Response Graph, which shows an input current value of 8A from the first second with gradual decline in its control value to zero towards the end of its control period of 10 seconds.

6.1.3.6 Specify Required MPC Algorithm Design Condition 1

The sixth step in the 'Matlab' MPC design process is to change MPC algorithm design condition of its reference output voltage as well as its prediction horizon. As shown in FIGURE A-6 (in Annex A), a reference signal of step output of -0.1V is set which equals to setting a final reference output voltage of 2.5V (2.6V – 0.1V). The simulation duration, which is equal to the prediction horizon, is set to 30 seconds instead of 10 seconds, based on our rough understanding of the discharge performance of the supercapacitor used in this research.

6.1.3.7 Specify Required MPC Algorithm Design Condition 2

The seventh step in the 'Matlab' MPC design process is to change MPC algorithm design condition of its important input constraint which is a distinctive strength and characteristics of MPC theories.

As shown in FIGURE A-7 (in Annex A), the input constraint in our case is set to -0.08A (80 mA) as both its minimum and maximum values. Also, the control horizon and prediction horizon are set to the same value throughout the whole duration of the prediction horizon. Such design settings reflect our specific input constraint situation that the manipulated input is the current supplied by the plant to power the WSN embedded system, and that its value is -0.08A (80 mA) when the WSN embedded system is in active operation.

6.1.3.8 Final MPC Algorithm Design Computation of Required Supercapacitor Discharge Time

This is the final step in the 'Matlab' MPC design process which shows our MPC algorithm design's output response as shown in FIGURE A-8 (in Annex A).

After the input constraint condition is set in our design process 7, selecting the 'Apply' function allows the designed MPC algorithm to compute both the input response and output response. As shown in the output response graph, the duration of discharge from 2.6V to 2.5V is about 26 seconds (25.78 seconds to be exact). We can see in the later part of this chapter that this parameter is instrumental to the completion of the energy control algorithm design.

A set of 'Mathlab' Simulink MPC Design files are submitted with the submission of this thesis. Please refer to Annex C for these files, which show the comprehensive design and simulation results.

6.1.3.9 Final Outcome of 'Matlab' MPC Design Computation

Using the design methods as above, MPC algorithm design at each voltage output operation point, separated by -0.1V each, ranging from 4.1V to 2.5V, is conducted accordingly. Results of the design and simulations are summarized as in the below table:

Table 6-1 'Matlab' MPC Algorithm simulation result on SPBL energy harvester

MPC Algorithm Operating point of V_3 (Supercapacitor Terminal Voltage), in V	Manipulated Input of Current Consumed by WSN (I_c), in mA	Starting Voltage of V_3, in V	End Voltage of V_3, in V	Time elapsed after discharge of 0.1V, in seconds
4.1	80	4.1	4.0	27.73
4.0	80	4.0	3.9	27.60
3.9	80	3.9	3.8	27.47
3.8	80	3.8	3.7	27.34
3.7	80	3.7	3.6	27.21
3.6	80	3.6	3.5	27.08
3.5	80	3.5	3.4	26.95
3.4	80	3.4	3.3	26.82
3.3	80	3.3	3.2	26.69

MPC Algorithm Operating point of V_3 (Supercapacitor Terminal Voltage), in V	Manipulated Input of Current Consumed by WSN (I_c), in mA	Starting Voltage of V_3, in V	End Voltage of V_3, in V	Time elapsed after discharge of 0.1V, in seconds
3.2	80	3.2	3.1	26.56
3.1	80	3.1	3.0	26.43
3.0	80	3.0	2.9	26.30
2.9	80	2.9	2.8	26.17
2.8	80	2.8	2.7	26.04
2.7	80	2.7	2.6	25.91
2.6	80	2.6	2.5	25.78

From the resulting parameters in TABLE 6-1, the nonlinear discharge characteristics of the supercapacitor can be seen. The supercapacitor has a faster discharge rate at a lower terminal voltage, although the extend of nonlinearity is rather small.

Theoretically, for totally precise control actions, one needs to use the precise discharge time at each voltage operating point as our design reference. However, as this application is not a mission critical type of application (in which no control deviation can be tolerated, such as similar energy control application in a spacecraft), an average discharge time is used in order to simplify the final algorithm coding. Average discharge time of discharging of 0.1V (with current consumed by the WSN equals to 80 mA) as given by the above simulation table is 26.94 seconds.

It will be shown in section 6.2.1 that this important parameter of 26.94 seconds in every discharge of 0.1V of V_3 allows the calculation of the desirable maximized duty cycle % ($D_{s,\,max}$%) in an indirect manner.

6.1.3.10 Experimental Validation of 'Matlab' MPC Design Computation

As the MPC algorithm computation depends heavily on the accuracy of the state space model of the plant, there exists a possibility that its computation may deviate from reality should the state space model used or its parameters identification are inaccurate. A separate discharge test (at every voltage point starting from 4.1V to 2.5V, discharge is performed using a precision constant sink instrument Fig_5_4 to discharge the supercapacitor with a constant current of 80 mA, and discharge duration is recorded with a smart phone timer when supercapacitor terminal voltage drops by 0.1V) is conducted to validate the

accuracy of table 6.1.

Discharge test result is shown in TABLE 6-2 as follows.

Table 6-2 Experimental Validation of 'Matlab' MPC Design Computation

MPC Algorithm Operating point of V_3 (Supercapacitor Terminal Voltage), in V	Time elapsed after discharge of 0.1V, in seconds, computed by MPC algorithm	Time elapsed after discharge of 0.1V, in seconds, measured by constant current discharge test	% difference of MPC algorithm computed data from discharge test data
4.1	27.73	28.84	-3.85
4.0	27.60	28.15	-1.95
3.9	27.47	29.12	-5.67
3.8	27.34	28.43	-3.83
3.7	27.21	28.03	-2.93
3.6	27.08	28.42	-4.71
3.5	26.95	27.49	-1.96
3.4	26.82	27.62	-2.90
3.3	26.69	27.65	-3.47
3.2	26.56	27.17	-2.25
3.1	26.43	27.78	-4.86
3.0	26.30	27.40	-4.00
2.9	26.17	27.37	-4.38
2.8	25.04	26.07	-3.95
2.7	25.91	26.69	-2.92
2.6	25.78	26.37	-2.24

As can be seen from above TABLE 6-2, the data computed by 'Matlab' MPC algorithm differs from the discharge test data from the smallest difference of -1.95% to the largest difference of -5.67%. Average difference is -3.5%. This small difference is a result of several possible reasons. The first possible reason is that the Two Branch Equivalent Model of the supercapacitor used may have a certain discrepancy from the supercapacitor's real discharge characteristics. The second possible reason is the measurement inaccuracies during the numerous charging and discharging tests to determine the state space model parameters. The third possible reason may be due to the accuracy tolerance specification of the testing instruments which include the constant current sink, the constant current source and the current

meter. It may also be possible that all these possible reasons are combined to produce the small data discrepancy. Section 7.2 provides more detail elaboration of these data inaccuracies Sec_7_2.

As a whole, the average data discrepancy of less than 5% is a totally acceptable figure based on the measuring limitations as presented in section 7.1 Data Error Analysis. It also reflects the successful use of a correct plant's state space model as well as the successful design of MPC algorithm with the use of 'Matlab' MPC Designer tool.

6.1.4 Explicit MPC Algorithm Design used in this research

There is a possible question to be answered regarding the offline MPC algorithm computation method (with a laptop computer) used in this research to compute the important control parameters (the discharge time of 0.1 V at every operable voltage point of the supercapacitor, average time computed by the MPC algorithm is 26.94 seconds).

The possible question is that if the MPC algorithm is not used in an online manner with the microcontroller in the wireless sensor node, can we still regard the resulting close loop feedback control algorithm by using the important parameters as computed by an offline MPC algorithm, as a legitimate MPC control algorithm ?

The answer is affirmative as provided by most MPC theories textbooks [30], [33] & [34] as well as on the Matlab MPC Design website (www.mathworks.com/help/mpc/explicit-mpc-design.html) with a term called 'Explicit MPC Design'.

Matlab 'Explicit MPC Design' documentation explains the reasons why in many circumstances when computation power is limited, there is a need to use offline computation. However, as the important control parameters are generated by MPC algorithm, the resulting close loop feedback controller is considered as an 'Explicit MPC controller'.

Below detail description (www.mathworks.com/help/mpc/explicit-mpc-design.html) serves to provide further clarification :

"**Fast model predictive control using precomputed solutions instead of run-time optimization**

Explicit model predictive control uses computations to determine all operating regions in which the optimal control moves are determined by evaluating a linear function. Explicit MPC controllers require fewer run-time computations than traditional (implicit) model predictive controllers and are therefor useful for applications that require small sample times. To implement explicit MPC, first design

a traditional (implicit) model predictive controller for your application, and then use this controller to generate an explicit MPC controller for use in real-time control. For more information, see Design Workflow for Explicit MPC. “

As one can see in this thesis, this research does exactly what the above description mentions to “generate an explicit MPC controller for use in real time control”, with the 0.1 V discharge steps as the ‘regions’ used in our explicit MPC calculations. However, the resulting controller still requires three new design principles to provide a practical solution for the addressed technological problem.

Explicit MPC control algorithm is used extensively in most application areas when a microcontroller is used, instead of using a more powerful industrial microcomputer. Examples are commonly seen in petrochemical plants when there are chemical reactions done in a tank where dozens of input chemical material needs to be controlled after a certain prediction time horizon to achieve a desirable chemical reaction and end products with desirable qualities. For these types of close loop feedback control, microcontrollers located in control boxes alongside the reaction tanks are almost used exclusively using MPC control algorithm. However, again almost exclusively MPC control algorithm are not run in real time in the microcontrollers for the computation of important control parameters (as these control parameters will not change over time/real time, there does not exist a need to perform real time computation in the relatively slow speed microcontroller). Understandably, those control parameters are obtained by running MPC control algorithm in fast speed laptop/desktop computers and then transported to the program memory of the microcontrollers for real time feedback control.

It is worth it to mention that there are debates and objections raised by different parties as to whether an ‘Explicit MPC Controller’ can be considered as an online feedback controller. Strongest objections come from research communities that are familiar with the design of fast speed real time close loop controllers such as the PID Controllers. PID Controllers have been used for a long time in different scientific application areas and once dominated a very high application/market share in the design of real time close loop feedback controller. For PID Controllers researchers and designers, PID control algorithm runs in a real time manner with microcontroller to provide feedback control action. For them, there has never been a need for ‘offline computation’ and ‘Explicit Controller’ appears to be a myth for them. It may be this regular practice and understanding that it is difficult for them to accept the idea of an offline ‘Explicit MPC Controller’.

There is no intention in this research and thesis to provide a resolution and answer for the debate (which is not relevant to achieve the goal of this research), but to follow the regular practice and recommendations made by the MPC design communities. At the same time, the core values of this

research lie mostly on the three new design principles Sec_6_2_1 to augment what the MPC algorithm fails to achieve in this specific technological problem for energy control in IOT application. Instead of highlighting the exclusive importance of an established theory (MPC theory in this research) to solve a technological problem, this research does quite the opposite to show that very often common sense and intuition are more important to provide a simple and direct solution. In this research, MPC theory alone will for sure not be able to solve the problem we intend to solve. There is no intention in this research to provide an extensive comparison and analysis between MPC control algorithm with other close loop control algorithm. The comparison does not provide the necessary value to this research as it is very likely that other control algorithm (Fuzzy Logic control algorithm, LQR control algorithm etc.) will/may be able to solve the same technological problem when the necessary new design principles are used to augment these theories. Although MPC theory is employed as a tool (even the best tool as considered in this research), this research has never put any focus or intention to improve on MPC theory already well established and this research is for sure not a research on MPC theory.

6.1.5 Rationale on the choice to use Explicit MPC Algorithm

Using MPC algorithm provided by Matlab Simulink MPC toolbox, important parameters of the discharge of every 0.1V at every voltage point of the supercapacitor's operating voltage range (from 4.1 V to 2.5 V) are computed. As the non-linearization of the discharge characteristics is very minor (less than 5%) and our selected greenhouse application can surely tolerate this minor discharge duration prediction inaccuracy, the choose in this research is to use a simplified average discharge duration of 26.94 seconds as shown in previous computation.

However, although MPC algorithm provides a systematic and efficient method to compute the required discharge time of the supercapacitor for a desirable real time feedback control to conserve energy in a supercapacitor to sustain a required period of WSN maximized operation, it is not used in an online feedback manner to address other online disturbances in this research as explained in the next paragraph. Typical online disturbance in this application will possibly include the current harvested by the miniature solar panel at any time. When an online current of solar energy harvested is measured by an analog to digital circuit (with an inevitable increase in energy harvester hardware cost), online MPC algorithm running in the microcontroller can provide its full power to allow a bigger current consumption from the supercapacitor, which in turn will provide an upside of the service duty cycle of the wireless sensor node.

The decision to avoid using MPC algorithm running online in the microcontroller in this research

application is deliberate and calculated, due to the consideration of various trade-offs with the focus of WSN hardware cost reduction. As MPC algorithm computation is intense, online computation will require a very fast speed microcontroller with large memory which is very often impractical with commercial consideration. It is decided instead in this research, after careful consideration, that the upside of real time and interactive solar energy harvested can be addressed in an indirect manner. When there is high level of solar energy harvested in the daytime, this upside input current disturbance will be reflected indirectly by a fully charged state of the supercapacitor, with a fully charged voltage level of more than 4.1 V. When a voltage level of more than 4.1 V is detected by the energy harvester's analog to digital signal conversion circuit, a service duty cycle of 100% of the WSN can be used in theory (although it is decided to use a much lower service duty cycle to avoid excessive data sending in this research). When voltage level of the supercapacitor is over 4.1V, there exists a free option to choose any service duty cycle to improve the WSN service duty anyway. It is noticed that even in a cloudy day with moderate solar irradiation, the supercapacitor is charged up very rapidly to its fully charged state, usually within 30 minutes. As such, the upside by running the MPC algorithm feedback control in real time to utilize the positive solar irradiation current impact is rather insignificant in this research application.

With this indirect method to provide the desirable upside for WSN performance, online real time MPC algorithm computation is avoided to provide a big saving in hardware cost which includes using an inexpensive microcontroller and with just one voltage sensing circuit to detect the terminal voltage of the supercapacitor. This practical approach in this research is significant when we see that many past related research focusing on using solar irradiation prediction model fail to avoid a high rate of WSN system shut down due to energy depletion of the energy harvester. The hardware cost increase of using one more analog to digital sensing circuit to sense the solar energy current harvested, and the use of an unreliable solar irradiation prediction model (unreliable when unexpected weather fluctuates within days) are not able to avoid the undesirable high rate of system shutdown. The crucial reason behind the failure is that solar energy harvested when there is sunlight is not the most important factor to be considered (as said, supercapacitor is charged up very rapidly, even in a cloudy day), to conserve the energy while at the same time maximize the service duty of the WSN (at a 'maximized' rate subject to a constraint that there is a need to sustain for 22 hours of zero energy harvesting period) when there is no energy harvested is instead the most important factor that an energy control algorithm has to address. To put it simply, we do not have to concern too much about the charging up of the supercapacitor, but we have to put our major consideration to fully utilize the discharge characteristics of the supercapacitor. One of the major reasons of the failure of past research is their wrong/unnecessary focus on the charging of the supercapacitor, instead of on the most important aspect of the discharging of the supercapacitor when no

new solar energy is harvested.

With the consideration of the pros and cons, it is decided that an Explicit MPC Algorithm is used in an offline manner in this research, instead of using an implicit MPC algorithm in an online/real time manner.

Although MPC algorithm's full power lie on its online feedback capability to handle multiple variables, it is used as an offline computation tool in this research instead due to a practical consideration. As such, alternative methods can be used to compute the important parameter of the discharge time of 26.94 seconds per 0.1 V of the discharge of the supercapacitors. Alternate methods include solving the two differential equations of the supercapacitor's precise two branch equivalent model directly, or simply by performing experimental discharge tests of the supercapacitor.

However, with other methods and tools available, MPC algorithm is still chosen to do the required offline computation (known as 'Explicit MPC Controller' by the MPC design communities) in this research to provide a general, practical and most importantly expandable theoretical framework and design guidelines for other more sophisticated applications. While it is important to focus on the core objective in this research to solve a targeted technological problem in an embedded system with a single input parameter, it is also valuable to provide useful theoretical reference value (in this case, MPC control theory) to solve similar technological problems in other more sophisticated applications. In applications in the energy control of a spacecraft or in an autonomous driving vehicle, there will be large number of multiple input variables and disturbances that require crucial online MPC algorithm computation. In those applications, the cost to use a very fast speed microcontroller with large memory will be an insignificant consideration.

6.2 Augmented MPC Energy Control Algorithm Formulation

6.2.1 Augmented MPC Energy Control Algorithm Design Approach

To reflect the weather condition in Vancouver, the design objective is set to ensure the supercapacitor will supply power that allows the wireless sensor node to operate with maximized service duty for a further 22 hours (measured from sunrise at 6am), during such period there is no new solar energy harvested.

Using MPC algorithm computation, the average discharge time of the supercapacitor of every 0.1 volt is found to be 26.94 seconds. While this parameter identification is important, the successful implementation of the energy control algorithm based on MPC theory must be augmented. There are

three important theoretical anchor points to be implemented:

(1) Mitigation of the impact of sleep mode current of the wireless sensor node and of the leakage current of the supercapacitor. Both are uncontrollable.

(2) Optimization/Maximization of the service duty cycle of the wireless sensor node's operation, which is controllable and is the core objective of the energy control algorithm.

(3) Management of the impact of sleep mode current on the maximized service duty cycle discharge period.

These three points are explained in the following paragraphs.

Point (1) Mitigation of the Impact of Sleep Mode Current

The extent of sleep mode current of the wireless sensor node and the leakage current of the supercapacitor depends on the hardware platform selection. They are not controllable and cannot be eliminated, because they are always present when the system is operating.

These uncontrollable currents, however, determine the voltage range of operation of the supercapacitor. They determine specifically the minimum operable terminal voltage of the supercapacitor ($V_{t,\,min}$). $V_{t,\,min}$, needs to be identified and to be mitigated in our energy control algorithm.

The test conducted show that the sleep mode current of the wireless sensor node equals to 0.17 mA. In the MPC algorithm computation, it is found that 80 mA current discharge in 26.94 seconds resulted in a discharge of 0.1 V of the supercapacitor.

So, 0.17 mA sleep mode discharge current in a discharge of 0.1 V will last for :-

*80/0.17 * 26.94 seconds = 12677.6 s* (3.522 hours)

ΔV_s is defined as the total voltage discharged of the supercapacitor due to sleep mode current, in 22 hours.

ΔV_s *= 0.1 V * 22/3.522 = 0.625 V* $\approx$ *0.7 V* (to be conservative)

ΔV_l is defined as the total voltage discharged of the supercapacitor due to leakage current, in 22 hours. Self discharge experiment conducted shows that ΔV_l = 0.1V

ΔV_{sl} is defined as the total voltage discharged of the supercapacitor due to sleep mode current and leakage current, in 22 hours.

ΔV_{sl} = 0.7 V + 0.1 V = *0.8 volt*

As the minimum operable voltage of V_t powering the DC-DC converter is 2.5 volt, no sensing and wireless transmission operation should be allowed once V_t is discharged to 2.5 + 0.8 = 3.3 volt. This is because of the need to reserve 0.8 volt to sustain the sleep mode operation of the embedded system under the continuous effect of sleep mode current and leakage current for the desirable operation time (which is set to be 22 hours in our case).

However, if the energy control algorithm works properly, V_t would never be discharged down to 2.5 volt.

Point (2) Optimization / Maximization of the Service Duty Cycle

After mitigating the sleep mode current and leakage current impact with the calculated minimum allowable operating voltage ($V_{t, min}$ = 3.3V), the design to maximize the WSN service duty cycle during the discharge of the supercapacitor from $V_{t, max}$ (4.1V) to $V_{t, min}$ (3.3V) is to be considered.

The design consideration is complicated because there are two parallel operating currents running at the same time. The first operating current is the sleep mode current, which is uncontrollable and cannot be turned off. The second operating current is the WSN operating current, which is controllable. Our objective is to maximize the WSN operating current (hence the WSN service duty cycle) during a desirable discharge period.

It is finally decided to design firstly the optimization / maximization of the service duty cycle, with an assumption that the sleep mode current is negligible. In the next point, that is anchor point 3, the sleep mode current will be evaluated for its impact on the discharge period.

Definition of WSN (wireless sensor node) service duty cycle % ($D_s\%$) = service time of WSN/total time elapsed.

$D_{s, max}\%$ is defined as the maximized service duty cycle % allowed for a sustained period during which no new solar energy is harvested.

Under a $D_{s,max}\%$ of 100%, discharge time equals to 26.94 seconds for discharge of 0.1 volt of the supercapacitor. If a discharge time of 22 hours is needed (i.e. 3,600 * 22 = 79,200 seconds), it is

necessary to divide the 100% $D_{s,\,max}$ % by a factor equal to 79,200/26.94 = 2,939.87.

As such, $D_{s,max}$ % in the discharge of V_t of 0.1 V in 22 hours = 100%/2,939.87 = 0.034%.

In one hour, 0.034% = 3,600 seconds * 0.034% = 1.2 seconds.

And as known by experiment that each WSN operation (sensing + wireless data sending) takes 0.1284 seconds,

Maximized number of WSN operations per hour = 1.2/0.1284 = 9.35 times ≈ 9 times (to be conservative).

That is, it shows that the WSN should sleep for 9 times and should wake up for 9 times to send out 9 data frames per hour. Thus, each sleep time duration = 3,600/9 = 400 seconds (6.67 minutes).

As every discharge of 0.1 volt will allow a $D_{s,max}$ % of 0.034% , the discharge of V_t from 3.4 volt to 3.3 volt will allow a $D_{s,max}$ % equal to 0.034%, and the discharge of V_t from 3.5 volt to 3.3 volt will allow a $D_{s,max}$ % equal to 0.034% * 2 = 0.068%.

Following the same logic, for every 0.1 volt that when V_t is higher than 3.3 volt, one additional 0.034% should be added to our $D_{s,max}$ %.

Point (3) Management of the Impact of Sleep Mode Current on the Maximized Service Duty Cycle Discharge Period

For the newest generation of microcontrollers, their sleep mode currents are reduced to a very small magnitude of 10 μA to 20 μA. The sleep mode current can therefore be approximated as negligible. However, as the sleep mode current of the microcontroller (Microchip pic24f) in our WSN hardware platform is significantly larger (170 μA or 0.17 mA), its impact on the maximized service duty cycle discharge period is also significant.

The impact of sleep mode current on the maximized service duty cycle discharge period is calculated below:

From point (1), sleep mode discharge current in a discharge of 0.1V will last for 3.522 hours.

From the discharge of $V_{t,\,max}$ (4.2V) to $V_{t,\,min}$ (3.3V), discharge duration by sleep mode current

$$= 3.522 \text{ hours x } \frac{(4.2-3.3)}{0.1}$$

$$= 3.522 \text{ hours x } 9$$

= 31.698 hours

By our design in point (2), discharge duration by the WSN maximized operation is known to last for 22 hours, if there is no sleep mode current.

In the presence of significant amount of sleep mode current, combining the two operating currents together results in :

Discharge duration from $V_{t,\,max}$ (4.2V) to $V_{t,\,min}$ (3.3V) under WSN maximized operation

$= 22 \text{ x } (\frac{31.698}{22+31.698})$

$= 22 \text{ x } (\frac{31.698}{53.698})$

= 12.9866 hours

≈ 13 hours

The average nighttime duration from sunset to sunrise in Vancouver in Winter usually lasts for 12 hours. The above resulting discharge duration from $V_{t,\,max}$ to $V_{t,\,min}$ of 13 hours is enough to allow the WSN for a full night maximized service duty operation, even in the worst solar harvesting season in Winter.

6.2.2 Augmented MPC Energy Control Algorithm Design for 22 hours Continuous Maximized Operation

Using these computed parameters, a maximized service duty cycle % ($D_{s,max}$ *%)* and sleep mode period table based on a 22 hours continuous maximized operation duration (with an assumption of negligible sleep mode current, using our hardware platform for testing, and the duration reduced to 13 hours as explained in point (3) of the last section) is constructed below.

Table 6-3 AMPC Algorithm parameters for Augmented MPC Energy Control Algorithm for 22 hours continuous operation

V_t (volts)	$D_{s,max}$ %, for 22 hours operation	Sleep times/hr	Sleep time duration (s) - See note 5	No. of service duty/hr
> 4.1	Can be 100%, set at 0.034% (See note 1)	72	48	72

V_t (volts)	$D_{s,max}$ %, for 22 hours operation	Sleep times/hr	Sleep time duration (s) - See note 5	No. of service duty/hr
4.1 – 4.0	0.034* 8 =0.272	72	48	72
4.0 – 3.9	0.034* 7 =0.238	63	64	63
3.9 – 3.8	0.034* 6 =0.204	54	80	54
3.8 – 3.7	0.034* 5 = 0.17	45	80	45
3.7 – 3.6	0.034* 4 =0.136	36	96	36
3.6 – 3.5	0.034* 3 =0.102	27	128	27
3.5 – 3.4	0.034* 2 =0.068	18	208	18
3.4 – 3.3	0.034	9	400	9
3.3 – 2.6 Minimized operation	0.35/3600 % =0.00972 See note 2	1	3,600	1
2.5	0.00972 See note 3	1	3,600	1
< 2.5 Dead time	See note 4			

Notes to Table 6.3:

Note 1: when V_t > 4.1volt, supercapacitor is fully charged up which indicates a surplus energy situation harvested from solar energy harvester. Under this situation, $D_{s,max}$ % can be set to 100% in principle. However, for practical usage to avoid excessive data sending, it is set to be the same 0.272% for V_t from 4.1 to 4.0 volts.

Note 2: minimized service duty is maintained by sending out one wireless data frame per hour. Power consumption is almost negligible.

Note 3: wireless sensor node embedded system will be shut down due to energy depletion of the supercapacitor down to the minimum operable voltage at 2.5 volt. Before system shut down, one

last data frame will be sent out.

Note 4: when V_t drops under 2.5 volt, wireless sensor node will be shut down and no more voltage recording of V_t is possible.

Note 5: for simpler algorithm programming into the microcontroller, a time base of 16 seconds is used. As such, sleep time duration is rounded up to the closest multiples of 16 seconds.

The above table is implemented in C codes into the WSN embedded system for field tests. The next chapter will present the results of the field tests.

6.3 Conclusion

In this chapter, a new design of an energy control algorithm is proposed. It is based on the use of MPC algorithm to compute important control parameters and on the employment of three new design principles to handle two mingled input variables. Detailed elaboration on the use of 'Matlab' MPC toolbox design tool is provided. The need and the principles behind the proposed new algorithm design are also presented in this chapter.

A design is constructed to cater for 22 hours continuous maximized operation of a WSN embedded system without any new solar energy harvesting and under a condition that sleep mode current of the WSN is negligible. Since the sleep mode current of the WSN is significant as in our choice of the testing hardware platform, the duration of continuous maximized operation of the WSN, for testing purpose, is reduced to 13 hours, which is still sufficient for a full night operation in Winter.

The resulting new energy control algorithm based on the design is ready to be implemented on a WSN hardware platform. Its performance and robustness are validated in the next chapter.

CHAPTER 7: SYSTEM IMPLEMENTATION AND FIELD TESTS

7.1 Algorithm Implementation in WSN Embedded System

Using the results in Table 6-3 in last chapter, the control algorithm is written in C codes and is implemented in the Microchip pic24f microcontroller in the self designed WSN embedded system.

Programming of the algorithm using C codes is straight forward. It involves the sensing of the supercapacitor's terminal voltage, with decision loops to determine the on and off duration of the XBee wireless transmitter.

If only for conducting the research of the novel MPC control algorithm, it is not necessary in this research to build a self designed wireless sensor node embedded system. However, a system is built in order to allow the best control and flexibilities in conducting the research and experiments. As the research focus of this thesis is not on the detailed design of the embedded system, only a brief description of the self-constructed system is included in this paper.

Below FIGURE 7-1 is a photo of the self designed wireless sensor node embedded system:

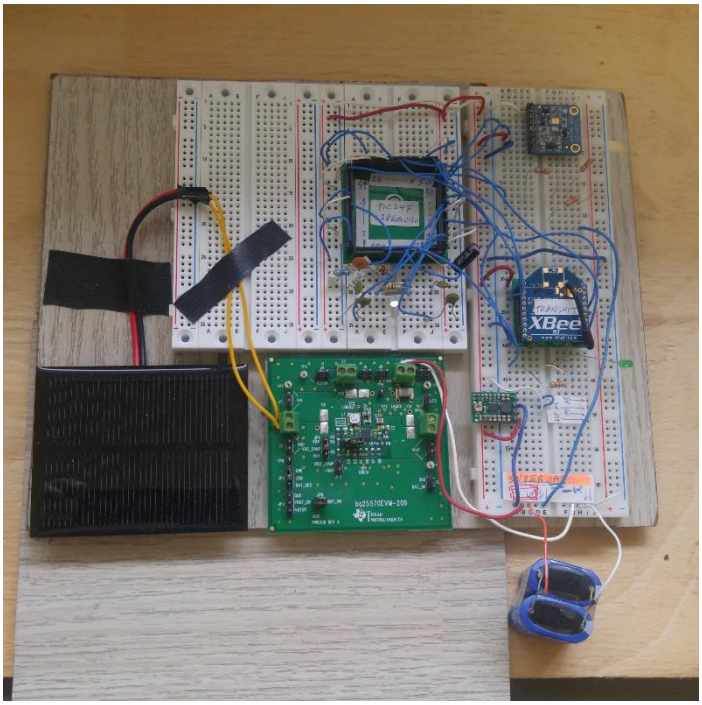

Figure 7-1 Self designed wireless sensor node embedded system

The self designed wireless sensor node embedded system is composed of these components:

(1) A 16 bit 'Microchip' pic24f 16 bit microcontroller,

(2) A 'Texas Instrument' light spectrum sensor integrated circuit TCS34725,

(3) A 'Xbee' S1 Zigbee low power wireless transmitter using IEEE 802.15.4 protocol,

(4) A 'Texas Instrument' solar power energy harvester module BQ25570,

(5) A 'Pololu' DC-DC converter module (2.5V – 5.5V converted to 3.3V, using a TPS63060 DC converter integrated circuit),

(6) 4 pcs of 'AXA' model 1637 (5.5V, 5F) supercapacitors connected in parallel, and

(7) 1 pcs of 5.5 V, 100 mA miniature solar panel.

At the beginning of the hardware design stage, the DC charger output voltage of the 'Texas Instrument' BQ25570 energy harvester module was fixed at 4.2 volt as referred by the manufacturer's datasheet. However, at the time of ordering the energy harvester module to put together the hardware testing system, the DC charger output of the energy harvester module was upgraded by the manufacturer to 5.5 volt. This hardware change improved the performance of the energy control algorithm which was designed originally based on a maximum charging voltage of 4.2 volt.

7.2 Data Error Analysis

It is mentioned earlier in section 5.2, the importance to use a precise two branch model for the supercapacitor, in order to allow for an accurate MPC algorithm prediction. On the other hand, it is also obvious that the inevitable data measuring errors in the state space model parameters identification as elaborated in section 5.3.2 will generate errors in the resulting state space parameters.

However, the theoretical analysis of the impact of the propagation of state space model parameters measuring and identification errors to the prediction output, is an in-depth research topic by itself which attract many research work and papers written for the topic. The analysis difficulty of the problem arises from the error propagation with hundreds of matrices computations in a typical MPC algorithm computation, along with other consideration. It is also mentioned in various MPC theory textbooks that these propagation errors can be mitigated by a 'tuning process' of a MPC controller to correct the inaccuracy of state space model parameters identification [30], [32], [33] & [34].

Although there is no intention to provide a detail analysis of the 'impact of model parameters error on MPC prediction' in this research and thesis, there are significant efforts in this research to ensure that all data measured are done with acceptable measuring errors. Data Error Analysis is also done with focus on the measurement for the parameters identification of the two branch state space model, and most importantly, on the accuracy of the data (terminal voltage value of the supercapacitor) obtained by the ADC (Analog to Digital Converter) sensing circuit in the microcontroller.

Firstly, effort is spent to find out the required number of samples of the measurement of the voltage value and milliampere value (measured by a multimeter with 1% accuracy) and time duration (in seconds, measured by a smart phone stop watch with 1% accuracy) during the state space model parameters identification process as seen in section 5.3.2. As a deviation of the prediction output of 5% in the targeted sustained operation of the WSN (i.e. a deviation of 22 hours x 0.05 = 1.1 hour) in this selected greenhouse automation application would be tolerable to the overall algorithm performance, an error percentage of 5% is selected as our model parameters identification measurement requirement.

Experiments show that standard deviation of the measurement of voltage, milliampere and the discharge time duration is within about 5% when a sampling size of ten is used. As a result, sample sizes of ten are used to obtain the mean values of measured data during the parameters identification process which results in much more accurate measurements than determined by the measurement equipment alone.

Secondly, the most important possible error generated by the sensing and measuring of the

supercapacitor terminal voltage by the microcontroller is analyzed and mitigated. There is a need to find out whether the potential sensing error is acceptable or not, by the below analysis:

Microchip pic24f microcontroller (16 bit) used in this research uses a 10-bit ADC (Analog to Digital Converter).

A 10-bit ADC has 2^{10} or 1,024 possible codes. So for the measurement of 5V, the resolution (accuracy) is 5V/1,024, or 4.88 mV.

Error % of measuring 5V = 4.88 mV/5V = 0.0976%

The above analysis shows that the measurement error % of the voltage value of the supercapacitor will be kept within a deviation of 0.1% in this research. On the other hand, it is decided not to perform a detail MPC model parameter errors analysis due to the limitation of time and scope in this research. Instead, sampling size of ten samples is chosen during the model parameters identification process to calculate the mean of measured data so that a standard deviation is kept within 5%. An error analysis is elaborated in section 6.1.13.10. Sec_6_1_3_10

7.3 Field Validation and Testing of Augmented MPC Energy Control Algorithm

To validate the new energy control algorithm's effectiveness, as well as its robustness, four types of field tests are conducted in a period of about two months.

The four types of tests are conducted under different testing conditions to see whether the wireless sensor node powered by the new design of energy control algorithm can sustain a continuous maximized WSN operation for a desired period of 22 hours without any new solar energy harvesting.

To conduct the field tests, the WSN embedded testing system is put in a transparent plastic case and placed on a sundeck to provide solar harvesting environment similar to that in a greenhouse. The transparent plastic case protects the embedded system from the rain while allowing solar irradiation to pass through to the miniature solar panel. FIGURE 7-2 in the following page is a photo showing the testing environment.

The wireless data frame transmits by the WSN through a 'Xbee' wireless transmitter is captured

by a 'Xbee' wireless receiver connected to a laptop computer which saves the data into a file. A serial terminal software called 'XCTU' supplied by 'Xbee' is used in the laptop computer for the wireless data recording. However, other popular serial terminal software such as Hyperterminal or Tera Term can also be used to do the data recording.

Figure 7-2 WSN embedded system placed in a plastic case on top of a sundeck for field tests

The four types of field tests conducted use the new energy control algorithm design to sustain a continuous operation of 22 hours without any new solar energy harvesting. Details of these tests are as follows.

(1) Normal Test - the wireless sensor node embedded system is placed in a plastic waterproof container and is placed on a sundeck to simulate a greenhouse operating environment;

(2) Stress Test I - to test the algorithm's robustness under an abnormal and unpredictable situation - half of the miniature solar panel is covered by a black adhesive tape, to simulate a possible field situation that the solar panel's surface is obstructed by a leaf or any other material;

(3) Stress Test II - to test the algorithm's robustness under another abnormal and unpredictable situation - half of the supercapacitor bank composed of 4 pieces of 5.5V, 5F supercapacitors is disconnected, to simulate a possible field situation that half of the supercapacitors become defective;

(4) Extreme Test – to conduct an extraordinarily challenging test by placing the wireless sensor node embedded system in an indoor environment, with an aim to create a failure situation for the energy control algorithm operating under an extremely adverse situation.

The field tests results are shown in the following four graphs.

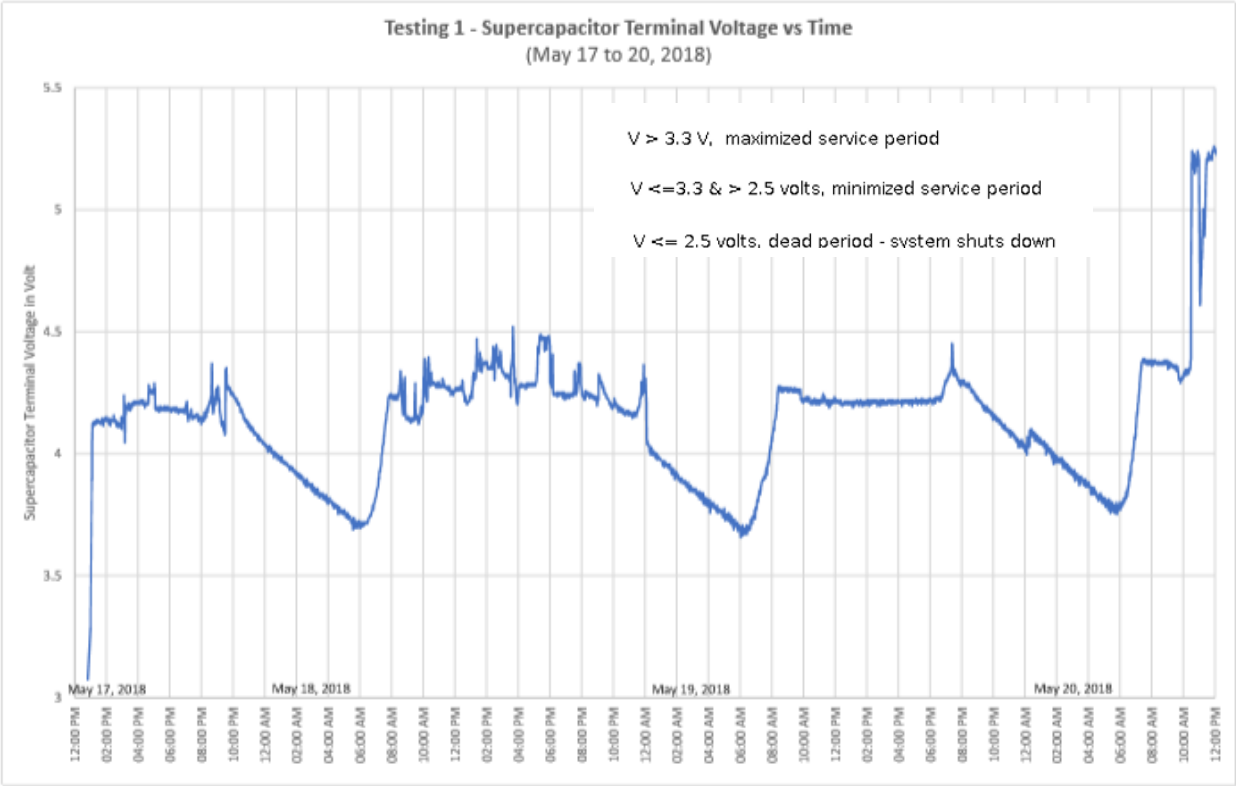

Figure 7-3 Graph (1) Field Test under simulated greenhouse operating environment

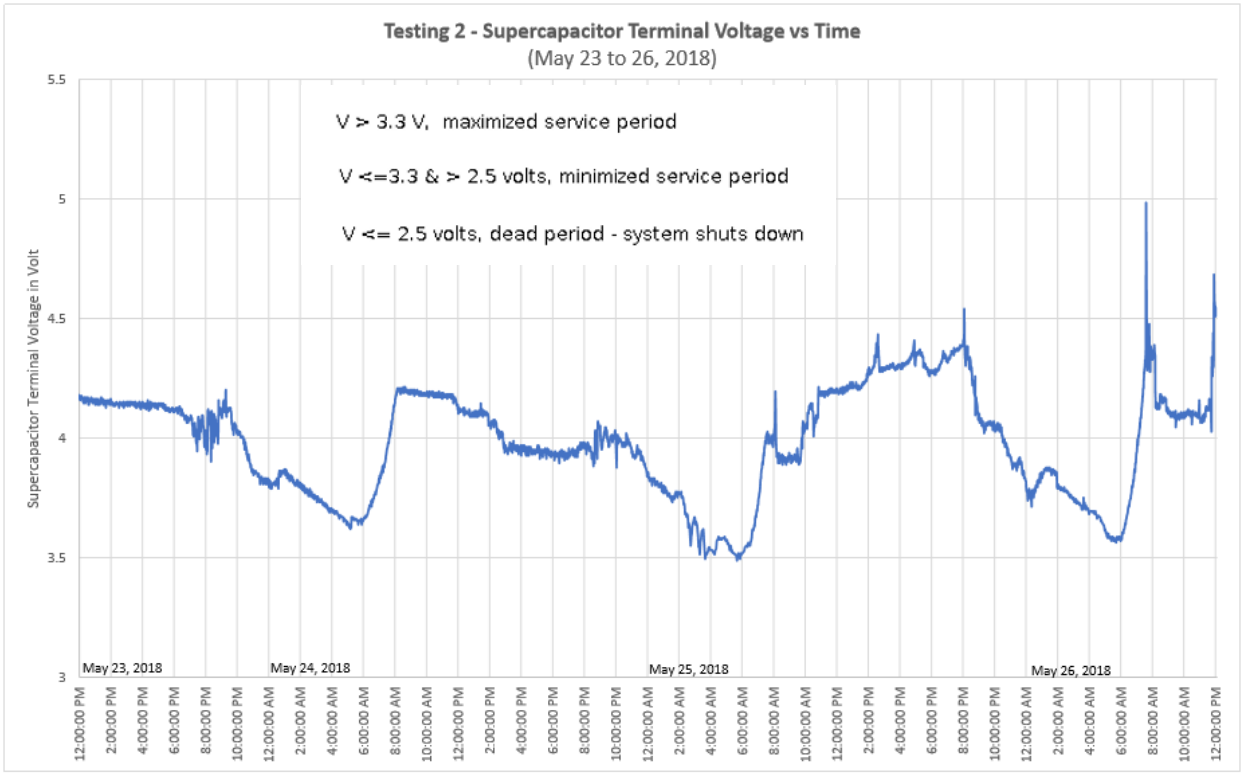

Figure 7-4 Graph (2) Field Test under Stress Test I

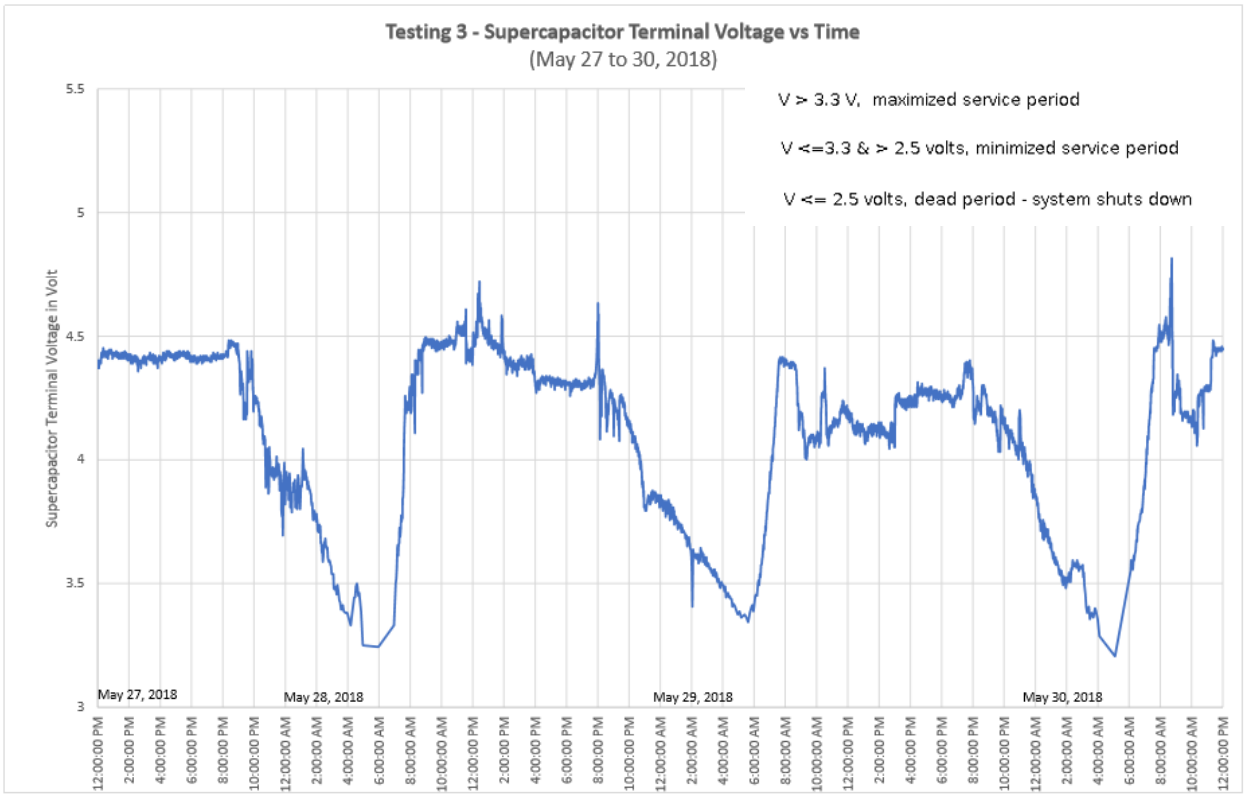

Figure 7-5 Graph (3) Field Test under Stress Test II

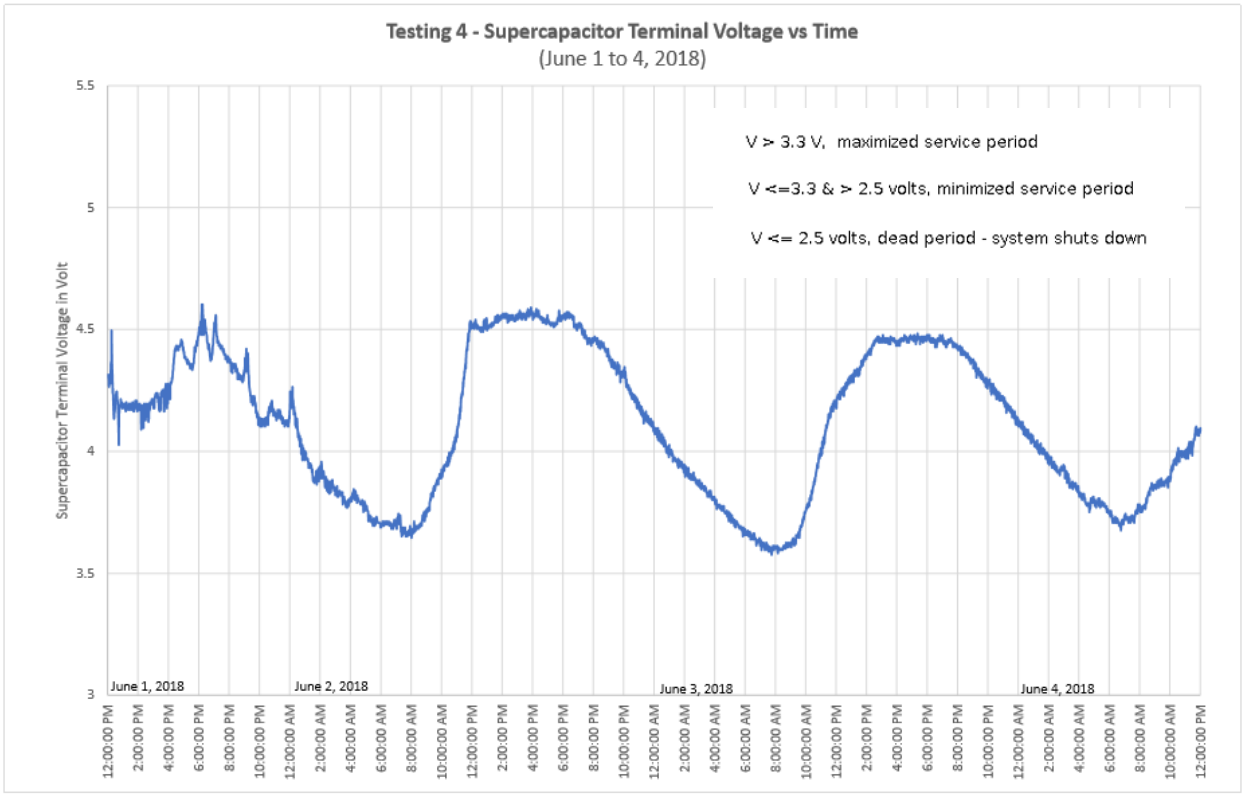

Figure 7-6 Graph (4) Field Test under extreme abnormal operating condition

7.4 Interpretation of field test results

FIELD TEST (1)

In field test (1), the wireless sensor node was placed in a plastic case on a sundeck to simulate a greenhouse operating environment. Three days of testing was conducted, with a total period of 72 hours, which was more than 3 times of the desired continuous operation of 22 hours under zero energy harvesting situation.

The precipitation in the three days of testing were 0 mm on May17, 2018 and 0 mm on May 20, 2018. The three days testing period was typical Vancouver (Canada) summer weather, where little precipitation was present and solar energy irradiation was quite strong. The intention of the test was to find out the performance of the wireless sensor node in a normal weather situation. The test started at noon time with a relatively low voltage level of about 3 volt at the supercapacitor terminal voltage. A

relatively low starting voltage was used due to the ideal summer sunny weather condition. On the other hand, if the testing was conducted on a raining winter weather condition, a much higher starting terminal voltage would be used to conduct the testing.

FIGURE 7-3: Graph (1), normal testing condition reflects an encouraging result. From noon to 9 pm on May17, 2018, the terminal voltage of the supercapacitor was charged up rapidly to about 4.2 volt with a maximized wireless sensor node operation of sending 72 data frames in every hour. After sunset at about 9 pm, the supercapacitor terminal voltage V_t gradually discharged during the nighttime. At 6 am of May 18, supercapacitor terminal voltage was discharged to about 3.75 volt. At this voltage level, the wireless sensor node continued its service duty of sending 45 data frames per hour. Once sun rose at around 6 am, the supercapacitor was charged up again by the solar energy harvester rapidly in two hours to about 4.25 volt at 8 am. It stayed at a relatively high voltage level between 4.25 volt and 4.5 volt until 10 pm before the sun set. At this voltage level, the wireless sensor node provided its maximized service duty of sending 72 data frames every hour. The weather of May 19 was almost the same as May 18. During the daytime period of May 19, a maximized service duty cycle of the wireless sensor node was performed according to our algorithm parameters set in AMPC Table 6-3 , with 72 wireless data frames sent out per hour.

It is interesting to note that on May 20, 2018, the last day of the test, it was a very bright sunny day with high solar irradiation. The test data reflected in the chart shows that the supercapacitor was charged up to more than 5 volt at about noon time and stayed at a high voltage level throughout the day.

Results as summarised below:

- no dead time recorded;

- 0.5 hours out of 72 hours (0.7%) were in minimized service duty operation;

- 71.5 hours out of 72 hours (99.3%) were in maximized service duty operation.

FIELD TEST (2), UNDER STRESS TEST I

Upon completion of test (1), we proceeded to test (2) where the performance of the algorithm under the first simulated stress condition was tested. Also labelled as Stress Test I, half of the miniature solar panel was covered with a black adhesive tape, simulating a situation that a piece of leaf or other material fell on the solar panel.

To cater for the challenge of the stress test, the terminal voltage of the supercapacitor was charged

up to 4.15 volt, at the beginning of our test. This was done due to the anticipation of the unfavourable solar energy harvesting situation resulted from the deliberate covering of half of the miniature solar panel.

Test was done from May 23, 2018 to May 26, 2018. The weather situation was similar to that in the previous test, with precipitation of 0 mm on May 23, 2018 and 0 mm on May 26, 2018.

Test result as shown in FIGURE 7-4: graph (2) reflects that the reduction of solar energy harvesting with solar panel half covered resulted in a lower supercapacitor terminal voltage in the daytime. With half of the solar panel covered, the supercapacitor terminal voltage remained at voltage level between 4.15 volt and 4.0 volt during the day. In comparison, the supercapacitor was further charged up gradually during the day in the previous test. Apparently, at a maximized service duty of sending out 72 data frames per hour, solar energy harvested was just enough to fulfill the maximized service duty of the wireless sensor node. That is, with the maximized service duty provided to the wireless sensor node, the energy control algorithm was able to optimize and maximize the wireless sensor node's performance while optimally maintaining the supercapacitor's terminal voltage. In fact, graph (2) looks like graph (1), both of which performed maximized service duty during the whole testing period. The performance of this stress test was actually better than the first normal test. In the first normal test, we recorded a minimized service duty operation of the wireless sensor node at 0.7% of total testing time. This time, there was no minimized service duty operation recorded. This was obviously due to the use of a much higher supercapacitor terminal voltage to start off the stress test. It is also noted that the voltage level of the supercapacitor spiked at certain time during the day. The wide fluctuation of the solar irradiation caused the spikes in solar energy harvester's charging current to the supercapacitor.

Results as summarised below:

- no dead time recorded;

- 72 hours out of 72 hours (100%) were in maximized service duty operation.

FIELD TEST (3), UNDER STRESS TEST II

It is the intention to find out what would happen to the algorithm's performance should some of the supercapacitors fail.

Stress Test II was conducted with a disconnection of half of the four-supercapacitors bank. This reduced the 20 Farad supercapacitor bank into a 10 Farad supercapacitor bank. To cater for the unfavourable condition of the stress test, the supercapacitor terminal voltage was charged up to 4.4 volt to start off the test.

The weather condition during this test was similar to that in our last two tests, with no precipitation during the 3 days testing period from May 27, 2018 to May 30, 2018.

FIGURE 7-5: Graph (3) shows that the size reduction of the supercapacitors bank due to failure (deliberate disconnection) of half of the supercapacitors did not affect much the charging of the supercapacitor but affected to some extend the rate of discharge of the supercapacitor. This was to be expected as the sunny weather was able to charge up the supercapacitors relatively rapidly despite its size difference, but the energy control algorithm's performance was affected to some extend due to the failure of half of the supercapacitors. It is noted that in the graph, from 5 am to 6 am of May 28, and from 4 am to 5 am of May 30, the supercapacitors' terminal voltage discharged below 3.3 volt. 3.3 volt was set in our design as the minimum voltage for executing the maximum duty cycle of the wireless sensor node. The test result showed that a minimum duty cycle was executed in those two hours, sending only one wireless data frame performed per hour. Even in this adverse situation, no dead time was recorded. However, we can imagine that the result might had been much worse if the test was done in the raining winter season in Vancouver.

Results as summarised below:

- no dead time recorded;

- 2 hours out of 72 hours (2.8%) were in minimized service duty operation;

- 70 hours out of 72 hours (97.2%) were in maximized service duty operation.

FIELD TEST (4), UNDER EXTREME WEATHER CONDITION

With the previous three tests completed, we put our system in an extremely abnormal environment in which failure was likely.

An extreme situation may be an acute/disastrous weather condition with very heavy rain lasting for months and with very little solar irradiation.

However, it would have been very difficult, if not impossible, to simulate such an environment during our testing period which was the sunny summer season in Vancouver. It was decided that putting the WSN system to operate in an indoor environment would create a similar situation. Based on separate tests, the current harvested from the miniature solar panel was only 1/15 when it was placed indoors compared to outdoors. Such a prolonged raining situation is very unlikely to happen, but the extreme test was conducted just to find out how badly the energy control algorithm would fail.

To cater for the unfavourable condition of the stress test, the supercapacitor terminal voltage was charged up to 4.3 volt to start off the test. At the same time, the embedded system under test was placed indoor close to a bright window to allow significant amount of indirect solar irradiation to be harvested by our testing system.

To our big surprise, results in FIGURE 7-6: graph (4) reflects that the anticipated high percentage of dead time of the operation of the wireless sensor node did not happen. We noticed that there was some discharge of the supercapacitors bank during the day and a much earlier constant discharge of the supercapacitors bank starting at 7 pm everyday. The performance was inferior to the supercapacitors' charging and discharging performance in our last three tests. This was to be expected due to the much weaker indoor solar irradiation. However, for the whole time during the three days testing period, the supercapacitors' terminal voltage maintained a healthy voltage level above 3.5 volt, which was a surprising performance. As such, the energy control algorithm allowed the wireless sensor node to operate with a maximized service duty for the whole 3 days testing period. There was also no deadtime recorded. In a way, it seems that our objective to simulate a heavy raining weather was not totally successful by putting the testing system in an indoor environment. A real test under heavy raining weather for many days is needed to find out the real stress impact to our energy control algorithm. On the other hand, the good performance of this stress test showed that the design of the energy control algorithm is robust and resilient under unexpected and unfavourable operating environment.

Results as summarised below:

- no dead time recorded;

- 72 hours out of 72 hours (100%) were in maximized service duty operation.

CONCLUSION OF THE FOUR FIELD TESTS

Among the 4 field tests with the use of the design of the new energy control algorithm, there was no deadtime recorded and in most of the time during the four tests, the wireless sensor node operated at our designed maximized service duty effected by our energy control algorithm. At the same time, the augmented MPC energy control algorithm shows strong robustness even when it is subject to unexpected operating environment.

Although the field tests demonstrate an encouraging performance of the new energy control algorithm, it is fair to say that the relatively short period of testing with the good summer weather

condition has its limitation of accuracies to truly reflect the performance of the new energy control algorithm. Only a prolonged period of field test for several months can determine with certainty if the energy control algorithm can achieve a 100% success rate in continual operation under different weather condition and in different locations.

7.5 Conclusion

In this chapter, the new energy control algorithm is implemented in a self designed WSN embedded system hardware, for the purpose of conducting four field tests. The four field tests presented shows that the new energy control algorithm fulfills the design objectives with strong robustness to changing environment and unexpected hardware failures. While many related researches validate their energy control algorithms with software simulation, validation of the design in this research is based on both software simulation and comprehensive field tests with the algorithm implemented in a self designed hardware platform. The new energy control algorithm can create useful contribution both in the targeted 'IoT' applications as well as in many other applications that require precise energy control of stored energy in a specific prediction period.

CHAPTER 8: CONCLUSION AND SUGGESTION FOR FUTURE WORKS

The research objective in this thesis is to solve a bottleneck problem to allow a solar powered batteryless wireless sensor node embedded system to operate autonomously and continuously for more than 20 years without the use of and the need to replace any batteries. The shortfalls of past research are analyzed, and a novel energy control algorithm is developed and proposed. The new design is based on MPC theories augmented with necessary principles to isolate the two mingled input variables of active operating current and sleep mode current. The uncontrollable input variable is mitigated, and the other controllable input variable is maximized in the design to provide the desirable maximized wireless sensor node service duty. The proposed energy control algorithm achieves the desired continuous operation in adverse weather situation and has the robustness to operate under unexpected hardware failures.

In order to allow the best control in this research, a wireless sensor node embedded system powered by a solar energy harvester with a supercapacitor bank is designed and constructed. Although the hardware constructed is still far away from performing as a commercial product, it nonetheless demonstrates its capability as a very usable wireless sensing device in a typical "Internet of things" application. The new augmented MPC energy control algorithm resulted from this research can be implemented in numerous other application areas where one needs to optimize the energy usage out from a storage device and simultaneously sustain a continuous operation for a desired period.

A very famous past example in which our energy control algorithm might have potential to provide life saving value is the Apollo 13 spacecraft back to the earth mission (in April 1970). A single oxygen fuel tank powering fuel cells was operable for only a few days in its journey back to the earth from the orbit of the moon. Without a suitable energy control algorithm, a team of engineers and scientists in NASA struggled to calculate how to use the scarce energy remained.

Apart from these mission critical applications, there are many other general applications where one must control our energy resources wisely. The emerging market in electric cars and unmanned autonomous vehicles is another example. Future efforts will be continued to improve this research in energy control algorithm both in depth and in breath with the goal of enabling its full application.

BIBLIOGRAPHY

[1] M.M. Group, “Internet Usage Statistics 2017,” *Internet world statistics*, 2017. [Online]. Available: http://www.internetworldstats.com/stats.htm. [Accessed: 15-Jun-2017].

[2] Harvard Business Review Analytics, “INTERNET OF THINGS: SCIENCE FICTION OR BUSINESS FACT?,” *Harvard Business Review Analytics*, 2014. [Online]. Available: https://hbr.org/resources/pdfs/comm/verizon/18980_HBR_Verizon_IoT_Nov_14.pdf. [Accessed: 15-Jun-2017].

[3] M. Maiman, “Internet-of-things-4-key-elements,” *Intelligent Products Solution*, 2015. [Online]. Available: https://intelligentproduct.solutions/blog/internet-of-things-4-key-elements/. [Accessed: 15-Jun-2017].

[4] M. Elgan, “Google, A.I. and the rise of the super-sensor,” *Computerworld*, 2017. [Online]. Available: https://www.computerworld.com/article/3197685/internet-of-things/google-a-i-and-the-rise-of-the-super-sensor.html. [Accessed: 12-Feb-2018].

[5] Wikipedia, “Wireless Sensor Network,” *Wikipedia*, 2018. [Online]. Available: https://en.wikipedia.org/wiki/Wireless_sensor_network. [Accessed: 10-Jun-2017].

[6] D. Ha, “Research Trend and Technical Challenges on Small Scale Energy Harvesting,” *Virginia Tech - Multifunctional Integrated Circuits and Systems Group (MICS) Newsletter*, pp. Vol1, No.1, 12-Dec-2012.

[7] J. Drew, “Energy Harvester Produces Power from Local Envronment, Eliminating Batteries in Wireless Sensors (Application Note, Linear Technology Inc.),” *Linear Technology*, 2010. [Online]. Available: https://www.analog.com/media/en/reference-design-documentation/design-notes/dn483.pdf. [Accessed: 17-Mar-2018].

[8] F. Schmidt, “The Advantages of Batteryless Power,” *Power Systems Design*, Mar-2015. [Online]. Available: https://www.powersystemsdesign.com/articles/the-advantages-of-batteryless-power/95/9032. [Accessed: 17-Mar-2018].

[9] D. Bruelli, L. Benini, C. Moser, and L. Thiele, “Design of a Solar-Harvesting Circuit for Batteryless Embedded Systems,” *IEEE Trans. Circuits Syst.*, vol. 56, no. 11, 2009.

[10] O. Lopex-Lopena, M. Penella, and M. Gasulla, “A New MPPT Method for Low-Power Solar Energy Harvesting,” *IEEE Trans. Ind. Electron.*, vol. 57, no. 9, 2010.

[11] O. Lopex-Lopena, M. Penella, and M. Gasulla, “A Closed-Loop Maximum Power Point Tracker for Subwatt Photovoltaic Panels,” *IEEE Trans. Ind. Electron.*, vol. 59, no. 3, 2012.

[12] S. Keeping, “Techniques to Limit Switching DC/DC Converter Inefficiency During Low Loads,” *Electronic Products Magazine*, Jul-2012. [Online]. Available: https://www.digikey.ca/en/articles/techzone/2012/jul/techniques-to-limit-switching-dcdc-converter-inefficiency-during-low-loads. [Accessed: 17-Mar-2018].

[13] S. Keeping, “Using PFM to Improve Switching DC/DC Regulator Efficiency at Low Loads,” *Electronic Products Magazine*, Feb-2014. [Online]. Available: https://www.digikey.ca/en/articles/techzone/2014/feb/using-pfm-to-improve-switching-dc-dc-regulator-efficiency-at-low-loads. [Accessed: 17-Mar-2018].

[14] U. Sengupta, “PWM and PFM Operation of DC/DC Converters for Portable Applications (Texas Instrument Application Article),” *Texas Instrument*, 2006. [Online]. Available: https://pdfs.semanticscholar.org/c885/a1d9de3a1873e46ee4cecf33983184e6006a.pdf. [Accessed: 17-Mar-2018].

[15] C. Moser, D. Bruelli, L. Thiele, and L. Benini, “Real time scheduling for energy harvesting sensor nodes,” *Real-Time Syst.*, vol. 37, no. 3, pp. 233–260, 2007.

[16] X. Jiang, J. Polastro, and D. Culler, “Perpetual environmentally powered sensor networks,” in *4th Int. Symp*, 2005, pp. 463–468.

[17] R. Bonert and L. Zubieta, “Characterization of double-layercapacitors for power electronics applications,” *IEEETrans.Ind.Appl.*, vol. 36, no. 1, pp. 199–205, 2000.

[18] T. Wei, X. Qi, and Z. Qi, “An improved ultracapacitor equivalent circuit model for the design of energy storage power systems,” in *2007 International Conference on Electrical Machines and Systems (ICEMS)*, 2007.

[19] R. Faranda, M. Gallina, and D. Son, “A new simplified model of Double-Layer Capacitors,” in *2007 International Conference on Clean Electrical Power*, 2007.

[20] Y. Zhang and H. Yang, “Modeling and Characterization of supercapacitors for wireless sensor network applications,” *J. Power Sources*, vol. 196, no. 8, pp. 4128–4135, 2011.

[21] Y. Zhang and R. Chai, “A Practical Supercapacitor Model for Power Management in Wireless Sensor Nodes,” *IEEE Trans. Power Electron.*, vol. 30, no. 12, 2015.

[22] A. G. Watts, “Managing Energy-Harvesting Environmental Monitoring Systems,” University of Alberta, 2014.

[23] N. L. Trong, O. Sentieys, O. Berder, A. Pegatoguet, and C. Belleudy, “Power Manager with PID controller in Energy Harvesting Wireless Sensor Networks,” in *2012 IEEE International Conference on Green Computing and Communications*, 2012, pp. 668–670.

[24] M. A. Kansal, J. Hsu, S. Zahedi, and M. B. Srivastava, “Power Management in Energy Harvesting Sensor Networks,” *ACM Trans. Embed. Comput. Syst.*, vol. 6, no. 4, Article 32, 2007.

[25] C. Moser, L. Thiele, D. Brunelli, and L. Benini, “Adaptive power management in energy harvesting systems,” in *Proceedings of the conference on Design, automation and test in Europe*, 2007, pp. 773–778.

[26] C. M. Vigorito, D. Ganesan, and A. G. Barto, “Adaptive Control of Duty Cycling in Energy Harvesting Wireless Sensor Networks,” in *2007 4th Annual IEEE Communications Society Conference on Sensor, Mesh and Ad Hoc Communications and Networks*, 2007.

[27] S. Peng and C. P. Low, “Throughput optimal energy neutral management for energy harvesting wireless sensor networks,” in *IEEE Wireless Communications and Networking Conference (WCNC)*, 2012.

[28] F. A. Aoudia, O. Gautier, and O. Berder, “Fuzzy Power Management for Energy Harvesting Wireless Sensor Nodes,” in *IEEE ICC 2016 Ad-hoc and Sensor Networking Symposium*, 2016.

[29] J. A. McEvoy, *THE UNIVERSE, FROM ANCIENT BABYLON TO THE BIG BANG*. Robinson Publisher, 2010.

[30] E. Mosca, *Optimal, Predictive & Adaptive Control*. Prentice Hall, 1995.

[31] J. A. Rossiter, "Video on model predictive control," *University of Sheffield, Department of Automatic Control and Systems Engineering*, 2018. [Online]. Available: https://www.sheffield.ac.uk/acse/staff/jar/mpcmaster. [Accessed: 12-Feb-2018].

[32] J. M. Maciejowski, *Predictive Control with Constraints*. Pearson Education (US), 2002.

[33] J. Rawlings and D. Q. Mayne, *Model Predictive Control: Theory and Design*. Nob Hill Publishing, 2015.

[34] L. Wang, *Model Predictive Control System Design and Implementation Using MATLAB®*. Springer-Verlag London Limited, 2009.

[35] J. Åkesson, "MPCtools 1.0 — Reference Manual," *Lund University*, 2006. [Online]. Available: http://lup.lub.lu.se/search/ws/files/4720262/8627312.pdf. [Accessed: 13-Feb-2018].

[36] M. Editor, "Application Note - Test Procedures for Capacitance, ESR, Leakage Current and Self-Discharge Characterizations of Ultracapacitors," *Maxwell Technologies, Inc.*, 2015. [Online]. Available: http://studylib.net/doc/18470417/test-procedures-for-capacitance--esr--leakage-current. [Accessed: 13-Feb-2018].

[37] Kyocera Editor, "'AVX' SCM Series Supercapacitor Modules datasheet," *Kyocera Corporation*, 2017. [Online]. Available: http://www.farnell.com/datasheets/2606177.pdf. [Accessed: 17-Mar-2018].

[38] A. Bemporad, M. Morari, and N. L. Ricker, "Model Predictive Control ToolboxTM Getting Started Guide," *The MathWorks, Inc.*, 2017. [Online]. Available: https://www.mathworks.com/help/pdf_doc/mpc/index.html. [Accessed: 17-Mar-2018].

[39] A. Bemporad, M. Morari, and N. L. Ricker, "Model Predictive Control ToolboxTM User's Guide," *The MathWorks, Inc.*, 2017. [Online]. Available: https://www.mathworks.com/help/pdf_doc/mpc/index.html. [Accessed: 17-Mar-2018].

[40] Wikipedia, “Internet of things,” *Wikipedia*, 2019. [Online]. Available: https://en.wikipedia.org/wiki/Internet_of_things. [Accessed: 01-Nov-2019].

[41] Wikipedia, “Wireless sensor networks,” *Wikipedia*, 2019. [Online]. Available: https://en.wikipedia.org/wiki/Wireless_sensor_network. [Accessed: 01-Nov-2019].

[42] Wikipedia, “Model predictive control,” *Wikipedia*, 2019. [Online]. Available: https://en.wikipedia.org/wiki/Model_predictive_control. [Accessed: 01-Nov-2019].

[43] Wikipedia, “Buck-boost converter,” *Wikipedia*, 2019. [Online]. Available: https://en.wikipedia.org/wiki/Buck–boost_converter. [Accessed: 01-Nov-2019].

[44] Wikipedia, “RC circuit,” *Wikipedia*, 2019. [Online]. Available: https://en.wikipedia.org/wiki/RC_circuit. [Accessed: 01-Nov-2019].

[45] Wikipedia, “Maximum power point tracking,” *Wikipedia*, 2019. [Online]. Available: https://en.wikipedia.org/wiki/Maximum_power_point_tracking. [Accessed: 01-Nov-2019].

ANNEX A ‘MATLAB’ MPC DESIGN PROCESS WITH SCREEN SHOTS

A.1 'Matlab' MPC Design Process 1 – Define Plant's State Space Model

'Matlab' simulation software 2017b is opened and shows the below screen display menu:

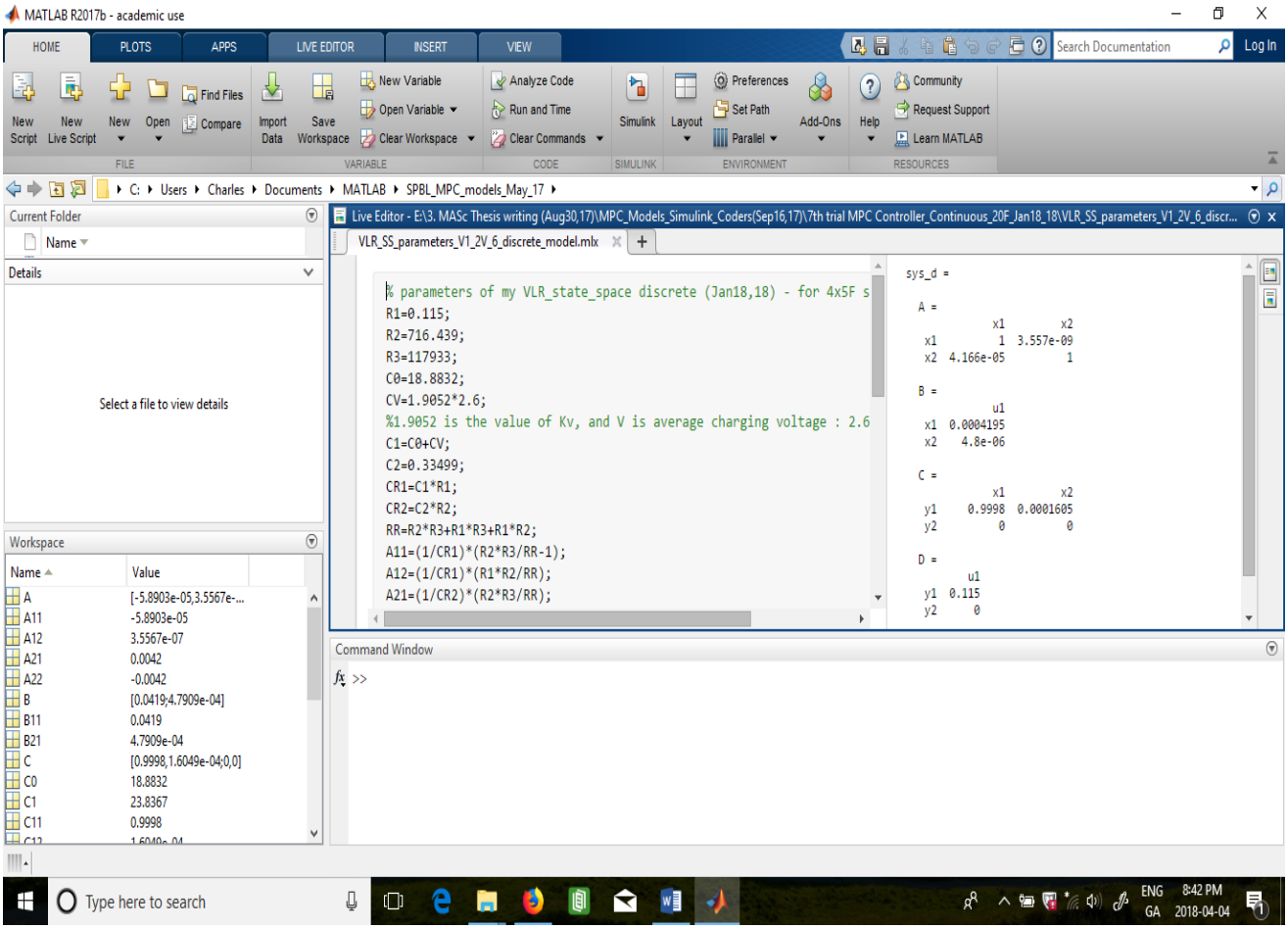

Figure A-1 'Matlab' MPC Design Process 1 - Define Plant's State Space Model

The first step in using 'Matlab' Simulink MPC designer is to define the controller plant's precise state space model. In this case, the controlled plant is the solar energy harvester state space model as defined precisely previously in section 6.1.2.

A.2 'Matlab' MPC Design Process 2 – Create 'Simulink' Plant's Model connected to a MPC Controller

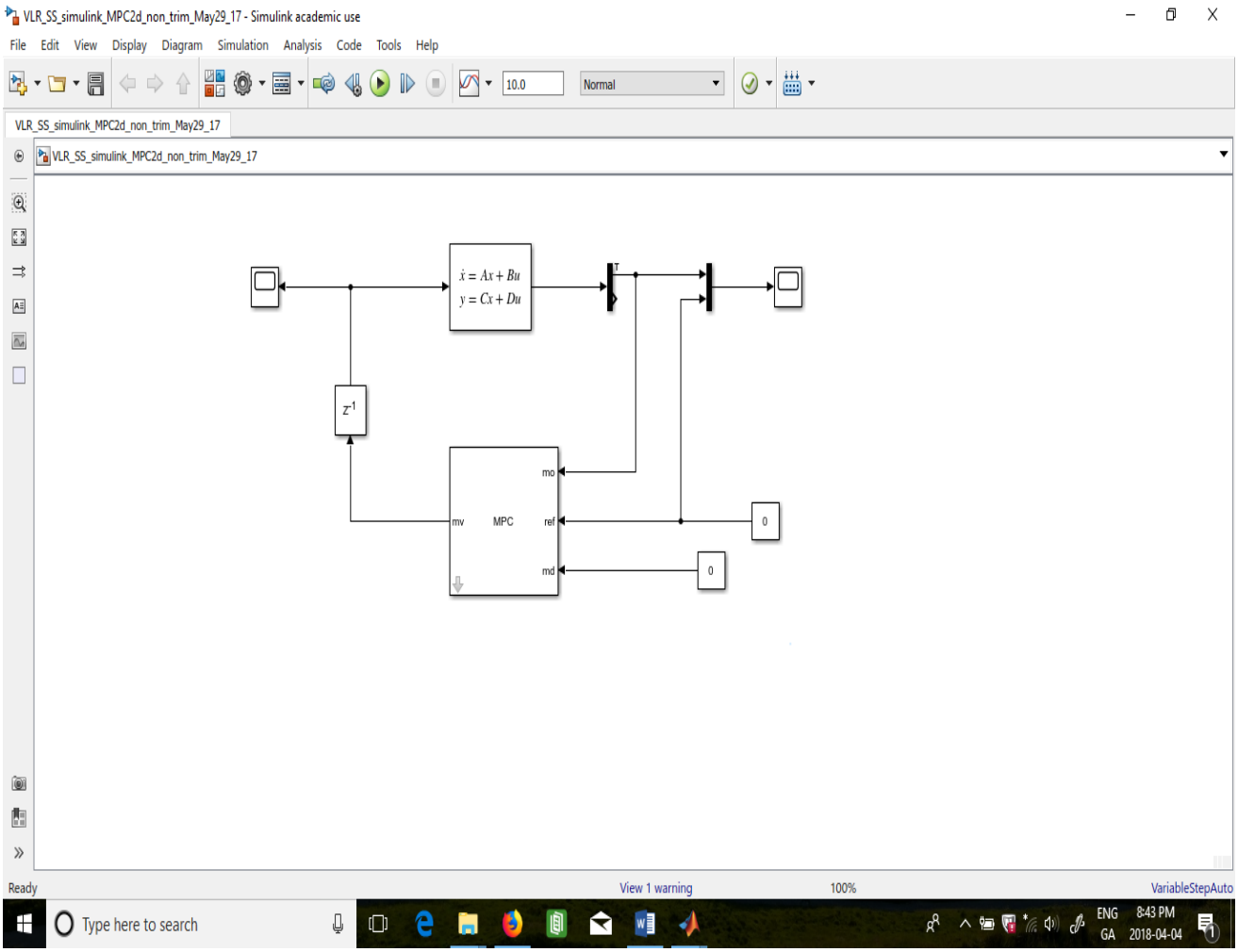

Figure A-2 'Matlab' MPC Design Process 2 - Create 'Simulink' Plant's Model connected to a MPC Controller

The second step in the 'Matlab' MPC design process is to create a 'Simulink' plant's model connected to a MPC controller as shown in above figure. Note that in this case, there is no external disturbance and there is no external reference and these manipulated inputs are set to zero constant. A delay block with defaulted delay time value is connected from the manipulated variable output from the MPC controller to the manipulated input port of our plant as a design requirement of the 'Matlab' controller. The output from the plant is highlighted with a 'Trim' function T so that a linearization point of the plant output can be defined in the later design process of plant's linearization at a particular operating point.

A.3 'Matlab' MPC Design Process 3 – Open 'Simulink' MPC Designer Design Function for Plant's Linearization

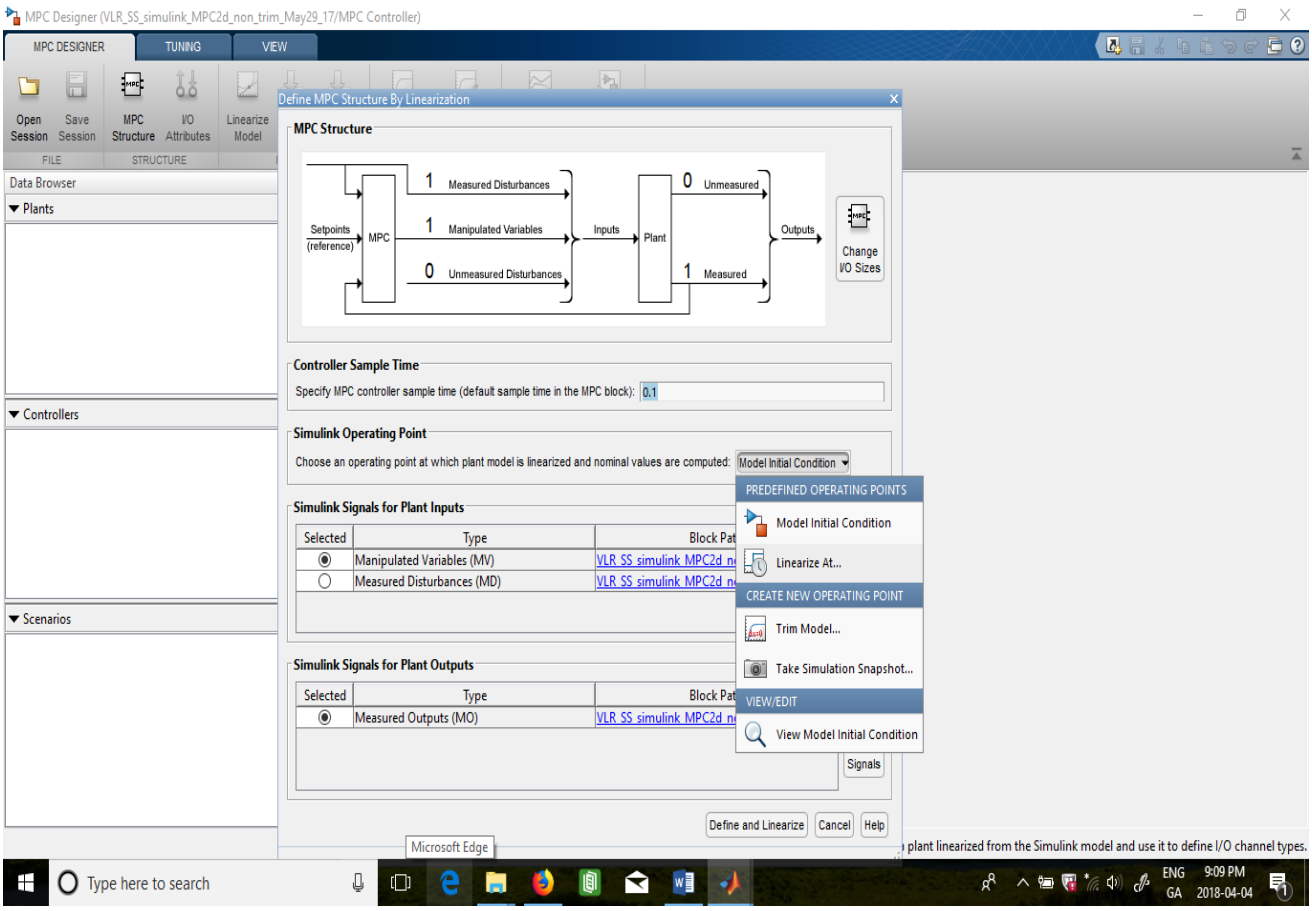

Figure A-3 'Matlab' MPC Design Process 3 - Open 'Simulink' MPC Designer Design Function for Plant's Linearization

The third step in the 'Matlab' MPC design process is to open 'Simulink' MPC Designer design function for plant's linearization. Select the MPC controller icon to go into the MPC Designer's main menu. In the MPC Designer's main menu, select function of MPC structure so that the option to create a new operating point (function of 'Trim Model') can be seen as shown in above Fig A-3.

A.4 'Matlab' MPC Design Process 4 – Specify Operating Point of Linearization

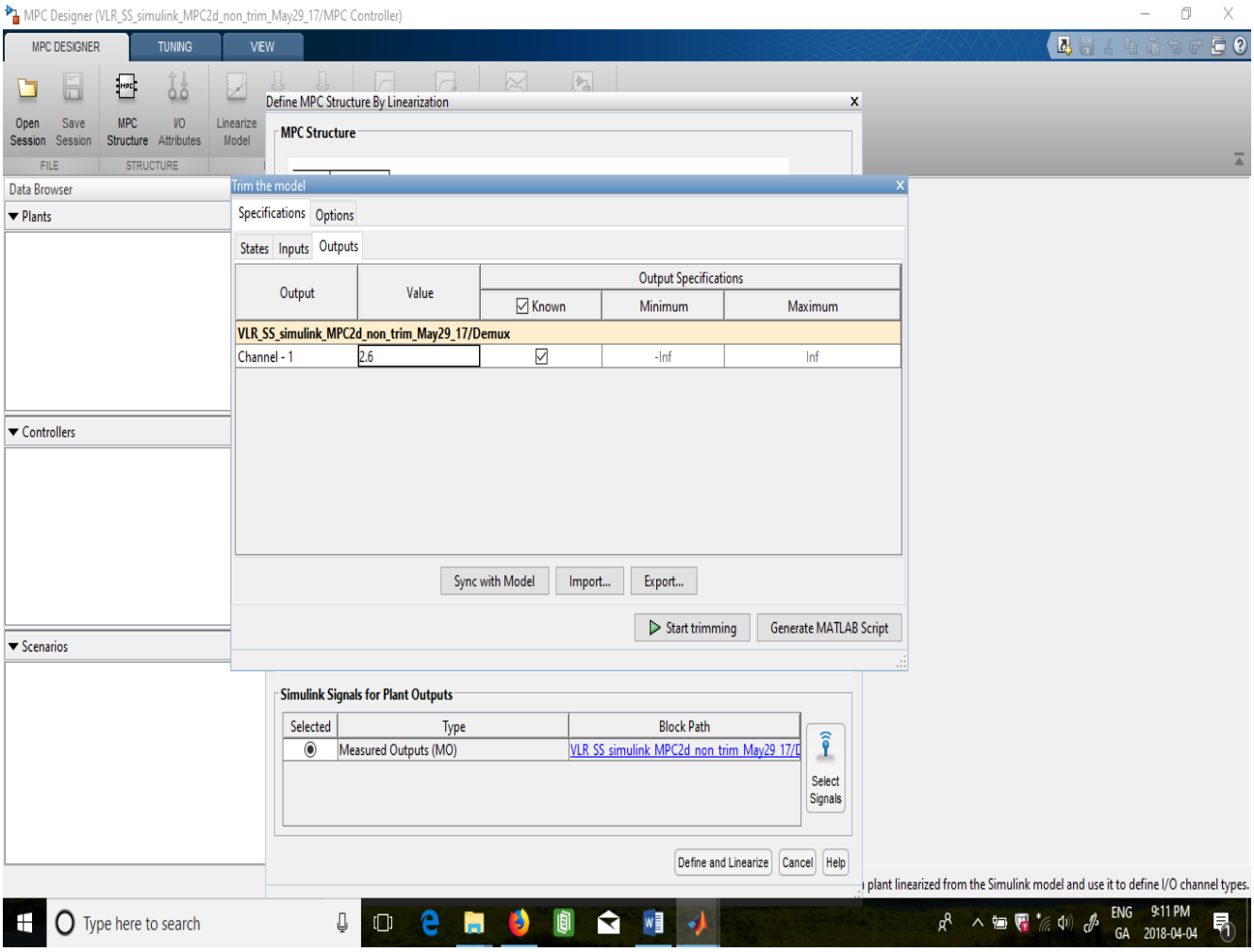

Figure A-4 'Matlab' MPC Design Process 4 - Specify Operating Point of Linearization

The fourth step in the 'Matlab' MPC design process is to specify the operating point of linearization of the plant by defining the plant's output voltage. Select the 'Trim Model' function in design process 3 so that a menu to specify the linearization point can be seen as shown in above Fig. A-4. The plant's output voltage is the terminal voltage of the supercapacitor which is this MPC computation is set to 2.6 volts.

A.5 'Matlab' MPC Design Process 5 – Observe Defaulted MPC Algorithm Design

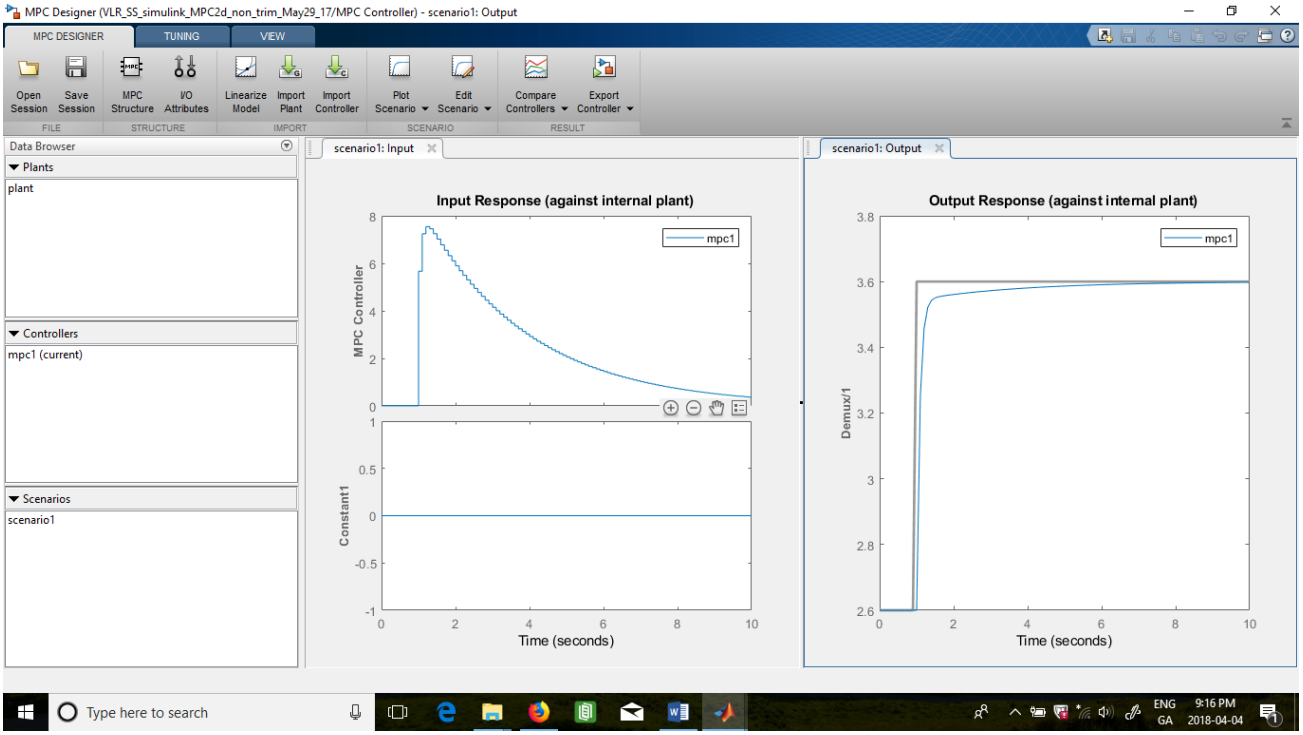

Figure A-5 'Matlab' MPC Design Process 5 - Observe Defaulted MPC Algorithm Design

The fifth step in the 'Matlab' MPC design process is to observe how the defaulted MPC algorithm generates a defaulted output response with a defaulted manipulated controller's input. After clicking the 'Start trimming' function in design process 4, the MPC controller generates a defaulted MPC control algorithm with defaulted output and defaulted manipulated input at the specified operating point (in this case, at output voltage of 2.6V).

As shown in above figure, the defaulted MPC algorithm design condition is defined with a prediction horizon of ten seconds, and with a control horizon set from the first second to the end of the ten seconds period, and its output reference at the end of the prediction horizon is set at 3.6 volts. With this defaulted design criterion, its manipulated control input can be seen from the Input Response Graph in Fig A-5, which shows an input current value of 8A from the first second with gradual decline in its control value to zero towards the end of its control period of 10 seconds.

A.6 'Matlab' MPC Design Process 6 – Specify Required MPC Algorithm Design Condition 1

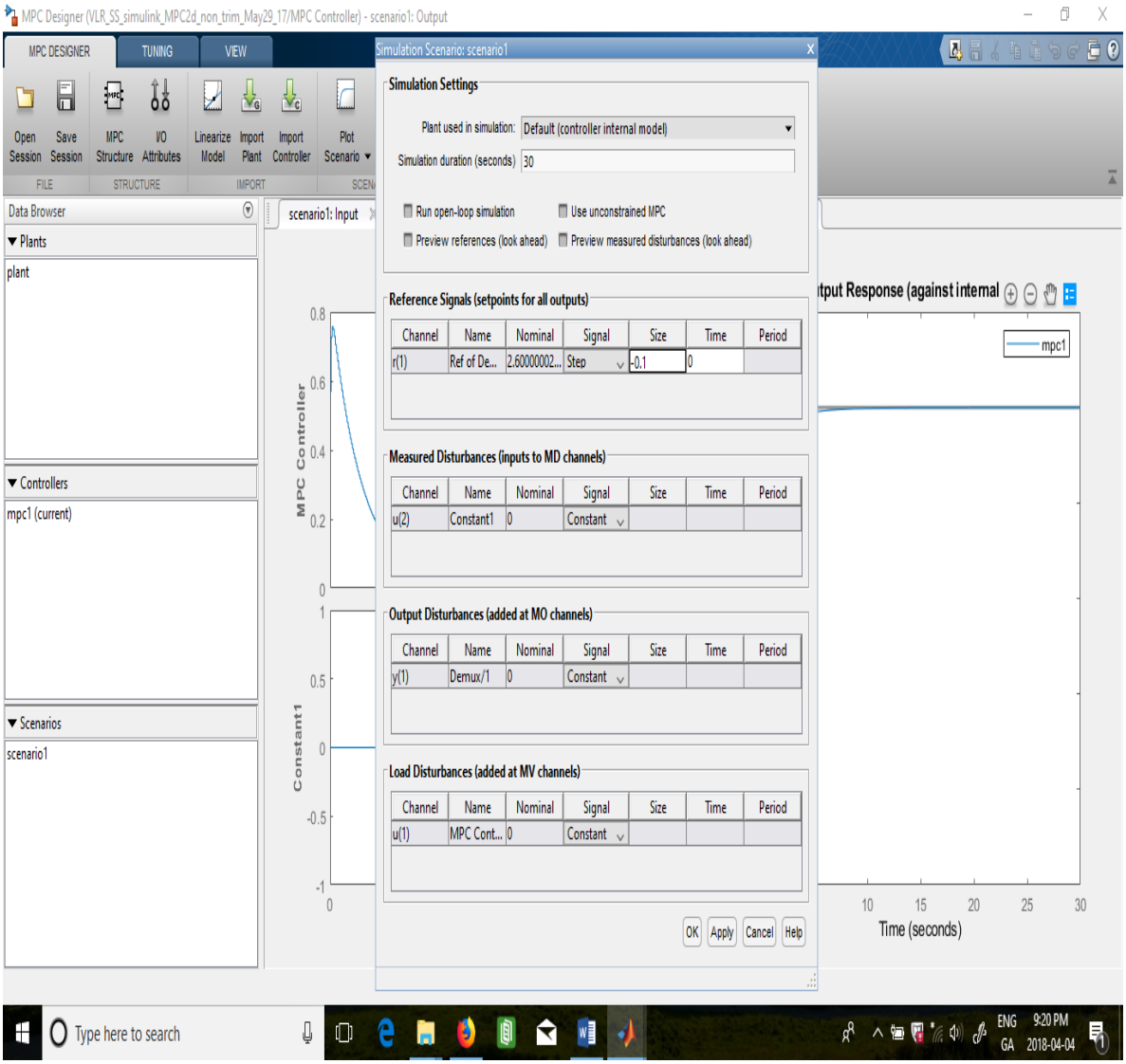

Figure A-6 'Matlab' MPC Design Process 6 - Specify Required MPC Algorithm Design Condition 1

The sixth step in the 'Matlab' MPC design process is to change MPC algorithm design condition of its reference output voltage as well as its prediction horizon. As shown in above Fig A-6, a reference signal of step output of -0.1V is set which equals to setting a final reference output voltage of 2.5V (2.6V – 0.1V). The simulation duration which is equal to the prediction horizon, is set to 30 seconds instead of 10 seconds.

A.7 'Matlab' MPC Design Process 7 – Specify Required MPC Algorithm Design Condition 2

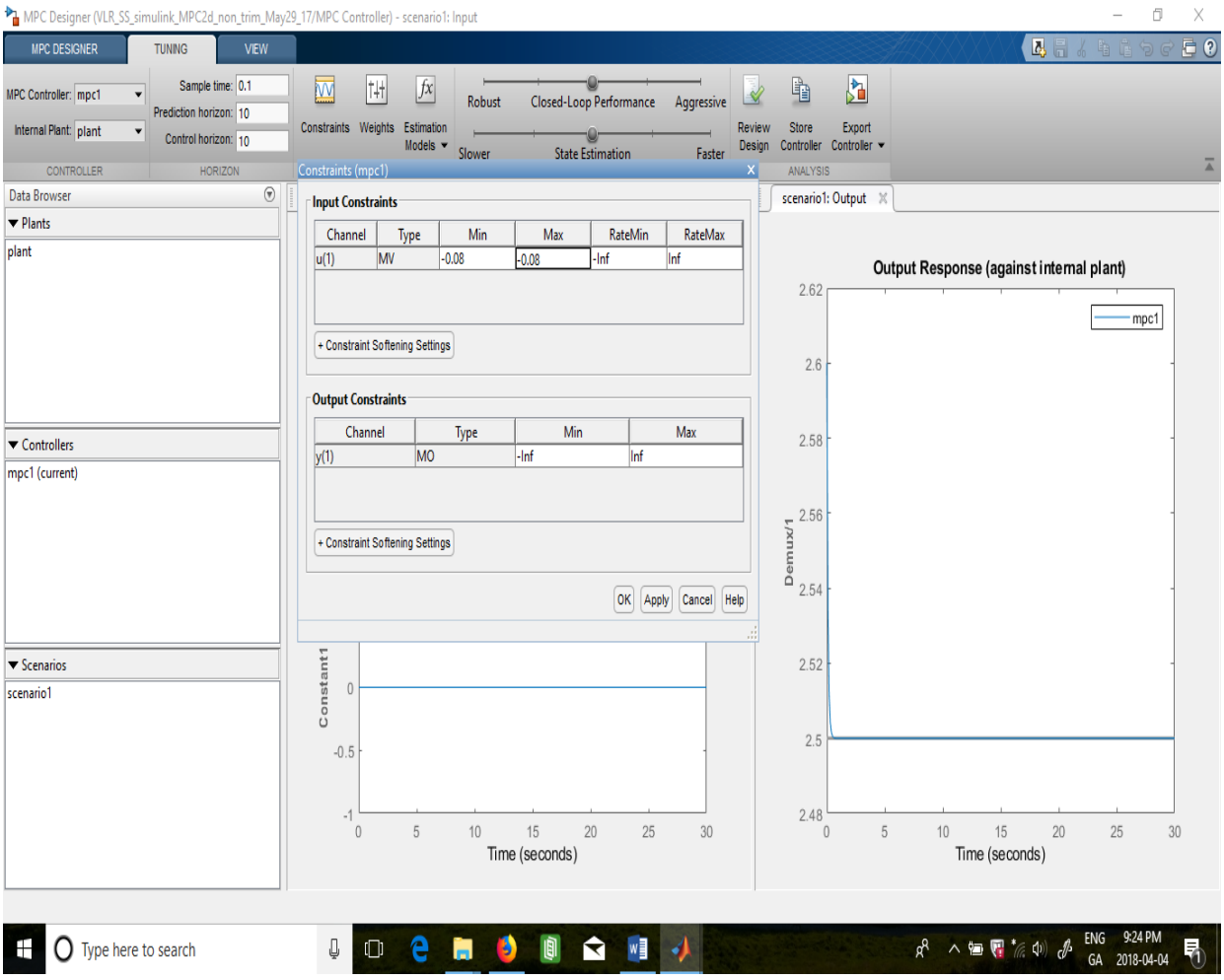

Figure A-7 'Matlab' MPC Design Process 7 - Specify Required MPC Algorithm Design Condition 2

The seventh step in the 'Matlab' MPC design process is to change MPC algorithm design condition of its important input constraint which is a distinctive strength and characteristics of MPC theories. As shown in above Fig. A-7, the input constraint in our case is set to -0.08A (80 mA) as both its minimum and maximum values. Also, the control horizon and prediction horizon are set to the same value throughout the whole duration of the prediction horizon. Such design settings reflect our specific input constraint situation that the manipulated input is the current supplied by the plant to power the WSN embedded system, and that its value is -0.08A (80 mA) when the WSN embedded system is in active operation.

A.8 'Matlab' MPC Design Process 8 – Final MPC Algorithm Design Computation of Required Supercapacitor Discharge Time

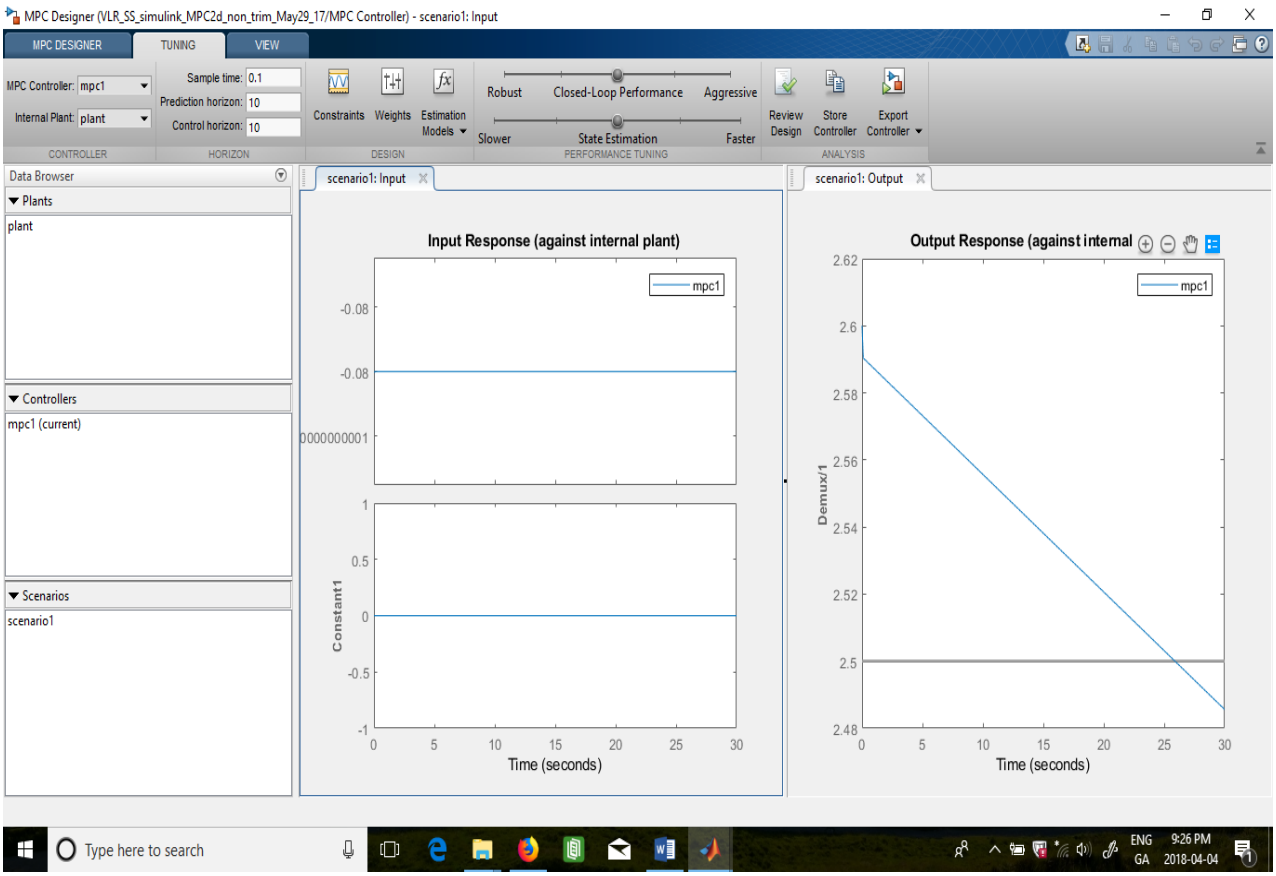

Figure A-8 'Matlab' MPC Design Process 8 - Final MPC Algorithm Design Computation of Required Supercapacitor Discharge Time

This is the final step in the 'Matlab' MPC design process which shows our MPC algorithm design's output response as shown in above Fig A-8. After the input constraint condition is set in our design process 7, select the 'Apply' function allows our designed MPC algorithm to compute both the input response and output response. As shown in the output response graph, the duration of discharge from 2.6V to 2.5V is about 26 seconds (25.78 seconds to be exact). We can see in the later part of this chapter that this parameter is instrumental to our completion of our energy control algorithm design.

ANNEX B FOUR SETS OF TESTING DATA

Please see attached testing data files.

ANNEX C THREE SETS OF MATLAB DESIGN FILES

Please see attached design files.